CANADIAN THESES ON MICROFICHE

I.S.B.N.

THESES CANADIENNES SUR MICROFICHE

National Library of Canada
Collections Development Branch

Canadian Theses on
Microfiche Service

Ottawa, Canada
K1A 0N4

Bibliothèque nationale du Canada
Direction du développement des collections

Service des thèses canadiennes
sur microfiche

NOTICE

The quality of this microfiche is heavily dependent upon the quality of the original thesis submitted for microfilming. Every effort has been made to ensure the highest quality of reproduction possible.

If pages are missing, contact the university which granted the degree.

Some pages may have indistinct print especially if the original pages were typed with a poor typewriter ribbon or if the university sent us a poor photocopy.

Previously copyrighted materials (journal articles, published tests, etc.) are not filmed.

Reproduction in full or in part of this film is governed by the Canadian Copyright Act, R.S.C. 1970, c. C-30. Please read the authorization forms which accompany this thesis.

THIS DISSERTATION
HAS BEEN MICROFILMED
EXACTLY AS RECEIVED

AVIS

La qualité de cette microfiche dépend grandement de la qualité de la thèse soumise au microfilmage. Nous avons tout fait pour assurer une qualité supérieure de reproduction.

S'il manque des pages, veuillez communiquer avec l'université qui a conféré le grade.

La qualité d'impression de certaines pages peut laisser à désirer, surtout si les pages originales ont été dactylographiées à l'aide d'un ruban usé ou si l'université nous a fait parvenir une photocopie de mauvaise qualité.

Les documents qui font déjà l'objet d'un droit d'auteur (articles de revue, examens publiés, etc.) ne sont pas microfilmés.

La reproduction, même partielle, de ce microfilm est soumise à la Loi canadienne sur le droit d'auteur, SRC 1970, c. C-30. Veuillez prendre connaissance des formules d'autorisation qui accompagnent cette thèse.

LA THÈSE A ÉTÉ
MICROFILMÉE TELLE QUE
NOUS L'AVONS REÇUE

NL-339 (r. 82/08)

Canada

0-315-06022-0

National Library of Canada | Bibliothèque nationale du Canada

Canadian Theses Division | Division des thèses canadiennes

Ottawa, Canada
K1A 0N4

53942

PERMISSION TO MICROFILM — AUTORISATION DE MICROFILMER

• Please print or type — Écrire en lettres moulées ou dactylographier

Full Name of Author — Nom complet de l'auteur

HRABOK, Metro M.

Date of Birth — Date de naissance	Country of Birth — Lieu de naissance
Sept 17, 1947	Canada

Permanent Address — Résidence fixe

Box 254
Cudworth, Saskatchewan
S0K 1B0

Title of Thesis — Titre de la thèse

Stiffened Plate Analysis by the Hybrid Stress Finite Element Method.

University — Université

University of Alberta

Degree for which thesis was presented — Grade pour lequel cette thèse fut présentée

Structural Engineering (Ph.D.) Dept of Civil Engineering

Year this degree conferred — Année d'obtention de ce grade	Name of Supervisor — Nom du directeur de thèse
Fall 1981	Dr. T. M. Hrudey

Permission is hereby granted to the NATIONAL LIBRARY OF CANADA to microfilm this thesis and to lend or sell copies of the film.

The author reserves other publication rights, and neither the thesis nor extensive extracts from it may be printed or otherwise reproduced without the author's written permission.

L'autorisation est, par la présente, accordée à la BIBLIOTHÈQUE NATIONALE DU CANADA de microfilmer cette thèse et de prêter ou de vendre des exemplaires du film.

L'auteur se réserve les autres droits de publication; ni la thèse ni de longs extraits de celle-ci ne doivent être imprimés ou autrement reproduits sans l'autorisation écrite de l'auteur.

Date	Signature
Oct. 07, 1981	MHrabok

NL-91 (4/77)

THE UNIVERSITY OF ALBERTA

Stiffened Plate Analysis by the Hybrid Stress Finite Element Method

by

© *Metro M. Hrabok*

A THESIS

SUBMITTED TO THE FACULTY OF GRADUATE STUDIES AND RESEARCH

IN PARTIAL FULFILMENT OF THE REQUIREMENTS FOR THE DEGREE

OF *Doctor of Philosophy*

IN

Structural Engineering

Department of Civil Engineering

EDMONTON, ALBERTA

Fall 1981

THE UNIVERSITY OF ALBERTA

RELEASE FORM

NAME OF AUTHOR *Metro M. Hrabok*

TITLE OF THESIS *Stiffened Plate Analysis by the Hybrid Stress Finite Element Method*

DEGREE FOR WHICH THESIS WAS PRESENTED *Doctor of Philosophy*

YEAR THIS DEGREE GRANTED Fall 1981

Permission is hereby granted to THE UNIVERSITY OF ALBERTA LIBRARY to reproduce single copies of this thesis and to lend or sell such copies for private, scholarly or scientific research purposes only.

The author reserves other publication rights, and neither the thesis nor extensive extracts from it may be printed or otherwise reproduced without the author's written permission.

(SIGNED) M Hrabok

PERMANENT ADDRESS:

Box 254

Cudworth, Saskatchewan

S0K 1B0

DATED September 25, 1981

THE UNIVERSITY OF ALBERTA

FACULTY OF GRADUATE STUDIES AND RESEARCH

The undersigned certify that they have read, and recommend to the Faculty of Graduate Studies and Research, for acceptance, a thesis entitled *Stiffened Plate Analysis by the Hybrid Stress Finite Element Method* submitted by *Metro M. Hrabok* in partial fulfilment of the requirements for the degree of *Doctor of Philosophy* in *Structural Engineering*.

.....
T.M. Hrudey
(Supervisor)

.....
J.S. Kennedy

.....
G.L. Kulak

.....
D.W. Murray

.....
S.H. Simmonds

.....
R.L. Taylor
(External Examiner)
(Berkeley, California)

Date....September 25, 1981.....

ABSTRACT

The hybrid stress finite element method is used for the analysis of stiffened plates. A computer program, called *HYBSLAB*, is developed with the objective that it become a regular analysis aid for practising engineers. The program is intended for the analysis of floor systems under serviceability conditions where the behavior is assumed to be linearly elastic and the loads static. The elastic constants can be those of an orthogonally isotropic (orthotropic) material.

Prior to writing the program an extensive literature search was conducted and the results are summarized in a 'table of existing plate elements'. Some of the simpler elements are then used in an element evaluation study.

The program generates stiffness matrices for a variety of plane elasticity and flexural elements ranging in shape from a triangle to a 6-sided polygon. After verifying that the program and its elements are capable of satisfying the 'patch test', its use is demonstrated on full-size floor systems. The program also provides the user with the option of modelling the finite size of various shaped column cross sections and the finite width of beam stems. The error introduced by coupling beam elements to a plate is examined.

Separate from the above, is a proposed formulation for including the effects of stress singularities at reentrant corners. The formulation is tested by generating stiffness matrices and analysing plates with reentrant corners.

ACKNOWLEDGEMENTS

The writer would like, first and foremost, to thank Dr. T.M. Hrudey for giving freely of his time and for the technical competence demonstrated during the course of this investigation. Next the writer would like to express his appreciation to the members of the examining committee, especially Dr. R.L. Taylor, for taking time from a busy schedule to read the manuscript and offer constructive criticism.

A special acknowledgement is given to a colleague, T.A. Casey, who unselfishly shared his knowledge on computer operations and text formatting. The author is also grateful to the National Sciences and Engineering Research Council for contributing financial support and to the University of Alberta for providing exceptional computer facilities and an environment conducive to research.

Table of Contents

Chapter		Page
1	INTRODUCTION	1
	1.1 General Information	1
	1.2 Scope and Objectives	4
	1.3 Organization and Presentation	5
2	LITERATURE REVIEW	8
	2.1 Review of Developments in Plate Bending	8
	2.2 Existing Elements	24
3	EVALUATION AND TESTING OF ELEMENTS	52
	3.1 Selection Criteria for Test Elements	52
	3.2 Test Cases and Results	59
	3.3 Discussion of Results and Conclusions	61
4	THE HYBRID STRESS METHOD	79
	4.1 Theory of The Hybrid Stress Method	79
	4.2 Polygonal Element In-Plane Matrices	93
	4.3 Polygonal Element Flexural Matrices	98
	4.4 L-Shaped Singularity Elements	109
5	THE COMPUTER PROGRAM '*HYBSLAB*'	126
	5.1 Introduction	126
	5.2 General Description	127
	5.3 Modelling of Eccentric Stiffeners	132
	5.4 Modelling of Columns	138
6	VERIFICATION OF ELEMENT MATRICES	144
	6.1 Introduction	144
	6.2 Plane Stress Problems	145
	6.3 Pure Bending Problems	149

6.4 Singularity Problems 154
6.5 Errors in Modelling Eccentric Stiffeners 157
7 APPLICATIONS TO FULL-SCALE FLOOR SYSTEMS 178
7.1 Introduction 178
7.2 Typical Floor of an Apartment Building 179
7.3 Experimental Test Floor 184
8 SUMMARY AND CONCLUSIONS 198
8.1 Summary 198
8.2 Conclusions 200
8.3 Recommendations for Future Studies 203
References 205
Appendix A 226

List of Tables

Table		Page
2.1	Classification of Finite Element Methods.	33
2.2	A Table of Existing Plate Elements.	34
3.1	Deflection and Moment Comparisons – Square Plate with Simply Supported Edges.	64
3.2	Deflection and Moment Comparisons – Square Plate with Clamped Edges.	65
3.3	Deflection and Moment Comparisons – Square Plate with Simply Supported Corners.	66
3.4	Deflection and Moment Comparisons – Square Plate with Clamped Corners and Edge $W,n=0$.	67
3.5	Normalized Moment Comparisons for Uniform Loading.	68
3.6	Normalized Moment Comparisons for Point Load.	69
6.1	Cantilever Beam In-Plane Displacements.	162
6.2	Cantilever Beam Flexural Displacements.	162
6.3	Clamped Plate: Deflections and Moments for Various Shaped Elements (Uniform Load).	163
6.4	Clamped Plate: Deflections and Moments for Various Shaped Elements (Point Load).	164
6.5	Deflections and Moments for the Singularity Test Case with the Free Edge Opening (Uniform Load).	165
6.6	Deflections and Moments for the Singularity Test Case with the Free Edge Opening (Point Loads).	166
6.7	Deflections and Moments for the Singularity Test Case with the Clamped Edge Opening (Uniform Load).	167
6.8	Error Comparison for Modelling of Eccentric Stiffeners.	168

Table Page

7.1 Comparison of Forces for the Finite Element Model and an Equivalent Frame Model. 189

7.2 Experimental Floor, Comparison of Column Forces. 190

List of Figures

Figure		Page
3.1	Square Test Plate with Typical 4×4 Grid.	70
3.2	Plate Deflections: Uniform Load, Simply Supported Edges.	71
3.3	Plate Deflections: Point Load, Simply Supported Edges.	72
3.4	Plate Deflections: Uniform Load, Clamped Edges.	73
3.5	Plate Deflections: Point Load, Clamped Edges.	74
3.6	Plate Deflections: Uniform Load, Corners Simply Supported.	75
3.7	Plate Deflections: Point Load, Corners Simply Supported.	76
3.8	Plate Deflections: Uniform Load, Corners Clamped, Edge *W*,n=0.	77
3.9	Plate Deflections: Point Load, Corners Clamped, Edge *W*,n=0.	78
4.1	Typical L-Shaped Element and Coordinate Systems.	125
5.1	Some Possible Element Configurations.	143
5.2	Regions for Evaluating [*H*hh], [*H*hp] and [*H*pp].	143
6.1	Test Cases for Constant Strains and Curvatures.	169
6.2	Additional Test Cases for Pure Shear and Pure Twist.	170
6.3	Cantilever Beam Test Case and Element Grids.	171
6.4	Clamped Plate Test Case and Element Grids.	172
6.5	Singularity Test Plate and Element Grids.	173
6.6	Free Edge Opening; Moments along Edge a-b.	174
6.7	Clamped Edge Opening; Moments along Edge a-b.	175

Figure Page

6.8 T-Beam and Representation of Cross Sections. 176

6.9 Beam and Plate Models for Eccentric Stiffeners. ...177

7.1 Typical Floor of a High-Rise Building. 191

7.2 Finite Element Grid for Typical Floor. 192

7.3 Contour Plots of Bending Moment *Mx*, (ft.kips/ft.). 193

7.4 Contour Plots of Bending Moment *My*, (ft.kips/ft.). 194

7.5 Experimental Test Slab. 195

7.6 Finite Element Grid for Experimental Slab. 196

7.7 Contour Plots of Displacement *W*, (feet/1000). 197

A.1 Rotations at the Midsurface of the Plate. 227

List of SYMBOLS, NOTATIONS and SIGN CONVENTIONS

The text of this thesis deals with the finite element analysis of plates. Both a right-handed Cartesian coordinate system (x,y,z), and a right-handed polar coordinate system (α,r,z), are used.

The following degrees of freedom are defined at the midsurface of the finite element plates:

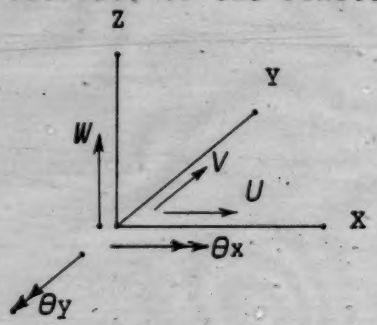

where,
- W = transverse displacement,
- θx = rotation about the X axis,
- θy = rotation about the Y axis,
- U = in-plane displacement (in the X direction),
- V = in-plane displacement (in the Y direction),

The directions of moments and shears are defined according to the tensor sign convention as shown below:

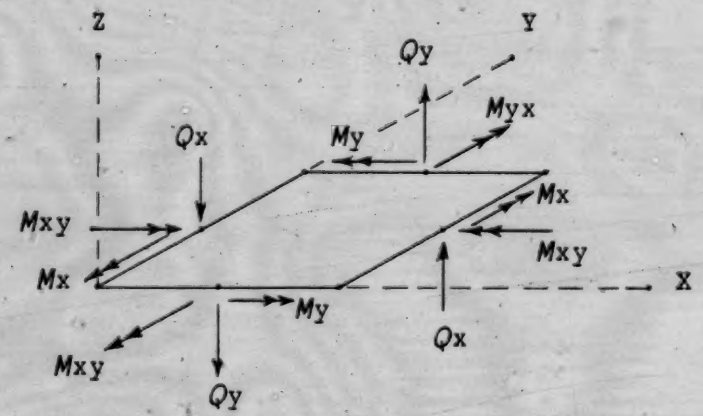

The following is a list of symbols, notations and nomenclature used in the text. The notations for the beam element and the Lagrange element are presented last. The notations are also defined in the text where they first appear.

Matrix Symbols

[ ] : denotes a rectangular matrix,

$[\ ]^T$: denotes the transpose of a rectangular matrix,

{ } : denotes a one-dimensional column matrix,

< > : denotes a one-dimensional row matrix,

( ),$_i$: denotes the partial differential of the quantity in brackets with respect to the variable 'x_i',

( ),y : denotes the partial differential of the quantity in brackets with respect to the variable 'y',

{o} : denotes a null vector,

Displacements

W = Z displacement of any point in the element,

$\{\underline{W}\}$ = nodal displacements of W for the element,

W,ij = second derivative of W (index notation),

θx = rotation about the X axis at any point in an element,

θy = rotation about the Y axis at any point in an element,

θn = rotation normal to an element side,

θt = rotation tangent to an element side,

θx_i = rotation θx at node 'i',

$\{\underline{\theta x}\}$ = nodal rotations θx for an element,

θy_i = rotation θy at node 'i',

$\{\underline{\theta y}\}$ = nodal rotations θy for an element,

U = X displacement of any point in an element,

$\underline{u}_i$ = value of U at node 'i',

V = Y displacement of any point in an element,

$\underline{v}_i$ = value of V at node 'i',

U_i = index notation for any translational displacement, of a point in a solid,

$\bar{U}_i$ = prescribed values of U_i,

$\{\underline{U}\}$ = matrix notation for all nodal displacements,

$[L]$ = matrix relating field values of displacements to nodal degrees of freedom,

Stresses, Stress Resultants and Tractions

σ_{ij} = stress tensor in index notation,

M = moment stress resultant (force×length/length),

M_{ij} = moment tensor in index notation,

M_n = moment normal to an element side,

M_{nt} = twisting moment about a normal to a side,

Q = ordinary transverse shear at a plate edge,

V = Kirchhoff shear,

T_i = traction vector in index notation,

$\{T\}$ = traction vector in matrix notation,

$\bar{T}_i$ = prescribed values of T_i,

S_x, S_y = Southwell stress functions,

Strains and Material Properties

ϵ_{ij} = strain tensor in index notation,

C_{ijkl}, D_{ijkl}, E_{ijkl} = fourth order tensors of material constants,

$\left.\begin{matrix}[C]\\[D]\\[E]\end{matrix}\right|$ = constitutive tensors in matrix form,

Energy Terms

$\mathfrak{E}$ = strain energy,

Π = potential energy,

Πc = complementary potential energy,

Πmc = modified complementary potential energy,

General Terms

a_i = coefficients of the patch test polynomials,

Fi = body force components (index notation),

$H^o_{i,2}$ = Hermitian interpolation polynomials as functions of ρ, where the
- superscript 'o' denotes the order of the family or the number of derivatives which the polynomial can interpolate,
- subscript '1' denotes the displacement being interpolated (either W or its derivative),
- subscript '2' denotes the node at which the function has a unit value,

$dH^o_{i,2}$ = derivative of above Hermitian with respect to 'ρ',

$\mathfrak{L}$ = length along the side of an element,

ni = component 'i' of a unit normal vector,

ρ = non-dimensional parameter used to denote length along a beam or element side,

q_o = uniform loading in the Z direction,

q = non-uniform loading in the Z direction,

Hybrid Stress Matrices

$[P]$ = matrix of terms for the stress functions without the β parameters,
$[Ph]$ = $[P]$ for the homogeneous solution,
$[Pp]$ = $[P]$ for the particular solution,
$[Ps]$ = $[P]$ for the singularity solution,

[*NP*]= matrix product of a matrix operator [*N*] and the polynomial matrix [*P*],
[*NP*h]= [*NP*] for the homogeneous solution,
[*NP*p]= [*NP*] for the particular solution,
[*NP*s]= [*NP*] for the singularity solution,

[*H*hh], [*H*pp], [*H*ss], [*H*hp], [*H*hs], [*H*ps], [*H*ph], [*H*sh], [*H*sp] = matrices used to evaluate the strain energy of an element,

[*G*hh], [*G*pp], [*G*ss] = matrices used to evaluate the potential of edge tractions for an element,

$\{\beta\}$ = vector of β_i terms from the stress functions, where,
$\{\beta h\}$ = β parameters from the homogeneous solution,
$\{\beta p\}$ = β parameters from the particular solution,
$\{\beta s\}$ = β parameters from the singularity solution,

[GHG] = stiffness matrix for a hybrid stress element,

{Peq} = work equivalent load vector for the hybrid element,

Singularity Functions (Section 4.4)

W_s = deflection function for stress singularities,

$\overline{W}_s$ = values of W_s without β,

$W_{s,\alpha r}$= second derivative of W_s, with respect to 'α', and 'r',

$\nabla^2 W = W_{,xx} + W_{,yy}$

[B_w] = a matrix of singularity displacement functions,

C_i = constants of W_s evaluated from the boundary conditions prescribed along the reentrant edges,

α = polar coordinate of rotation,

β_o = β_i from the singularity function W_s,

λ = an eigenvalue,

ν = Poisson's ratio for an isotropic material,

M_α = moment normal to an edge,

F = a function used to denote part of the singularity function, W_s,

$\dddot{F}$ = third derivative of F with respect to the angle, α,

G_1, G_2, G_3 = functions calculated from W_s to obtain moments and shears,

$\dot{G}_2$ = first derivative of G_2 with respect to 'α',

$r^{(-1)}$ = radius 'r' raised to the power '-1',

$r^{(\lambda)}$ = radius 'r' raised to the power 'λ',

Offset Beam Element Matrix

e_1 = 'Y' eccentricity of a beam element,

e_2 = 'Z' eccentricity of a beam or offset plate element,

γ = angle of rotation of a beam element in the X-Y plane,

k_i = stiffness coefficient for a beam element,

[Kb] = beam stiffness matrix in global coordinates,

[$\underline{K}$] = beam stiffness matrix in local coordinates,

[Te] = linear transformation matrix relating geometric degrees of freedom between the local and global coordinate systems,

[Tr] = rotation transformation matrix used to rotate a beam in plan,

Lagrange Element (Appendix A)

θ_x = rotation about the X axis of a normal with respect to a tangent at the midsurface,

θ_y = rotation about the Y axis of a normal with respect to a tangent at the midsurface,

$\langle N_i \rangle$ = shape functions used to relate the values of W, θx, θy, λx, and λy, to their respective nodal parameters,

$\langle N_i,x \rangle$= partial derivative of $\langle N_i \rangle$ with respect to 'x',
$\{N_i,x\}$= partial derivative of $\{N_i\}$ with respect to 'x',
$\langle N_i,y \rangle$= partial derivative of $\langle N_i \rangle$ with respect to 'y',
$\{N_i,y\}$= partial derivative of $\{N_i\}$ with respect to 'y',

$\{F_1\}$ = work equivalent load vector for W load,
$\{F_2\}$ = work equivalent load vector for θx load,
$\{F_3\}$ = work equivalent load vector for θy load,

λx = Lagrangian multipliers in the X direction,

λy = Lagrangian multipliers in the Y direction,

$\{\underline{\lambda} x\}$ = nodal values of λx,

$\{\underline{\lambda} y\}$ = nodal values of λy,

$\mathrm{I\!I}$ = Lagrangian functional,

$[L^{(i)}]$= matrices evaluated from the product of the Lagrangian and the displacement shape functions,

$[K^{(i)}]$= stiffness submatrix number 'i'.

Chapter 1

INTRODUCTION

1.1 General Information

The development of the finite element method over the last two decades ranks as perhaps one of the most significant achievements in the history of engineering. This analysis technique has a sound base in variational calculus and with the aid of a computer provides a means of solving complex problems which would otherwise be intractable. With its use now well established in many fields of engineering, the research frontiers in the finite element method have moved to areas such as non-linear applications and the modelling of complex material behavior. As discussed recently by Clough[1], even in these fields the rewards for research have reached the point of diminishing returns. Also as discussed by Clough, the trend now is towards analytical-experimental research in an attempt to model actual behavior and verify the theoretical model.

Theoretical developments in the finite element field experienced a very rapid growth rate during the latter part of the 1960's and the early 1970's. In addition to the analytical-experimental type of research described by Clough, present day efforts are directed at either edging back the frontiers established during that period or making practical use of existing theoretical formulations for

problem solving. The present study falls into both of these categories, with the major portion being in the latter.

The need for practical-oriented studies is great. Methodology employed by the majority of consulting firms today lags seriously behind the state of the technology. For example, the majority of structural consulting firms still use beam/column elements to model plane stress and plate bending structures.

The reluctance of practitioners to use the finite element method can be attributed to a number of factors. Probably the most significant is the lack of familiarity and experience with the finite element method. This is mostly due to lack of training in the area, compounded by the nature of the solution which requires choosing a grid and later interpreting the output. The would-be user is also faced with finding or writing a suitable computer program. The issue is further complicated by the fact that within the finite element method there exist a number of different formulations. The one most familiar to engineers is the displacement method. In plate bending, for example, the use of the various formulations has resulted in a bewildering number of elements. After a program is obtained, the question of costs arises. With the capability and efficiency of present day computers, the dominant cost of the analysis is most likely to be associated with the cost of manpower. Many finite element programs require several man hours for preparation of input data and interpretation

of output data. The cost of actually 'running' the finite element program can no longer be regarded as a deterrent to its use.

The investigation presented here deals with the use of the finite element method for the analysis of flat plates. The study has two main goals. The first goal is a practical one and is to provide design engineers with a design aid in the form of a finite element plate bending computer program. This program differs from existing programs in the following ways:

(1) The program is based on the hybrid stress method. For reasons discussed in Chapter 3, this formulation appears to be best suited for the analysis of flat plate floor systems.

(2) In modelling the structure, any element shape ranging from a triangle to a six-sided polygon may be used. Floors of arbitrary planform can be analysed and the finite dimensions of column cross sections and the finite width of beams may be included in the analysis. Translational in-plane degrees of freedom have been included to allow for displacements, such as those caused by eccentric stiffeners. The same subroutine which generates the flexural matrices for the various shaped elements is also used to obtain the in-plane matrices.

(3) In developing the program, much emphasis has been placed on reducing the user manpower demands. This has been done by automating the input of data and by using graphical displays to aid in the checking of input data and the interpreting of output data.

The program is primarily intended for use by consulting firms where at present more approximate methods based on equivalent frames predominate. In this sense, it represents an advancement because plate structures can be analysed as

plates rather than a series of crossing beam elements with incompatible displacements. At the same time, the program has the capability of doing refined analysis of the type required for research purposes.

The second goal is to develop an element for the study of stress singularities at reentrant corners of plates. The formulation proposed in this thesis and the results obtained therefrom are believed to be original work.

1.2 Scope and Objectives

The scope of the investigation is restricted to the static analysis of linear elastic orthotropic plates. Classical Kirchhoff plate theory has been used to describe the behavior of the plate.

The objectives of the present study are:

(a) to conduct an extensive literature review and in summary to provide a table of elements which can serve as a guide and a quick reference to users of plate bending elements,

(b) to evaluate a number of plate bending elements and to choose the one which is most suited for the analysis of flat plate structures,

(c) to include in the analysis the modelling of eccentric stiffeners of finite width and of columns with finite-sized cross sections and various shapes,

(d) to study the effects of stress singularities at reentrant corners,

(e) to develop a computer program capable of modelling complex flat plate structures but intended for use by consulting firms,

(f) to illustrate the use of the program on actual floor systems and to demonstrate that it is a viable

alternative to more approximate and traditional approaches presently being adhered to; to incorporate graphical output for the purpose of reducing the time spent in checking of data, interpreting the results and preparing the working drawings.

1.3 Organization and Presentation

The presentation begins in Chapter 2 with an indepth literature review highlighting the more significant events in the development of plate bending elements. The number of elements which have evolved over the years is overwhelming and an attempt is made in Table 2.2 to chronologically catalogue most of these elements. In the table, each element is described by a sketch and accompanying comments. This type of table is expected to be of great assistance as a reference chart to both users and researchers of plate bending elements.

In Chapter 3 certain criteria are established to choose candidate elements for the desired plate bending program. The candidate elements are then evaluated on four test cases thought to be relevant to practise and the results are presented in tabular and graphical form. From these results, one element is chosen for the computer program.

The theory and use of the hybrid stress method for plate bending and plane elasticity problems is dealt with in Chapter 4. The in-plane matrices are necessary to model the in-plane displacements caused by eccentric stiffeners. The formulation for dealing with the stress singularities is

included in this discussion of the theory. This is followed by details on how various matrices are obtained for polygonal shaped plane stress and flexural elements and the L-shaped singularity elements. These matrices are then used to calculate stiffness matrices and work equivalent load vectors. With Chapter 4 as a basis, a computer program which will be referred to as *HYBSLAB* was developed.

The capabilities and the general set-up of the program *HYBSLAB* are described in Chapter 5. As well, the methods used in the program to model eccentric beam elements and finite-sized columns are explained in detail.

Chapter 6 deals with the test cases used to verify the element matrices of Chapter 4 and the program of Chapter 5. The patch test and other similar tests are used to verify the in-plane and the flexural stiffness matrices. Test problems are included to illustrate convergence trends for the various shaped elements. The L-shaped singularity elements are used to solve an example problem and the importance of considering the singuarity functions in the formulation is assessed. The chapter concludes with an investigation into the magnitude of error caused by coupling eccentric stiffeners to a plate.

The use of the program *HYBSLAB* to solve practical problems is demonstrated in Chapter 7. Two actual floor systems are considered. The first is a typical floor of a high-rise building, while the second is an experimental test slab with eccentric stiffeners. In the second case the

finite size of the columns and the finite width of the stiffeners are accounted for in the analysis.

The final chapter contains the summary and conclusions of this investigation. Also areas which still require additional research work are identified.

Chapter 2

LITERATURE REVIEW

2.1 Review of Developments in Plate Bending

Solutions to typical plane stress, plane strain and three-dimensional elasticity problems can be obtained by solving second order differential equations such as the Navier displacement equations. The energy functional associated with these problems contains only the first derivative of the displacements.

In comparison, plate analysis, even by a simple plate theory such as the classical Kirchhoff theory[14], requires the solution of a fourth order differential equation. For more refined theories such as those established by Reissner[15], Hencky[11], and Kromm[11], the integration order may increase from four to six. These more exact theories differ from the Kirchhoff plate theory by including the effects of transverse shear strains and thereby allowing the use of all three actual boundary conditions along the plate edges.

Plate analysis by the finite element method was started at the beginning of the 1960's by researchers such as Clough[7], Adini[3], Melosh[12], and Tocher[15]. These researchers used Kirchhoff plate theory and assumed functions for the deflected shape of the element. The finite element method provided a means of replacing the

displacement form of the differential equations of equilibrium by a set of linear algebraic equations. The equations were then solved for the unknown displacements; therefore, this approach came to be known as the 'displacement method'.

By the mid 1960's it was realized that this type of finite element analysis was based on the variational principle of minimization of potential energy for the structure. The strain energy expression contains second derivatives of the displacement functions and is calculated from the individual elements. For the variational principle to be valid, it is essential not to have any discontinuities in either the transverse displacement or its first derivatives at any point in the structure. This requirement of continuity for the prime variable and its first derivatives has come to be known as the 'C' continuity' requirement. Plane elasticity problems require continuity of the prime variable alone or 'C° continuity'. It is important to note that a complete linear polynomial function can provide C° continuity, but nothing less than a complete cubic polynomial will satisfy C' continuity.

For elements based on Kirchhoff plate theory, the prime variable is the transverse displacement. Its first derivatives along an edge are the normal and tangential slopes. The shape functions used most often are either the polynomial type obtained from Pascal's triangle or the

Hermitian type of interpolation functions.† With these types of functions there is no problem in obtaining full continuity of the transverse displacement and the tangential rotation along a common boundary. However, as early researchers soon discovered, obtaining the same continuity for the normal slope did prove to be difficult indeed. Physically, this incompatibility of normal slope represents a kink in the structure at the junction of two neighboring elements and hence these elements were labelled as 'displacement nonconforming' or simply 'nonconforming'. Most early plate elements were nonconforming and this caused much concern. The presence of the slope discontinuities violated one of the conditions of the variational principle and therefore there was no guarantee that the solution would converge.

Five papers which were presented in 1965 at a conference at the Wright Patterson Air Force Base are worthy of mention because they not only described the state of the art as it then was, but they set the stage for much of the research to come. The publications by Clough and Tocher[4], Bazeley, Cheung, Irons, and Zienkiewicz[5], and Bogner, Fox and Schmit[3] established the importance of the constant strain states and demonstrated that obtaining conformity for plate elements was not going to be easy. These papers marked the beginning of an era of plate bending research

---

† Other shape functions have been used on occasion; in 1964, Deak and Pian[13] used spline functions.

where the objective was either to provide C' conformity or else provide alternatives to it.

In all three papers, a displacement formulation and classical Kirchhoff plate theory were the bases for the element stiffness derivations. In addition to the above, the papers by Pian'[4] and Herrmann'[5] are included because they introduced the hybrid and mixed methods as alteratives to the displacement method. Further discussions on the contributions of these researchers follows.

Clough and Tocher's investigation was primarily a comparative study of displacement accuracy for 3 rectangular and 4 triangular elements. It consisted of 280 analyses involving 8 plates. All of the elements had corner nodes only and the 3 geometric degrees of freedom as nodal parameters. The geometric degrees of freedom are defined as the transverse displacement and the two rotations. The elements which were used are discussed in more detail in Section 2.2.

Clough and Tocher found that the rectangles generally provided better results than the triangular elements. Unfortunately, for certain cases, one of the nonconforming rectangles and all three of the nonconforming triangles converged to incorrect values. These researchers correctly identified the absence of a constant twist term, where applicable, as being responsible for the poor behavior. However, Clough'[4] stated in an earlier publication that complete conformity is essential for convergence. As well,

Clough and Tocher leave the impression that the lack of conformity is responsible for the poor performance of the triangles.

Bazeley, Cheung, Irons and Zienkiewicz took issue with this statement on conformity and set out to prove otherwise. They postulated that, although complete geometric conformity is useful because it ensures monotonic convergence of strain energy, it is not essential for convergence to the true values. Bazeley et al. stated that the only thing which is essential is that the element, regardless of size or shape, is capable of representing all the constant strain (or curvature) states.

Today it is agreed that for true convergence the individual elements must be able to represent the constant strain states exactly. Although this is a necessary condition, it not sufficient. Conformity together with the constant strain or 'completeness' condition guarantees true convergence but conformity is not essential; it can be replaced by the 'patch test'. One interpretation of the patch test is that any group of elements, when subjected to constant strain conditions around the periphery of the group, can reproduce exactly the constant strain conditions at all the interior points. For flat plates, elements of any size or shape are expected to meet these requirements. Irons'[10] is credited with the development of the patch test, but its origin was in the work of Bazeley et al. More details on convergence and the patch test are available in a

number of publications by Irons.

Bazeley et al. considered triangular elements only. They introduced the use of 'area' coordinates as a means of obtaining element shape functions which were geometrically isotropic and were not affected by the orientation of the element. Unfortunately, their shape functions could not satisfy the constant curvature conditions and it became necessary to add supplementary functions. These supplementary shape functions by themselves had zero-valued transverse displacement and slopes at each of the element nodes and therefore could be added to the existing shape functions in any proportion. The element could now represent the constant strain states, but still it was nonconforming. To make the element conforming they added parabolic corrective functions. These corrective shape functions were applied to the normal slope along element sides and eliminated departures from a linear variation between the nodes.

Although their formulation does become rather involved, Bazeley et al. do some example problems and present the following important results. First, without the corrective functions, the elements are nonconforming but they still converge to the correct results. Thus the importance of the constant strain conditions was established. Second, they were successful in obtaining C' continuity for a triangular element. More will be said about their method in the next section. Third, the nonconforming elements gave results

usually much superior to those obtained from the conforming triangle. This was especially true for the coarser grids, so much so that Bazeley et al. recommend these elements for actual use.

Bogner, Fox and Schmit[3] dealt with conforming rectangular elements. They used Hermitian interpolation functions to derive stiffness matrices for 12 and 24 degree of freedom rectangular elements. Each rectangle had corner nodes only, but the 24 degree of freedom element, in addition to the three geometric degrees of freedom, had curvatures as nodal parameters.

Bogner et al. did some example problems and concluded that the elements exhibited monotonic convergence and good accuracy. However, the convergence was to incorrect values because the constant twist term had been omitted. In an addendum to the paper, they removed this deficiency and rederived 16 and 36 degree of freedom stiffness matrices to replace the earlier 12 and 24 degree of freedom versions. The new elements exhibited extremely rapid convergence.

Although the work of Bogner et al. did show the importance of including all constant strain states, their main contribution is that they were successful in obtaining full conformity for rectangular elements. However, they found that in order to get conformity it was necessary to use the twist term which is a second derivative of the transverse displacement. Some clarification on this was provided in 1965 by Irons and Draper[13]. They showed that

it was impossible to use simple polynomials with only the 3 geometric degrees of freedom as nodal parameters and get complete conformity.

There was considerable discontent with the C' continuity requirement and researchers looked for alternate formulations. Not only was C' continuity difficult to obtain for most elements, but, when finally achieved, the resulting elements were often found to be too stiff. The research which followed went two separate ways. Followers of the displacement method turned to higher order polynomials and elements with more nodes or more nodal parameters. Other researchers abandoned the displacement method and searched for alternate formulations. These alternatives were also based on variational principles.

A logical alternative was to use the principle of minimum complementary potential energy and an 'equilibrium formulation'. It would appear that all one needs to do again is to use interpolation functions, but this time to describe the stress field. The chosen functions would be required to satisfy equilibrium at every point in the structure and the stress conditions on the boundaries. However, as described by Zienkiewicz[20], 'despite many trials of horrifying complexity' seldom has this been achieved directly with stresses as variables. One of the major difficulties is satisfying the kinematic boundary conditions.

Initial work in this field was done by de Veubeke[7]. To avoid a redundant force analysis, de Veubeke formed element flexibility matrices directly, inverted them to get stiffness matrices, and then proceeded with a displacement type of solution. Problems arose with this approach when the assembled stiffness matrix was found to be positive semi-definite; this indicated that the structure was kinematically unstable.

Another means of using the complementary energy principle is to use the 'flexibility' or 'force' approach where a set of redundant self-equilibrating forces is chosen as the unknowns. In finite element analysis, difficulties with automating the selection of the redundant force system have caused this approach to be all but abandoned.

Considerable clarification and simplification in the use of the equilibrium method is attributed to Morley[33,34] and Elias[9], who implemented the use of element stress functions. Stresses are calculated from the second derivatives of these functions and therefore the stress functions must still possess C' continuity, but choosing these functions is made easier by 'the principle of duality'. According to this principle, the Airy stress function, ϕ, from an equilibrium solution in plane elasticity, has the same form as the conforming displacement function, W, for a plate bending problem. Conversely, the conforming displacement functions, U and V, from a plane stress solution can serve as the Southwell stress functions,

S_x and S_y, for an equilibrium solution to a plate bending problem. These analogies have been discussed extensively in the literature by Southwell[177], Zienkiewicz and de Veubeke[180], Morley[133], Elias[70], and Sander[170]. In spite of Morley's and Elias' contributions, problems still exist with choosing the stress functions, defining the applied load state and specifying the boundary conditions for the stress functions. As well, the displacements do not possess unique values because they can only be obtained from integrating the strains. More detailed discussions on obtaining solutions from the principle of minimum complementary energy are given in Chapter 7 of Gallagher[84] and in Chapter 12 of Zienkiewicz[204].

Another alternative to the displacement method is the hybrid stress method of Pian[146,152]. Using a modified potential energy principle, Pian chose, to his advantage, stress polynomials for the interior of the element and displacements around the perimeter of the element. Since this method has traits of both the displacement and equilibrium methods, it became known as a hybrid stress method. In 1965, Pian[146] successfully used his method to derive stiffness matrices and obtain solutions for both in-plane and plate bending problems. His method has attracted the interest of researchers such as Severn[177], Henshell[84], Wolf[200], Cook[54], and Yoshida[204].

Other researchers, such as Hansteen[92], Tong[186], and Kikuchi and Ando[120], developed various displacement hybrid

approaches based on a modified principle of minimum potential energy. Due to difficulties in obtaining some of the component matrices and other problems identified by Mang and Gallagher[124], this approach does not enjoy the same success as Pian's stress hybrid.

A third alternative to the displacement method was presented at the same conference by Herrmann[81] and was based on a modified Reissner variational principle. Using this method, different combinations of displacements and stresses can be assumed on the interior as well as on the boundaries of the element. Herrmann relaxed the continuity requirements for displacements but imposed continuity conditions on the stress field. The result was that C^0 continuity was required from both sets of trial functions. Computations for the element stiffness are reduced because lower order polynomials can be used, but neither equilibrium nor compatibility may be satisfied in totality[83]. In general, with the mixed methods, Lagrangian multipliers are included in the final equations and the pivots must be chosen carefully because the equations are positive semi-definite[84,206].

The developments from the mid 1960's to the early 1970's are regarded by many writers as being the most significant in the development of the finite element method. The most important contribution from this era was the establishment of variational principles as the bases for the various finite element methods in structural engineering. A

comparison of these methods is presented in Table 2.1. This table is basically the same as that published in 1969 by Pian and Tong[52] except for the addition of the generalised displacement and the generalised equilibrium methods to the mixed category.

In the 'generalised displacement method', nonconforming elements are used in conjuction with interelement Lagrangian multipliers. The Lagrangian multipliers are present in the global equations and can be identified as forces which are attempting to remove the discontinuities in normal slopes between the elements. This approach appears to have been initiated by Jones[11], Greene et al.[8], Anderheggen[2], and Harvey and Kelsey[3].

Similarily, in the 'generalised equilibrium method', the Lagrangian multipliers are applied to the global set of equations but now are identified as displacements. These displacements restore equilibrium conditions between elements in an overall or integral sense. Such a solution was used in 1969 by Anderheggen[1] and later by Sander[10]. With these two mixed methods, as with the mixed method described earlier, Lagrangian multipliers are included in the final solution and the equations are positive semi-definite. Morley[37] has developed an approximation technique to ensure that the final equations are positive definite. Due to the increased number of unknowns and the more complicated nature of these solutions, they are seldom used.

The period from the early 1970's onward was considerably less rewarding in terms of plate bending element research. Nevertheless, there were many papers published primarily dealing with C' continuity or alternatives to it. This period saw the introduction of techniques such as reduced integration and penalty number formulations, the use of substitute shape functions and derivative smoothing, and the use of discrete Kirchhoff constraints. Some of these topics and the resulting elements are discussed in the next section.

One of the most significant developments which emerged from this period was the use of the displacement formulation based on Mindlin plate theory and reduced integration schemes. A discussion of these schemes and two related approaches follows after a brief description of the Mindlin plate theory.

Discontent with the C' continuity requirement and the desire to include shear deformations caused some researchers to abandon the Kirchhoff plate theory in favour of other theories such as that due to Mindlin[31]. For flexural equilibrium of plates, Mindlin's plate theory is very similar to Reissner's[45]. Both theories recognize three separate boundary conditions along the edge of a plate and Reissner's theory can be considered as a special case of the more general Mindlin theory. A comparison of the two methods is given by Mindlin[31].

In Mindlin plate theory the rotations at the plate midsurface are not solely dependent on the transverse displacement of the plate. For a finite element analysis, this means that independent shape functions can be used for the 3 geometric degrees of freedom. Only the first derivative of the variables appears in the energy functional and therefore only C^0 continuity is required of the shape functions. As well, the shape functions from plane elasticity elements can be used for the plate bending elements and the elements can be distorted or mapped into isoparametric shapes.

This approach worked fine for thick plates, but as the plate thickness decreased the shear stiffness became so large as to render the computations useless[2,8]. Therefore, for thin plates, it became necessary to either impose the Kirchhoff conditions of normality directly as constraints or else make the shear strain matrix rank deficient by using reduced integration. This type of approach had been used with some success in 1969 by Doherty et al.[4] for overly stiff plane stress elements. For plate bending, it was introduced simultaneously in 1971 by Zienkiewicz, Taylor and Too[2,9] and by Pawsey and Clough[1,3].

In both publications, its use was demonstrated on Ahmad's eight-node serendipity shell element[1]. In evaluating the shear strain energy, both research groups purposely underintegrated the shear strain terms while evaluating the flexural terms exactly. This procedure has

come to be known as 'selective reduced integration'. Zienkiewicz and co-workers also tried underintegrating all terms by one order of integration. Such a procedure is now referred to as 'uniform reduced integration'. Both methods gave much improved results and led to the method of selective reduced integration with Mindlin plate theory. This was to dominate the plate bending research field from the mid 1970's to the present. The main contributions to this area have come from research groups associated with Hughes[99,103,107] and Hinton[96,99]. Some of the elements from this development are used in the next chapter.

One alternative to using selective reduced integration for Mindlin plate elements is to impose, at the element level, the Kirchhoff constraints of normality at discrete locations such as the Gauss integration points or the Loof nodes[121]. Although this is a systematic approach, it is not always successful and C^0 continuity is not always preserved[206]. This idea was introduced in 1968 by Wempner et al.[196] and has been used for plates by researchers such as Stricklin[80], Baldwin[8], Fried[81], Irons[114], and Lyons[122].

A second alternative is to impose the Kirchhoff constraints in a weighted integral sense by using Lagrangian multipliers. The details of using this approach to obtain an element stiffness matrix are presented in Appendix A.

Neither of the last two approaches is as simple or effective as the selective reduced integration technique. In 1980, the use of the selective reduced integration scheme

was extended to hybrid stress formulations by Spilker[77].

All of the methods discussed thus far are not independent and a more comprehensive treatment of these topics and the equivalences between certain methods are discussed in Chapters 11 and 12 of Zienkiewicz[200] and in Chapter 12 of Gallagher[84]. As well, Malkus and Hughes[123] and Spilker[77] show the equivalence of selective reduced integration and some mixed methods.

A radically different approach to all the methods which have been discussed thus far is the 'direct method' introduced in 1975 by Bergan and Hanseen[21]. The method is not based on any variational principle, and any element matrix which satisfies certain conditions is acceptable. The conditions consist of representing the rigid body modes and the constant strain conditions and satisfying the patch test. The method does not require involved computations as some of the previous methods, and Bergan and Hanseen have derived a triangle which is quite accurate.

Various other methods exist for the finite element analysis of plates. One of these is the 'constraint' method used by Rossow[167]. Another approach, which has unlimited applicability, is to use three-dimensional elements for plate analysis. Neither of these methods is discussed in this review.

2.2 Existing Elements

The purpose of this section is to identify most of the elements which have resulted from the developments discussed in the review section. Some of the more prominent elements are discussed first and then a table of elements is presented. The rectangular elements are considered first and then the triangles. Quadrilateral elements can be obtained from rectangles by a transformation of coordinates, but unfortunately the constant curvature states are often destroyed[200]. Therefore quadrilateral elements are usually derived from triangles and will not be discussed separately.

The derivation of stiffness matrices for plate bending elements was initiated by three simple rectangles. All three elements had corner nodes only and the 3 geometric degrees of freedom at each node.

The most well known of these elements was presented at the beginning of the 1960's and is the Adini-Clough-Melosh or 'A C M' element. This is a displacement element based on a twelve term polynomial displacement function consisting of a complete cubic and two quartic terms. Although this element is nonconforming, its shape function does satisfy the plate's differential equation of equilibrium and biharmonic displacement equation. The principle of minimum potential energy does not require the shape functions to satisfy either of these two equations.

The second rectangle was presented in 1961 and is often referred to as the Melosh or 'M' element[128]. To derive the

stiffness matrix for this element, Melosh used the Hermitian beam functions along the edges of the element and assumed a linear decay to zero at the opposite and parallel side.

The third element is based on a product of two cubic Hermitian polynomials, one along the local X axis and the other along the Y axis. This element is sometimes referred to as the element with crossing-beam displacement functions. It was presented in 1959 by Papenfuss'[40], but did not receive much attention until rederived by Bogner, Fox and Schmit in 1965. Although conforming, this element suffers from the lack of a constant twist term and may not converge to the correct result.

The above three simple rectangular elements initiated the derivation of plate bending matrices. Several other rectangular elements based on various functions and formulations are presented in Table 2.2. Two of the more prominent types from these developments are the hybrid stress elements and those based on Mindlin plate theory and selective reduced integration.

The hybrid stress elements were put forward by Pian in the mid 1960's. Since that time a large number of elements have been derived by his method; several of these are presented in Table 2.2.

The rectangles based on selective reduced integration and Mindlin plate theory are a recent development due mainly to the efforts of researchers such as Hughes and Hinton. Most of the elements developed by this approach are included

in Table 2.2. Two of the more promising of these elements are the simple bilinear rectangle and the 'heterosis' element. These elements will be encountered again in the next chapter.

The derivation of stiffness matrices for triangular elements has been the most challenging of all. The problem with triangles arises from the fact that it is very difficult to obtain conformity and retain geometric isotropy because the number of terms in a suitable shape function seldom equals the total number of nodal parameters. Adding internal degrees of freedom does not help conformity. In the following paragraphs, a survey of element types originating from various solutions is presented.

Beginning with the work of Adini[3] in 1960, and Tocher'[8] in 1962, it was soon apparent that for the basic 9 degree of freedom triangle it was not going to be easy to obtain a stiffness matrix which converged to the correct result. The problems arose because a complete cubic displacement function has 10 terms but the basic triangle has only 9 degrees of freedom. Therefore, the choice regarding which terms to omit is almost arbitrary, but symmetry should be maintained. Clough and Tocher[7] presented 3 nonconforming triangles, none of which was satisfactory. One of these, derived earlier by Adini[4], had the xy term omitted and converged to an incorrect value. The second one, derived by Tocher'[8], had the x^2y and xy^2 terms combined. Unfortunately, for some orientations of the

element, problems are encountered with singular matrices[84,133,206]. The third triangle, known as the 'T-10' triangle, was also derived by Tocher. All 10 terms of the cubic polynomial were used and an internal degree of freedom was added to the triangle. This degree of freedom could be eliminated from the stiffness matrix by static condensation. It was found that the resulting stiffness matrices were too flexible and converged to incorrect values. The problem with this element is unique in the sense that it can satisfy the constant strain conditions but it cannot pass the patch test.

The fourth triangle presented by Clough and Tocher is conforming and marked the beginning of a method which Gallagher[83] has labelled as the 'subdomain approach'. To use this approach, a triangular element is subdivided into 3 subtriangles and independent displacement functions are chosen for each. Clough and Tocher used only 9 terms of the cubic function, but chose the local coordinates for each subtriangle in such a manner that geometric isotropy was preserved. They began with 27 degrees of freedom, but by imposing compatibility conditions at the nodes and along subtriangle boundaries, reduced the number of degrees of freedom to 9. This conforming triangle is known as the 'H C T' or Hsieh-Clough-Tocher element and has been found to be somewhat stiff. The excessive stiffness has been attributed to the constraint of linear variation of normal slopes between the nodes.

In 1968, Clough and Felippa[14] improved on this method by using all 10 terms of the cubic polynomial. In addition to obtaining a stiffness matrix for a triangular element, they also used 4 subtriangles to derive a conforming matrix for a quadrilateral. This element is one of the better plate bending quadrilaterals available and is still being used in the SAP4[24] computer program.

Several researchers have used the subdomain approach or variations of it. Elements derived by this approach are identified in Table 2.2 by showing the subtriangles within the element.

Instead of using the subdomain approach, a number of researchers devised 'single field' approaches[14]. Some of the elements resulting from these efforts are discussed below.

Bazeley et al.'s[25] approach of superimposing various shape functions was discussed in Section 2.1. Zienkiewicz[200] has labelled these types of displacement functions as 'conforming shape functions with nodal singularities'. The singularity refers to the fact that the second order derivatives or curvatures are not uniquely defined between elements. Because of this singularity, a high order of numerical integration is necessary to compute the stiffness matrix[200]. Bazeley et al.'s approach could probably be used to obtain shape functions which give results identical to Clough's subdomain approach, but in its present form it has not enjoyed the same usage.

A significant improvement to Bazeley's approach was presented by Irons and Razzaque[17],[44] through the use of 'substitute shape functions' and the 'smoothed derivative technique'. In a conforming element, the terms of the highest order complete polynomial govern the rate of convergence. Terms above this order are necessary for conformity, but these same terms are responsible for the excessive stiffness displayed by many conforming elements. The substitute shape functions replace the original functions but retain the same order of completeness and approximate the derivatives which appear in the stiffness matrix computations in a least squares sense[20]. The resulting elements are nonconforming and have convergence rates which parallel those of their conforming predecessors, but the new elements are much more accurate. A more detailed discussion is given in Chapter 11 of Zienkiewicz[20] and in Chapter 12 of Gallagher[4]. Two elements, a 9 and a 12 degree of freedom triangle, were derived by Razzaque and Irons and are included in Table 2.2.

Many attempts were made to get a single triangle to conform by using the complete cubic polynomial and an interior node. To obtain conformity, techniques ranging from constraint equations and Lagrangian multipliers to calculating of 'corrective matrices' have been used. A discussion of these approaches is given in Chapter 12 of Gallagher[4] and several of the resulting elements are included in Table 2.2.

To avoid the 9 degree of freedom triangle, some researchers reduced the number of nodal parameters to 6, while others kept on increasing the order of the polynomial. Some of the elements obtained from these various trials warrant mentioning.

The complete quadratic function with its 6 terms was used by Morley[134] to derive the 'constant moment triangle'. This triangle has 6 nodes and 6 degrees of freedom consisting of the transverse displacement at each vertex and a normal rotation at each midside node. Along element boundaries this element does not satisfy displacement continuity but it is able to meet all the conditions of equilibrium both internally and between elements. Therefore it can be derived from the complementary energy principle as an equilibrium element; this was done by Allman[4]. As well, the same element can be derived from a mixed method as was done by Herrmann[77]. Later the same stiffness matrix was obtained from a hybrid displacement method by Kikuchi and Ando[120] and from the hybrid stress approach by Yoshida[203]. The constant moment triangle in plate bending is analogous to the constant strain triangle in plane elasticity.

A discussion of triangular elements would not be complete without mentioning the quintic conforming triangle. The corner nodes of this element have 6 degrees of freedom consisting of the 3 geometric parameters plus the 3 curvatures. Since a complete quintic polynomial has 21 terms, midside nodes with the normal slope as a degree of

freedom were added to the element. The 21 degree of freedom matrix for this element was derived by Felippa[73], Withum[199], Bosshard[33], Argyris[15], Bell[24], and Irons[111]. Since the midside node does present an inconvenience, it can be eliminated by constraining the variation of the normal slope to be cubic. This was done independently and almost simultaneously by Cowper et al.[54], Argyris[13], Bell[28], and Butlin and Ford[34]. The resulting element has 18 degrees of freedom, is conforming, and gives results very similar to the 21 degree of freedom triangle[84]. These elements are often referred to as the 'T-21' and 'T-18' triangles. Continuing with higher order polynomials, Argyris used sextic and septic functions to complete his TUBA family[16]. This was followed by the work of Zenisek[205] who proposed and proved a general interpolation theorem for triangles of many orders.

The most recent elements are based on Mindlin plate theory and selective reduced integration. A triangular element based on the displacement method was presented in 1980 by Batoz and co-workers[23]. Also in 1980, Spilker[179] presented a series of 4-node hybrid stress quadrilaterals based on selective reduced integration and Mindlin plate theory.

The table which follows, presents all the elements discussed thus far and many more which have not received much coverage in the literature. An attempt has been made to present these in chronological order with rectangles

first and then the triangles and the quadrilaterals. An extensive list of references and bibliography is provided at the end of the text for the interested reader.

FINITE ELEMENT METHOD		VARIATIONAL PRINCIPLE	Assumed Functions inside the element	Along Interelement Boundaries	Unknowns in Final Equations	REFERENCES
DISPLACEMENT (Conforming)		Minimum Potential Energy	Continuous Displacements	Displacement Compatibility	Nodal Displacements	Courant(1943) Melosh(1963)
EQUILIBRIUM		Minimum Complementary Energy	Continuous and Equilibrating Stresses	Equilibrium Boundary Tractions	a) Generalized Displacements b) Stress Parameters	a) de Veubeke(1964) b) Morley(1967,68) Elias(1968)
HYBRID	HYBRID STRESS METHOD	Modified Complementary Energy	Continuous and Equilibrating Stresses	Assumed Compatible Displacements	Nodal Displacements	Pian(1964,1965)
	HYBRID DISPLACEMENT METHOD	Modified Potential Energy	Continuous Displacements	Assumed Compatible Displacements	Nodal Displacements	Tong(1970) Kikuchi & Ando(1972)
MIXED	REISSNER's PRINCIPLE	Reissner Method as modified by Herrmann	Continuous Stress and Displacement Functions	Combinations of Boundary Tractions and Displacements	Combinations of Displacements and Tractions	Herrmann(1965,1967) Pian & Tong(1969)
	GENERALIZED DISPLACEMENT METHOD	Modified Potential Energy	Continuous Displacements	Lagrangian multipliers (stresses)	Nodal Displacements and Lagrangian multipliers	Greene et al(1969) Anderheggen(1970) Harvey& Kelsey(1971)
	GENERALIZED EQUILIBRIUM METHOD	Modified Complementary Energy	Continuous and Equilibrating Stresses	Lagrangian multipliers (displacements)	Nodal Displacements and Lagrangian multipliers	Anderheggen(1969)

Table 2.1 Classification of Finite Element Methods.

ELEMENT	DESCRIPTION
1) 12 dof P 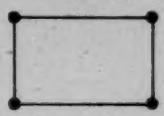	Displacement Type (Conforming) - Kirchhoff Plate Theory - Nodal dof= < W W,x W,y > - References: Papenfuss(1959), Clough and Tocher(1965) Bogner,Fox, and Schmit(1965) - used crossing-beam functions; twist term 'xy' omitted, erroneous convergence.
2) 12 dof A C M 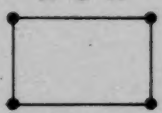	Displacement Type (Nonconforming) - Kirchhoff Plate Theory - Nodal dof= < W W,x W,y > - References: Adini and Clough(1960), Melosh(1963), Zienkiewicz and Cheung(1964),Dawe(1965) - 12 term polynomial(cubic and $x^3y + xy^3$) - Dawe also forms a consistent mass matrix.
3) 12 dof M 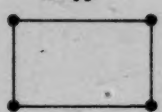	Displacement Type (Nonconforming) - Kirchhoff Plate Theory - Nodal dof= < W W,x W,y > - References: Melosh(1961) - cubic beam functions along edges with a linear variation to the opposite side.
4) 12 dof 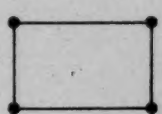	Hybrid Stress Type - Kirchhoff Plate Theory - Nodal dof= < W W,x W,y > - References: Pian(1964-68) - also stress-free edges, Severn and Taylor(1966), Henshell and co-workers(1972-73) - various combinations of W and M .
5) 16 dof BFS-16 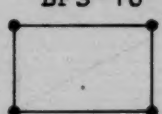	Displacement Type (Conforming) - Kirchhoff Plate Theory - Nodal dof= < W W,x W,y W,xy > - References: Bogner,Fox and Schmit(1965), Butlin and Leckie(1966), Hansteen(1966), Mason(1968).

Table 2.2 A Table of Existing Plate Elements.

ELEMENT	DESCRIPTION
6) 24 dof 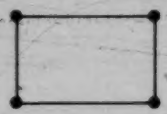	Displacement Type (Conforming) - Kirchhoff Plate Theory - Nodal dof=< W W,x W,y W,xx W,xy W,yy > - References: Bogner et al(1965)- Hermitian functions, Popplewell and MacDonald(1971), Gopalacharyulu(1973,1975)- quartic poly. Watkins(1974,1975)- blended Hermitians,
7) 36 dof	Displacement Type (Conforming) - Kirchhoff Plate Theory - Nodal dof= < W W,x W,y W,xx W,xy W,yy W,xxy W,xyy $W,xxyy$ > - References: Bogner,Fox and Schmit(1965).
8) 12 dof 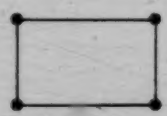	Displacement Type (Nonconforming) - Kirchhoff Plate Theory - Nodal dof= < W W,x W,y > - References: Dawe(1967)- modified the ACM polynomial to reduce the coefficients which were causing the W,n discontinuity.
9) 12 dof 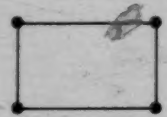	Mixed Type(Generalized Displacement Method) - Kirchhoff Plate Theory - Nodal dof= < W W,x W,y > - References: Greene,Jones,Mclay and Strome(1968,1969) Harvey and Kelsey(1971); (triangles). - Lagrangian multipliers are used at a global level to restore continuity.
10) 16 dof	Hybrid Stress Type - Kirchhoff Plate Theory - Nodal dof= < W W,x W,y W,xy > - References: Pian and Tong(1968), Pian(1973) - spurious energy modes may appear for this and other elements if assumed moments are linear - Pian & Mau(1972), Holand(1975).

ELEMENT	DESCRIPTION
11) 36 dof 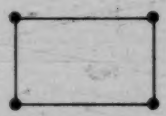	Displacement Type (Conforming) - Love's Moderateley Thick Plate Theory - Nodal dof= < W W,x W,y W,xx W,xy W,yy W,xxy W,xyy $W,xxyy$ > - References: Smith(1968), Smith and Duncan(1970) - also form a 24 dof rectangle by ignoring the last 3 nodal dof.
12) 12 dof 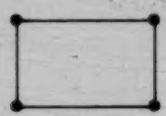	Hybrid Displacement Type(Simplified Method) - Kirchhoff Plate Theory - Nodal dof= < W W,x W,y > - References: Kikuchi and Ando(1972) - derived 4 rectangles and 4 triangles by using various displacement combinations, ('corrective' matrix enforces continuity)
13) 8 dof C M R 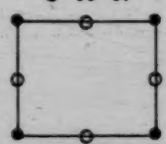 1 2	Hybrid Displacement Type - Kirchhoff Plate Theory - Node1 dof= < W > Node2 dof= < W,n or Mn > - References: Kikuchi and Ando(1972); (as above) Poceski(1975) - mixed method, - this is the 'Constant Moment Rectangle'.
14) 24 dof 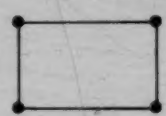	Displacement Type (Nonconforming) - Kirchhoff Plate Theory - Nodal dof=< W W,x W,y W,xx W,xy W,yy > - References: Wegmuller and Kostem(1972,1973) Wegmuller(1973) - complete quintic polynomial and the terms x^3y, x^3y^3, and xy^3.
15) 16 dof 1 2	Displacement Type (Discrete Kirchhoff) - Mindlin Plate Theory - Node1 dof= < W θx θy > Node2 dof= < θn > - References: (also a parallelogram) Razzaque(1972),Baldwin(1973),Irons(1976) - reduced 24 dof to 16 by using 8 discrete conditions at the Gauss points.

ELEMENT	DESCRIPTION
16) 16 dof 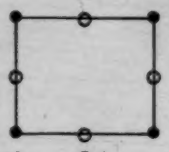 1 2	Displacement Type (Discrete Kirchhoff) - Mindlin Plate Theory - Node1 dof= < W θx θy > Node2 dof= < θn > - References; (also a quadrilateral) Baldwin,Razzaque and Irons(1973) - reduced 25 dof to 16 by using constraints at 8 Loof nodes and a perimeter integral.
17) 16 dof Semi-Loof 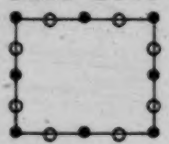 1 2	Displacement Type (Discrete Kirchhoff) - Mindlin Plate Theory - Node1 dof= < W > Node2 dof= < θn > , (Loof nodes) - References: Irons(1976), Martins and Owens(1978) - reduced 27 dof to 16 by using constraints at 8 Loof nodes and 3 area integrals.
18) 12 dof Bi.MPT 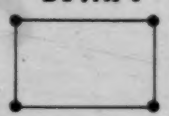	Displacement Type (Selective Integration) - Mindlin Plate Theory - Nodal dof= < W θx θy > - References: Pugh(1976), Pugh,Hinton and Zienk.(1978) Hughes,Taylor and Kanoknukulchai(1977) - bilinear displacement functions, - two spurious energy modes (Hughes1977-78)
19) 24 dof QSR	Displacement Type (Selective Integration) - Mindlin Plate Theory - Nodal dof= < W θx θy > - References:(Quadratic Serendipity Reduced Pugh(1976), Pugh,Hinton and Zienk.(1978) - basically the same as Ahmad's reduced integration plate element; may diverge or converge erratically (Pugh et al.1978)
20) 27 dof QLR	Displacement Type (Selective Integration) - Mindlin Plate Theory - Nodal dof= < W θx θy > - References: (Quadratic Lagrange Reduced) Pugh(1976), Pugh,Hinton and Zienk.(1978) - four spurious energy modes for S2x2 reduced integration, - can be mapped into a quadrilateral.

ELEMENT	DESCRIPTION
21) 36 dof CSR 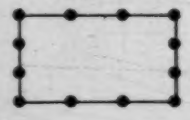	Displacement Type (Selective Integration) - Mindlin Plate Theory - Nodal dof= < W θx θy > - References: (Cubic Serendipity Reduced) Pugh(1976), Pugh,Hinton and Zienk.(1978) - no spurious energy modes for S3x3 reduced integration, but the element locks for S.S. and clamped plates (Pugh et al.1978)
22) 48 dof CLR 	Displacement Type (Selective Integration) - Mindlin Plate Theory - Nodal dof= < W θx θy > - References: (Cubic Lagrange Reduced) Pugh(1976), Pugh,Hinton and Zienk.(1978) - four spurious energy modes for S3x3 reduced integration.
23) 12 dof 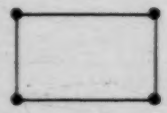	Displacement Type (Discrete Kirchhoff) - Mindlin Plate Theory - Nodal dof= < W θx θy > - References: Lyons(1977) - reduced 23 dof to 12 by using 8 Loof nodes and 3 shear integrals.
24) 16 dof 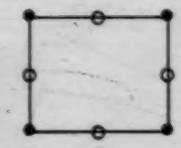 1 2	Displacement Type (Discrete Kirchhoff) - Mindlin Plate Theory - Node1 dof= < W θx θy > Node2 dof= < θn > - References: Lyons(1977) - reduced 27 dof to 16 by using 8 Loof nodes and 3 shear integrals.
25) 26 dof HETEROSIS 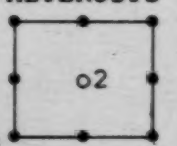 o2 1	Displacement Type (Selective Integration) - Mindlin Plate Theory - Node1 dof= < W θx θy > - Node2 dof= < θx θy > - References: (also 44 and 66 dof elments) Hughes(1978,1979) - Serendipity shape function for W and Lagrangian shape functions for θx and θy.

ELEMENT	DESCRIPTION
26) 12,24,36 dof 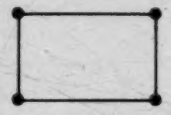	Hybrid Stress Type (Selective Integration) - Mindlin Plate Theory - Nodal dof= < W θx θy > - References: Spilker(1980) - derived matrices for thick and thin plate rectangles with 12, 24, and 36 dof, used Serendipity shape functions.
27) 12 dof LAGRANGE 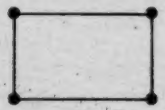	Displacement Type (Integral Kirchhoff) - Mindlin Plate Theory - Nodal dof= < W θx θy > - References: Hrudey and Hrabok(1981) - Kirchhoff normality conditions for thin plates are imposed in an integral sense by using Lagrangian multipliers.
28) 9 dof A (Adini) 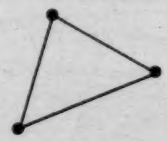	Displacement Type (Nonconforming) - Kirchhoff Plate Theory - Nodal dof= < W W,x W,y > - References: Adini(1961), Clough and Tocher(1965) - constant twist term 'xy' omitted; erroneous convergence (too stiff).
29) 9 dof T (Tocher) 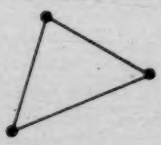	Displacement Type (Nonconforming) - Kirchhoff Plate Theory - Nodal dof= < W W,x W,y > - References: Tocher(1962), Clough and Tocher(1965) - combined x^2y and xy^2, - singular matrix encountered for certain shapes or orientations of the element.
30) 10 dof T-10 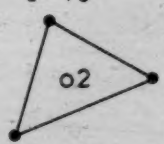	Displacement Type (Nonconforming) - Kirchhoff Plate Theory - Node1 dof= < W W,x W,y > Node2 dof= < W > - References: Tocher (1962), Clough and Tocher(1965) - element too flexible, does not pass the 'patch test'; can be reduced to 9 dof.

ELEMENT	DESCRIPTION
31) 9 dof H C T 	Displacement Type (Conforming) - Kirchhoff Plate Theory - Nodal dof= < W W,x W,y > - References: (Hsieh-Clough-Tocher element) Clough and Tocher(1965) - beginning of the 'subdomain approach', - 'geometric isotropy' preserved by special choice of axes; linear W,n enforced.
32) 9 dof B C I Z(nc) 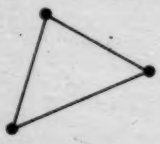	Displacement Type (Nonconforming) - Kirchhoff Plate Theory - Nodal dof= < W W,x W,y > - References: Bazeley,Cheung,Irons and Zienk.(1965) - introduced the use of 'area coordinates' to retain geometric isotropy; also begin the 'substitute shape function' approach.
33) 9 dof B C I Z(c) 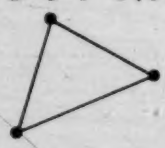	Displacement Type (Conforming) - Kirchhoff Plate Theory - Nodal dof= < W W,x W,y > - References: Bazeley,Cheung,Irons and Zienk.(1965) - as above, but corrective shape functions used to obtain conformity (very stiff), - requires very high order of integration.
34) 12 dof 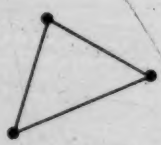	Mixed Type (modified Reissner Principle) - Reissner Plate Theory - Nodal dof= < W Mx My Mxy > - References: Herrmann(1965) Chatterjee and Setlur(1972) - assumed linear variation of W and M , - trial functions need only C^0 continuity.
35) 9 dof 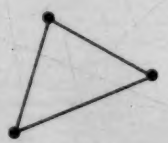	Displacement Type (Discrete Kirchhoff) - Mindlin Theory or (Thick Plate Theory - displacement functions for U, V, and W). - References: Melosh(1965),Utku(1967,71),Martin(1968) Wempner et al(1968), Dhatt(1969-70), Stricklin et al(1969), Fried(1973), Hinton et al(1975), Batoz et al(1980).

ELEMENT	DESCRIPTION
36) 9 dof 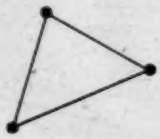	Equilibrium Type(Argyris' Natural Approach) - Kirchhoff Plate Theory - Nodal dof= < W W,x W,y > - References: Argyris(1965) - obtained a 6x6 flexibility matrix by using the Unit Load method.
37) 9 dof 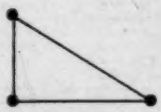	Hybrid Stress Type - Kirchhoff Plate Theory - Nodal dof= < W W,x W,y > - References: Severn and Taylor(1966) - assumed quadratic M and cubic W .
38) 21 dof T-21 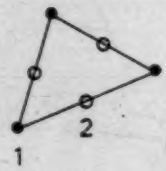	Displacement Type (Conforming) - Kirchhoff Plate Theory - Node1 dof=< W W,x W,y W,xx W,xy W,yy > - Node2 dof= < W,n > - References: Felippa(1966), Withum(1966) Argyris(1968), Bell(1968),Bosshard(1968) Visser(1968), Irons(1968) - used a complete quintic polynomial.
39) 6 dof C M T 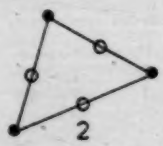	Methods : CONSTANT MOMENT TRIANGLE Displacement ; Morley(1971) Equilibrium ; Allman(1970) Hybrid Stress; Yoshida(1972) Hybrid Disp. ; Kikuchi and Ando(1972) Mixed ;Herrmann(1967),Hellan(1967) - Node1 dof= < W or Q > Node2 dof= < W,n or Mn >
40) 12 dof 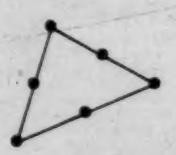	Equilibrium Type (Duality Approach) - Kirchhoff Plate Theory - Nodal dof= < Sx Sy > - References: Morley(1967,68), Sander(1970) - quadratic moment functions, - nodal parameters are the Southwell stress functions.

ELEMENT	DESCRIPTION
41) 9 dof 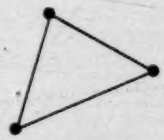	Hybrid Stress Type - Kirchhoff Plate Theory - Nodal dof= < W W,x W,y > - References Dungar,Severn and Taylor(1967), Allman(1970), Neale,Henshell and Edwards(1972), Yoshida(1972,1974), Batoz et al(1980).
42) 12 dof Lcct-12 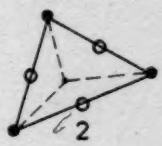	Displacement Type (Conforming) - Kirchhoff Plate Theory - Nodal dof= < W W,x W,y > - Node2 dof= < W,n > - References: Clough and Felippa(1968) -improved the subdomain approach by using a complete cubic and reducing 30 dof to 12.
43) 15 dof T-15 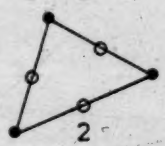	Displacement Type (Nonconforming) - Kirchhoff Plate Theory - Nodal dof= < W W,x W,y > - Node2 dof= < W W,n > - References: Bell(1968,1969) Chu and Schnobrich(1972) - used complete quartic shape functions.
44) 9 dof C P T 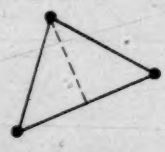	Displacement Type (Non-Conforming in W) - Kirchhoff Plate Theory - Nodal dof= < W W,x W,y > - References: Connor and Will(1968) - discarded the x^2y term, conforming in W,n but not in W along one of the sides, - used in the STRUDL2 computer program.
45) 12 dof L M T 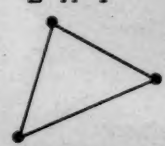	Equilibrium Type - Kirchhoff Plate Theory - Nodal dof= < W > - Side dof= < averaged integral value of W and 2 weighted edge rotations > - References: (Linear Moment Triangle) de Veubeke and Sander(1968), Somervaille(1974)-also presented Q M T.

ELEMENT	DESCRIPTION
46) 9 dof 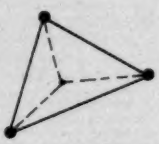	Displacement Type (Conforming) - Kirchhoff Plate Theory - Nodal dof= < W W,x W,y > - References: Shieh et al(1968) - used a quadratic function and reduced 18 dof to 9 dof, element cannot satisfy interior displacement comptability.
47) 18 dof T-18 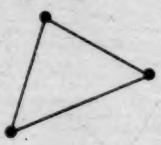	Displacement Type (Conforming) - Kirchhoff Plate Theory - Nodal dof=< W W,x W,y W,xx W,xy W,yy > - References: Cowper et al(1968), Argyris(1968), Butlin and Ford(1968), Bell(1968-69) - derived from T-21 triangle by imposing a a cubic variation of W,n .
48) 21 dof TUBA-6 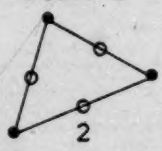	Displacement Type (Conforming) - Kirchhoff Plate Theory - Node1 dof= < W W,x W,y W,xx W,xy W,yy > Node2 dof= < W,n > - References: Argyris(1968) - identical to T-21, -complete quintic displacement polynomial, element has 6 nodes and 21 dof.
49) 28 dof TUBA-13 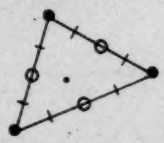	Displacement Type (Conforming) - Kirchhoff Plate Theory - Node1 dof= < W W,x W,y W,xx W,xy W,yy > Nodei dof= various dof at remaining nodes - References: Argyris(1968) -complete sextic displacement polynomial, element has 13 nodes and 28 dof.
50) 36 dof TUBA-15 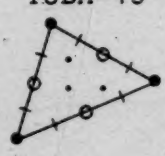	Displacement Type (Conforming) - Kirchhoff Plate Theory - Node1 dof= < W W,x W,y W,xx W,xy W,yy > Nodei dof= various dof at remaining nodes - References: Argyris(1968), Zenisek(1970) -complete septic displacement polynomial, element has 15 nodes and 36 dof.

ELEMENT	DESCRIPTION
51) 6 dof 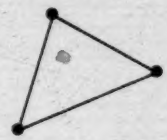	Equilibrium Type - Kirchhoff Plate Theory - Nodal dof= < Sx Sy > - References: Elias(1968), Sander(1970) - nodal parameters are Southwell functions, - assumed linear moment functions.
52) 12 dof 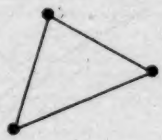	Mixed Type (Herrmann's Method) - Reissner Plate Theory - Nodal dof= < W Mx My Mxy > - References: Visser(1969), Boot(1978) - 9 dof obtainable by static condensation, - parabolic variation of W and a linear variation of M .
53) 18 dof 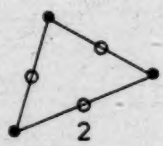	Displacement Type (Conforming) - Kirchhoff Plate Theory - Node1 dof= < W W,x W,y > Node2 dof= < W W,n W,nt > - References: Irons(1969) - used all 15 terms of a quartic plus 3 basic or 'singularity' functions.
54) 24 dof 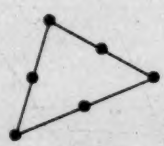	Mixed Type(Generalized Equilibrium Method) - Linear Stress Variation across thickness - Nodal dof= < Mx My Mxy > - Side dof= < 2 Lagrange multipliers to restore shear continuity > - References: Anderheggen(1969), Meek(1975)
55) 9 dof 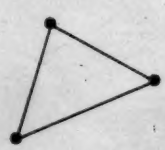	Hybrid Stress Type - Kirchhoff Plate Theory - Nodal dof= < W W,x W,y > - References: Dungar and Severn(1969), - various combinations of M and W, - variable thickness, also triangles with stress-free edges, and hybrid beams.

ELEMENT	DESCRIPTION
56) 9 dof 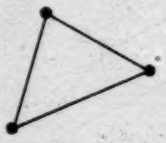	Hybrid Displacement Type - Kirchhoff Plate Theory - Nodal dof= < *W* *W*,x *W*,y > - References: Hansteen(1969),Yoshida(1972),Allman(1976) - Allman's cubic *W* for interior and edges is identical to a stress hybrid with cubic *W* and linear *M* .
57) 12 dof 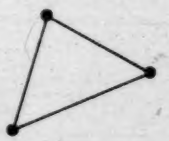	Mixed Type(Generalized Displacement Method) - Kirchhoff Plate Theory - Nodal dof= < *W* *W*,x *W*,y > - Side dof= < weighted average of *M*n (used to restore interelement continuity)> - References: Anderheggen(1970) - complete cubic, one dof is integral of *W*
58) 12 dof 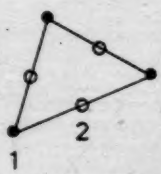	Hybrid Stress Type - Kirchhoff Plate Theory - Node1 dof= < *W* *W*,x *W*,y > Node2 dof= < *W*,n > - References: Allman(1970), Bartholomew(1976) - element with linear *M* and cubic *W* is identical to Razzaque's 'A-12'.
59) 9,10 dof 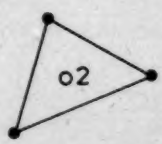	Mixed Type(Generalized Displacement Method) - Kirchhoff Plate Theory - Node1 dof= < *W* *W*,x *W*,y > - Node2 dof= < *W* >, can be condensed out. - References: Harvey and Kelsey(1971), Meek(1975) - Lagrangian multipliers restore continuity at a global level, similar to Anderheggen
60) 12 dof 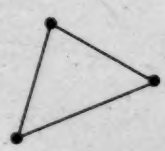	Mixed Type (Herrmann's Method) - Reissner Plate Theory - Nodal dof= < *W* *Mx* *My* *Mxy* > - References: Tahiani(1971) Bron and Dhatt(1972)

ELEMENT	DESCRIPTION
61) 24 dof 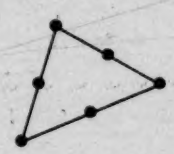	Mixed Type (Herrmann's Method) - Reissner Plate Theory - Nodal dof= < *W* *Mx* *My* *Mxy* > - References: Tahiani(1971) Bron and Dhatt(1972)
62) 9 dof 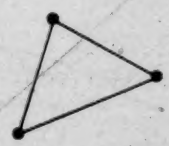	Displacement Type (Nonconforming) - Kirchhoff Plate Theory - Nodal dof= < *W* *W*,x *W*,y > - References: Irons and Razzaque(1972-73) - used 'derivative smoothing' and 'substitute shape functions', - identical results to Allman(1970) hybrid.
63) 12 dof 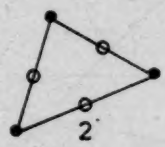	Displacement Type (Conforming) - Kirchhoff Plate Theory - Node1 dof= < *W* *W*,x *W*,y > Node2 dof= < *W*,n > - References: Irons and Razzaque(1972-73) - used 'derivative smoothing' but element identical to Allman's(1970) stress hybrid
64) 9 dof 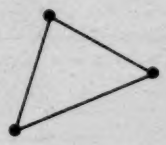	Hybrid Displacement Type(Simplified Method) - Kirchhoff Plate Theory - Nodal dof= < *W* *W*,x *W*,y > - References: Kikuchi and Ando(1972) - used a complete cubic and a 'corrective matrix' to derive 4 rectangles and 4 triangles.
65) 33 dof 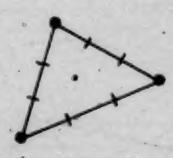	Displacement Type (Conforming) - Kirchhoff Plate Theory - Node1 dof=< *W* *W*,x *W*,y *W*,xx *W*,xy *W*,yy > Nodei dof= various dof at remaining nodes - References: Svec and Gladwell(1973) - similar to TUBA-15 but reduced to 33 dof, - 10 node element used for contact problems

ELEMENT	DESCRIPTION
66) 9 dof 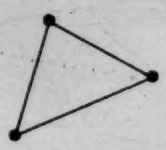	Hybrid Stress Type - Love's Plate Theory - Nodal dof= < W W,x W,y > - References: Cook(1972-74) - various aspects of the hybrid stress method; emphasis on transverse shear, - also formed quadrilaterals from triangles
67) 9 dof 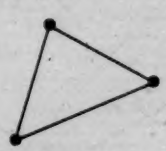	'Direct Approach' - Kirchhoff Plate Theory - Nodal dof= < W W,x W,y > - References: Bergan and Hanseen(1975) - not based on any variational principle but must satisfy constant strain states and pass the 'patch test'.
68) 8 dof 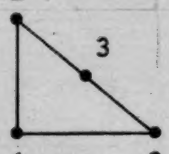	Mixed Type (modified Herrmann's method) - Kirchhoff Plate Theory - Node1 dof= < W Mx My >, Node2 dof= < W Mn >, Node3 dof= < W > ,(linear M along 2-2) (constant M along 1-2) - References: Poceski(1975) - stress polys. partly dependent on disps.
69) 12 dof 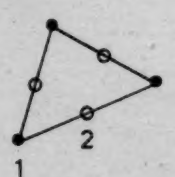	Displacement Type (Conforming) - Kirchhoff Plate Theory - Node1 dof= < W W,x W,y > Node2 dof= < W W,x W,y W,nt > - References: Caramanlian, Selby and Will(1978)
70) 9 dof 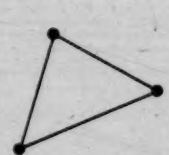	Displacement Type (Selective Integration) - Mindlin Plate Theory - Nodal dof= < W θx θy > - References: Batoz,Bathe and Ho(1980) - a study of 9 dof triangles which included conventional disp., hybrid stress, and discrete Kirchhoff elements.

ELEMENT	DESCRIPTION
71) 12 dof Rhombics 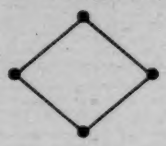	Methods: Displacement ; Sander(1970) Equilibrium ; Sander(1970) Hybrid Stress; Wolf(1973) - Nodal dof= < W W,x W,y > - References: Pian(1973)
72) 12 dof 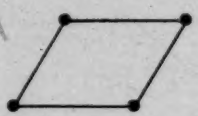	Displacement Type(Argyris' Natural Method) - Kirchhoff Plate Theory - Nodal dof= < W W,x W,y > - References: Argyris(1965) - derived 9x9 'natural flexibility matrix' from which the 12x12 stiffness matrix was obtained.
73) 12 dof 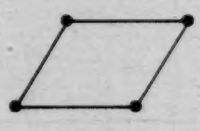	Displacement Type (Nonconforming) - Kirchhoff Plate Theory - Nodal dof= < W W,x W,y > - References: Dawe(1966), Ramstad and Holland(1966), Ramstad(1967) - Dawe uses the ACM polynomial in an oblique coordinate system.
74) 16 dof 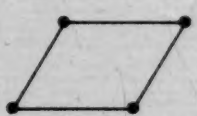	Displacement Type (Conforming) - Kirchhoff Plate Theory - Nodal dof= < W W,x W,y W,xy > - References: Granheim(1968)
75) 12,24,36 dof	Equilibrium Type (Duality Approach) - Kirchhoff Plate Theory - Nodal dof= < Sx Sy > - References: Sander(1970) - derived a family of equilibrium linear, quadratic, and cubic parallelograms and triangles (also sub- and hyper- elements)

ELEMENT	DESCRIPTION
76) 16 dof CQ-16 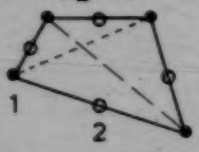 	Displacement Type (Conforming) - Kirchhoff Plate Theory - Node1 dof= < W W,x W,y > Node2 dof= < W,n > - References: Sander(1964), de Veubeke(1965,1968) - 12 dof quad. may be obtained by imposing a linear variation of normal slopes.
77) 12 dof 	Displacement Type (Conforming) - Kirchhoff Plate Theory - Nodal dof= < W W,x W,y > - References: Clough and Felippa(1968) - the quadrilateral used in the SAP4 computer program.
78) 24 dof 	Displacement Type (Conforming) - Kirchhoff Plate Theory - Nodal dof=< W W,x W,y W,xx W,xy W,yy > - References: Clough and Felippa(1968)
79) 16 dof 	Mixed Type(Generalized Displacement Method) - Kirchhoff Plate Theory - Nodal dof= < W W,x W,y > - References: Greene,Jones,Mclay and Strome(1968,1969) - used Lagrangian multipliers to restore continuity at a global level.
80) Polygons 	Hybrid Stress Type - Kirchhoff Plate Theory - Nodal dof= < W W,x W,y > - References: Allwood and Cornes(1969) - reported results for work done on polygons with 3 to 9 sides.

ELEMENT	DESCRIPTION
81) 24 dof	Displacement Type (C° Conformity) - Ahmad's quadratic thick shell element. - Nodal dof= < W θx θy > - References: Ahmad,Irons and Zienkiewicz(1968,1970) - a plate element obtained from a degenerated solid, found to be too stiff for thin plates.
82) 24 dof 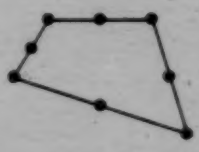	Displacement Type (Selective Integration) - Ahmad's shell element underintegrated. - Nodal dof= < W θx θy > - References: Pawsey and Clough(1971) Zienkiewicz,Taylor and Too(1971) - both 'selective' and 'uniform' reduced integration used to soften the element.
83) 12,24,36 dof	Mapping of Rectangles to Quadrilaterals. - Kirchhoff Plate Theory - Nodal dof= < W W,x W,y > - References: Henshell,Walters and Warburton(1972) - a quadrilateral can be obtained from a rectangle by a transformation of coordinates, but the constant curvature states may be destroyed (Zienkiewicz1977)
84) 16 dof	Mixed Type (Herrmann's Method) - Reissner Plate Theory - Nodal dof= < W Mx My Mxy > - References: Bron and Dhatt(1972) - linear W and linear M.
85) 24 dof	Mixed Type (Herrmann's Method) - Reissner Plate Theory - Nodal dof= < W Mx My Mxy > - References: Bron and Dhatt(1972) - quadratic W and quadratic M.

ELEMENT	DESCRIPTION
86) 12 dof	Hybrid Stress Type - Kirchhoff Plate Theory - Nodal dof= < W W,x W,y > - References: Torbe and Church(1975) - also derived the in-plane matrices.
87) 24 dof	Hybrid Displacement - Trefftz's Principle - Kirchhoff Plate Theory - Nodal dof=< W W,x W,y W,xx W,xy W,yy > - References: Jirousek and Leon(1977) - independent disp. functions for interior and perimeter; attempt to satisfy the differential equations of equilibrium.
88) 9 dof	Hybrid Stress Type (Selective Integration) - Mindlin Plate Theory - Nodal dof= < W θx θy > - References: Spilker(1980) - derived a series of 4-node quadrilaterals - also derived Serendipity quadratic and cubic elements for thick plates.

Chapter 3

EVALUATION AND TESTING OF ELEMENTS

3.1 Selection Criteria for Test Elements

From the literature review of the preceding chapter, it is obvious that there is a bewildering number of elements from which to choose. However, the intent of this research project is to develop a program for practical use and this will eliminate a considerable number of elements. The factors considered to be important for the selection process will be dealt with shortly. The property of conformity is felt to be of secondary importance and is not used in the selection of candidate elements.

As well, to aid in the search for the 'best' element, there exist a number of studies where various plate bending elements have been compared. The findings of two of these studies, one by Smith and Duncan[7,8] and the other by Abel and Desai[1], are thought to be particularly useful and will also be discussed.

The first selection criterion is that only the transverse displacement, W, and the two rotations, θx and θy, will be used as nodal degrees of freedom. These nodal parameters are often referred to as the 'engineering', 'geometric' or 'basic' degrees of freedom. Elements which have nodal parameters consisting of second and higher order derivatives of W have been labelled as elements with

excessive nodal continuities'[78],[204]. The terminology stems from the fact that in a displacement formulation based on classical plate theory the variational principle requires only C' continuity. In this chapter the phrase 'higher order parameters' will be used interchangeably with 'excessive nodal continuities'. The reasons for not using higher order parameters as nodal degrees of freedom are discussed in the following paragraphs.

A study by Smith and Duncan'[78] compared displacements and moments versus the number of unknowns for four different rectangular and parallelogram shaped elements. The four elements were the nonconforming A C M element, the Bogner, Fox and Schmit 16 and 36 degree of freedom conforming rectangles, and Smith's 24 degree of freedom rectangle. More information on these elements is contained in Table 2.2. Smith and Duncan formulated the stiffness matrices in terms of skew coordinates and analysed rhombic plates with various angles of skew. They concluded that for thin plate flexure there was no substantial improvement in using elements with excessive nodal continuities. This is one of the reasons for not insisting that the higher order degrees of freedom be used as nodal parameters. At the same time, however, it is necessary to mention that elements such as the T-18 triangles with curvatures as degrees of freedom are capable of providing very accurate results.

A second reason for choosing only the geometric parameters is that each degree of freedom of the structure

physically represents a displacement or load quantity which can easily be visualized. This makes it easier for a designer to specify the kinematic boundary conditions and the loading and later to interpret the results.

A third reason is that in some structures the higher order parameters are not continuous. For example, in a beam or plate with an abrupt change in cross section or moment of inertia, equilibrium requires that the bending moment remains continuous. If the member is homogeneous then the bending curvature cannot be continuous. This causes problems for elements with excessive nodal continuities. The problem can be resolved by using discontinuous degrees of freedom, but this is undesirable because it causes inconveniences in the modelling of the structure and increases the total number of unknowns.

A similar problem arises when coupling adjoining plate elements at such locations as corners of columns. The problem can again be rectified by using discontinuous degrees of freedom, but this has the same disadvantages as discussed in the above paragraph.

Another complication with the higher order parameters arises when coupling eccentric beam or plate elements to the main plate. The geometric degrees of freedom are zero and first order tensors in the X-Y plane, and, as such, have translational and rotational transformations which are simple to obtain because the coupling action between the degrees of freedom can be visualised. The same is not true

for the higher order nodal parameters where it is difficult to decide which degrees of freedom are coupled to which.

For the reasons discussed above, elements with excessive nodal parameters were eliminated in the preliminary selection process.

The second selection criterion deals with the number of nodes per element and the degrees of freedom at these nodes. For convenience of use and versatility in coupling beams to plates, any element without the same set of nodal parameters at each node is undesirable. This eliminates a large number of plate bending elements which have nodal parameters such as '*W*' and '*W*,n' at midside or interior nodes. Most higher order elements are of this type and therefore, after the second selection criterion is applied, most of the elements which remain are of the simple type with corner nodes only. Evidence to show that simple elements are not necessarily inferior to the higher order elements was presented by Abel and Desai' in 1972.

Abel and Desai did a displacement accuracy study and used 12 different elements to analyse simply supported and fixed square plates subjected to central point loads. The elements included the A C M and M rectangles, the H C T triangle, Clough and Felippa's triangle and quadrilateral, de Veubeke's displacement conforming quadrilateral and equilibrium triangle, Anderheggen's mixed method with equilibrium triangles, Elias' equilibrium triangle, Argyris' Tuba-6 triangle, the BFS-16 rectangle and Severn and

Taylor's hybrid stress rectangle. Details on these elements can be found in Chapter 2 and Table 2.2.

For all the cases, quadrilaterals or an equivalent assemblage of triangles were used. Abel and Desai compared displacement accuracy versus NB^2, where 'N' is the total number of unknowns and 'B' is the semi-band width. Their graphs indicate that the M rectangle is the best overall element and that the more complicated elements are really not superior to the simple rectangles.

Abel and Desai's, and Smith and Duncan's studies do not consider the work required to obtain the element matrix, but their comparisons are much more valid than most studies which simply compare displacements versus the number of elements. The latter type of comparison definitely favors the higher order elements.

The result of applying the two selection criteria is that the candidate elements must have nodes with only the 3 geometric degrees of freedom as nodal parameters. At this point it was decided to use rectangular elements for the evaluation. The reasons for making this choice are discussed in the paragraphs which follow. The test cases which were used are described in the next section.

The decision to use rectangular elements was based on two main considerations. First, most floor plans in practise can be represented almost entirely by a rectangular gridwork. This type of grid is desirable because it simplifies the operations of automatic mesh generation for

input data, post-processing of the solution data and production of graphical output. Second, for the simpler type of elements being considered here, rectangular elements usually provide better results than an equivalent number of triangles. This is to be expected of the displacement elements where the interpolation polynomials for a rectangle are usually of a higher order than for a triangle, but it has also been found to be true for other methods[11],[20]. Therefore, wherever possible, the use of rectangular elements is preferred.

Using the guidelines established thus far, it was decided to use the following rectangles in the evaluation:

(a) The well known A C M rectangle based on a displacement formulation and Kirchhoff plate theory. The displacement function for this element is a twelve-term polynomial consisting of a complete cubic and two quartic terms. The element is nonconforming. It was discussed in Chapter 2 and appears as element (2) in Table 2.2.

(b) A hybrid stress element similar to that initially developed by Pian and later by Severn and Taylor. The element has 12 displacement degrees of freedom and its derivation is based on a modified complementary potential energy principle and Kirchhoff plate theory. The internal bending moments are represented by complete quadratic polynomials, while along the element edges the transverse displacement and the normal rotation are represented by cubic and linear polynomials respectively. This element is listed as element (4) in Table 2.2.

(c) The element referred to as the Bi.MPT element in this study. This is a bilinear displacement element based on minimum potential energy, Mindlin plate theory and selective reduced integration. It appears as element (18) in Table 2.2. The flexural strain energy is evaluated exactly using a 2x2 order of Gauss integration while the shear strain energy is underintegrated by using a 1x1 Gauss order. The shear strain energy is purposely underintegrated to prevent 'locking'[8]. This

element was introduced by Hughes et al.[9] in 1977 and was quoted as being 'the simplest effective plate bending element yet proposed' and described as being 'highly efficient' and 'surprisingly accurate'.

(d) The fourth element of this study does not meet the requirement of having the same degrees of freedom at all nodes. However, the so-called 'heterosis' element developed in 1978 by Hughes and Cohen[8] is included because it looks sufficiently promising and has been highly recommended by Hughes. This element is listed as member (25) of Table 2.2. It is a higher order displacement element based on Mindlin plate theory and selective reduced integration. The element has nine nodes and uses Serendipidty shape functions for the transverse displacement, while Lagrangian shape functions are used for the rotations. The flexural strain energy is evaluated exactly using a 3x3 Gauss order of integration, while the shear strain energy is underintegrated by using a 2x2 order.

(e) The fifth and last element is a 12 degree of freedom displacement element where independent shape functions have been used to describe the transverse displacement and the rotations. Lagrangian multipliers are then used to impose the Kirchhoff conditions of normality. This element appears as member (27) in Table 2.2 and for lack of a better name is referred to as the 'Lagrange' element. The details of its derivation are given in Appendix A.

Details of the element evaluations are contained in the next section.

After this work was completed, the results of a similar study were published in 1980 by Batoz, Bathe and Ho[23]. However, the work of Batoz et al. deals only with basic 9 degree of freedom triangular elements and therefore, can be considered as being complementary to this study on rectangles.

3.2 Test Cases and Results

Four test plates were chosen for the element evaluations. The test cases were categorized according to the following sets of boundary conditions:

(1) Simply supported edges.

(2) Clamped edges.

(3) Corners simply supported and edges free.

(4) Corners clamped and edges free to displace but with zero normal slopes. In practise, this test case could represent a typical interior panel of a floor system.

Only square plates were used and each plate was analysed using 4 different finite element gridworks. The loading conditions for each plate consisted of a uniformly distributed load and a central point load. A sketch of the plate and a typical 4x4 grid are shown in Figure 3.1. For all cases, the plate was assumed to be isotropic and a Poisson's ratio of 0.30 was used.

The results of the analyses are presented in Tables 3.1 to 3.6 and in Figures 3.2 to 3.9. Numerical comparisons of deflections and moments for the four test cases and both load cases are presented in Tables 3.1 to 3.4. The deflections are those calculated at the centre of the plate. The location of the moments is indicated in the tables. The normalized values of these moments are shown in Tables 3.5 and 3.6. Graphs of 'displacement error' versus 'number of unknowns' on logarithmic axes are presented in Figures 3.2 to 3.9. Although the graphs and tables are for the most

part self-explanatory, the following information may be of interest.

The ratio of plate side dimension to the thickness (L/t) is 100, except for the Bi.MPT and heterosis elements. In an attempt to reduce the effects of shear deflections, values of 10^3 were initially used for the Bi.MPT element and 10^4 for the heterosis element. These were the upper limits of plate slenderness as recommended by Hughes et al.[99] for the Bi.MPT element and by Hughes and Cohen[98] for the heterosis element. For larger L/t values, the element matrices may be expected to degenerate numerically due to the overwhelming shear stiffness. To confirm that these limits were acceptable, the test cases were run for both elements using L/t values of 10^3, 10^4, and 10^5. For the heterosis element the ratio of 10^4 was also used. A comparison of the displacements from each of the L/t values revealed that numerical deterioration was evident for both elements for L/t ratios greater than 10^4. This was especially true for the finer grids. Based on these comparisons, it was decided to use $L/t=10^4$ for both the Bi.MPT and the heterosis element.

A second point of interest is the behavior of the Bi.MPT element for the last two test cases as indicated in Tables 3.3 and 3.4. For these applications, the Bi.MPT element matrix is almost singular and the results become very erratic, alternating between extremely large positive and negative numbers. The same problem was encountered by

Hughes et al.[10] when they attempted to analyse a pergola type structure supported at its centre by a single node.

The singular element matrix is caused by a 'spurious' or false zero-energy mode. A spurious energy mode is a deformed shape of the element which has zero strain energy. It occurs as a result of the low order of integration and usually does not appear for the structure as a whole because it has been eliminated by the kinematic boundary conditions and the assembly procedure. For the Bi.MPT element, Hughes and co-workers[10],[17] identify two such modes. One is an in-plane constant twist mode while the other is a *W*-hourglass mode. It is interesting to note that if the flexural strain energy had also been underintegrated, then the element would have four spurious energy modes. For structures which have only one suppressed transverse displacement, the *W*-hourglass mode is the spurious energy mode causing the singularity problem. Hughes et al.[10] have overcome this problem by suppressing additional transverse displacements. This type of remedial work was not done in the present study.

3.3 Discussion of Results and Conclusions

With the aid of the tables and graphs of the previous section, the process of element selection may begin. This is done in the following paragraphs by a process of successive elimination.

The first element to be eliminated is the heterosis element. A comparison of displacement accuracy versus number of unknowns in Figures 3.2 to 3.9 indicates that this element is not superior to the simpler elements. It is expected that a comparison based on NB^2 would make the element look even less favorable.

A second reason for not using the heterosis element is the presence of the centre node which does not have the same nodal parameters as the remaining nodes. Although the centre degree of freedom can be eliminated by static condensation, this does require additional computation and a modification to the work equivalent load vector. It is felt that this is not worth the effort because better elements exist.

The next element to be eliminated is the Bi.MPT element. Although the element provides good results for the first two test cases, it encounters difficulties with singular matrices for the last two. To obtain solutions for problems similar to the last two test cases, it is necessary to provide artificial constraints to suppress more transverse displacements. This complication is a feature which precludes its use in a practical analysis program. The Bi.MPT element is eliminated mainly for this reason, and also because it does not exhibit behavior superior to some of the other elements.

The third element to be eliminated is the Lagrange element. From the graphs in Figures 3.2 to 3.9, it can be

observed that this element's behavior is very similar to that of the A C M element. However, obtaining the stiffness matrix for the Lagrange element requires significantly more computational effort and therefore it is abandoned in favor of the A C M element.

The final choice is to be made between the A C M and the hybrid stress element. After studying the tables and graphs of displacements, it is clear that the hybrid element is the better overall element. A similar comparison of Tables 3.5 and 3.6 indicates that the same statement is again true for the stress resultants. In addition to the satisfactory performance of the element, there are two other factors which strongly influence the decision to use the hybrid stress method.

One factor is the ease with which stiffness matrices for nonrectangular shapes can be derived by this method. These special shapes will be required in situations where rectangular elements are not capable of modelling the geometry of the structure. The second factor is the capability of the method to include the effects of stress singularities in the formulation of the element matrix. These two factors, together with the accuracy demonstrated earlier, indicate that the hybrid stress method appears to be ideally suited for the analysis of flat plates. Thus it was decided to use the hybrid stress formulation for the remainder of this investigation. The chapters which follow deal solely with the theory and use of this method.

Uniform Load:

Deflection = Coefficient *(qL⁴/D)/1000					
Grid	A C M	Hybrid	Bi.MPT	Heterosis	Lagrange
2x2	5.06323	3.90625	3.18878	3.82544	4.88769
4x4	4.32819	4.05156	3.96899	4.02407	4.29079
8x8	4.12928	4.06166	4.04142	4.05473	4.12080
16x16	4.07910	4.06231	4.05721	4.06095	4.07703
Timoshenko (Navier's solution, 25 terms): 4.062353					
Moment(centre) = Coefficient * qL²/100					
Grid	A C M	Hybrid	Bi.MPT	Heterosis	Lagrange
2x2	6.602	4.906	3.316	-	-
4x4	5.217	4.827	4.771	-	-
8x8	4.892	4.799	4.790	-	-
16x16	4.814	4.791	4.789	-	-
Timoshenko (Levy's solution, 5 terms): 4.7886					

Central Point Load:

Deflection = Coefficient *(PL²/D)/1000					
Grid	A C M	Hybrid	Bi.MPT	Heterosis	Lagrange
2x2	13.7841	10.4498	12.7551	10.5131	12.9940
4x4	12.3272	11.3819	11.5093	11.3808	12.1528
8x8	11.8285	11.5514	11.5382	11.5464	11.7805
16x16	11.6694	11.5888	11.5786	11.5873	11.6560
Timoshenko (Navier's solution, 250 terms): 11.60083					
Twisting Moment(corners) = Coefficient * P /100					
Grid	A C M	Hybrid	Bi.MPT	Heterosis	Lagrange
2x2	7.008	5.768	7.144	-	-
4x4	6.440	6.484	6.840	-	-
8x8	6.212	6.192	6.296	-	-
16x16	6.128	6.120	6.140	-	-
Timoshenko (Levy's solution, 10 terms): 6.0953					

Table 3.1 Deflection and Moment Comparisons – Square Plate with Simply Supported Edges.

Uniform Load:

Deflection = Coefficient *(qL⁴/D)/1000					
Grid	A C M	Hybrid	Bi.MPT	Heterosis	Lagrange
2x2	1.47964	1.33501	0.00357	1.54093	1.25313
4x4	1.40334	1.23884	1.21124	1.23449	1.37122
8x8	1.30394	1.26009	1.25069	1.25722	1.29813
16x16	1.27518	1.26454	1.26165	1.26368	1.27388
Timoshenko (coefficient method, 20 equations): 1.265319					
Moment(centre) = Coefficient * qL²/100					
Grid	A C M	Hybrid	Bi.MPT	Heterosis	Lagrange
2x2	4.616	3.394	0.	-	-
4x4	2.778	2.250	2.519	-	-
8x8	2.405	2.295	2.331	-	-
16x16	2.319	2.292	2.300	-	-
Timoshenko (coefficient method, 20 equations): 2.3067					

Central Point Load:

Deflection = Coefficient *(PL²/D)/1000					
Grid	A C M	Hybrid	Bi.MPT	Heterosis	Lagrange
2x2	5.91856	5.34006	0.01429	6.16371	5.01253
4x4	6.13445	5.34963	4.84496	5.38977	5.95282
8x8	5.80257	5.55001	5.40373	5.55149	5.75670
16x16	5.67214	5.59801	5.55464	5.59683	5.65961
Timoshenko (coefficient method, 20 equations): 5.612017					
Moment(midside)= Coefficient * P /100					
Grid	A C M	Hybrid	Bi.MPT	Heterosis	Lagrange
2x2	14.20	14.48	0.0	-	-
4x4	11.78	12.85	7.75	-	-
8x8	12.33	12.61	9.16	-	-
16x16	12.50	12.57	10.54	-	-
Timoshenko (coefficient method, 20 equations): 12.5775					

Table 3.2 Deflection and Moment Comparisons – Square Plate with Clamped Edges.

Uniform Load:

Deflection = Coefficient *(qL⁴/D)/1000					
Grid	A C M	Hybrid	Bi.MPT	Heterosis	Lagrange
2x2	21.7898	25.4618	*	27.6998	21.8228
4x4	24.2956	25.5035	erratic	25.9715	24.3000
8x8	25.1778	25.5058	results	25.6244	25.1924
16x16	25.4219	25.5064	*	25.5374	25.4335
(Marcus:24.87), (Galerkin:26.48), (Lee&Ballesteros:26.48)					
Moment(centre) = Coefficient * qL²/100					
Grid	A C M	Hybrid	Bi.MPT	Heterosis	Lagrange
2x2	11.75	11.07	*	-	-
4x4	11.55	11.23	erratic	-	-
8x8	11.27	11.18	results	-	-
16x16	11.20	11.17	*	-	-
(Marcus:10.90), (Galerkin:11.09), (Lee&Ballesteros:11.04)					

Central Point Load:

Deflection = Coefficient *(PL²/D)/1000					
Grid	A C M	Hybrid	Bi.MPT	Heterosis	Lagrange
2x2	34.7041	38.9753	*	41.7874	34.7085
4x4	37.8161	38.9978	erratic	39.5096	37.7582
8x8	38.8260	39.0965	results	39.2225	38.8149
16x16	39.0718	39.1301	*	39.1622	39.0753
Moment(midside)= Coefficient * P /100					
Grid	A C M	Hybrid	Bi.MPT	Heterosis	Lagrange
2x2	20.96	20.26	*	-	-
4x4	19.87	20.86	erratic	-	-
8x8	20.34	20.42	results	-	-
16x16	20.29	20.33	*	-	-

Table 3.3 Deflection and Moment Comparisons – Square Plate with Simply Supported Corners.

Uniform Load:

Deflection = Coefficient *(qL⁴/D)/1000					
Grid	A C M	Hybrid	Bi.MPT	Heterosis	Lagrange
2x2	5.20833	5.20833	*	5.20834	5.20834
4x4	5.78512	5.67104	erratic	5.75558	5.72883
8x8	5.84288	5.75616	results	5.77021	5.81898
16x16	5.82276	5.78871	*	5.79110	5.81516
Bares (series solution): 5.81					
Moment = Coefficient * qL²/100					
Grid	A C M	Hybrid	Bi.MPT	Heterosis	Lagrange
2x2	2.780	1.809	*	-	-
4x4	3.712	3.854	erratic	-	-
8x8	3.643	3.599	results	-	-
16x16	3.600	3.588	*	-	-
Bares (series solution): 3.59					

Central Point Load:

Deflection= Coefficient *(PL²/D)/1000					
Grid	A C M	Hybrid	Bi.MPT	Heterosis	Lagrange
2x2	10.4167	10.4167	*	10.4167	10.4167
4x4	11.5702	11.3421	erratic	11.5112	11.4577
8x8	11.6858	11.5123	results	11.5404	11.6380
16x16	11.6455	11.5774	*	11.5821	11.6303
Moment(midside)= Coefficient * P /100					
Grid	A C M	Hybrid	Bi.MPT	Heterosis	Lagrange
2x2	8.748	8.752	*	-	-
4x4	6.016	6.812	erratic	-	-
8x8	6.148	6.276	results	-	-
16x16	6.112	6.144	*	-	-

Table 3.4 Deflection and Moment Comparisons –
Square Plate with Clamped Corners and Edge W, n=0.

Simply Supported Edges:

Moment normalized w.r.t. 4.7886 $qL^2/100$				
Grid	A C M	Hybrid	Bi.MPT	most accurate
2x2	1.379	1.025	0.692	hybrid
4x4	1.089	1.008	0.996	Bi.MPT
8x8	1.022	1.002	1.000	Bi.MPT
16x16	1.005	1.001	1.000	Bi.MPT

Clamped Edges:

Moment normalized w.r.t. 2.291 $qL^2/100$				
Grid	A C M	Hybrid	Bi.MPT	most accurate
2x2	2.015	1.481	0.0	hybrid
4x4	1.213	0.982	1.100	hybrid
8x8	1.050	1.002	1.017	hybrid
16x16	1.012	1.000	1.004	hybrid

Simply Supported Corners:

Moment normalized w.r.t. 11.17 $qL^2/100$				
Grid	A C M	Hybrid	Bi.MPT	most accurate
2x2	1.052	0.991	*	hybrid
4x4	1.034	1.005	erratic	hybrid
8x8	1.009	1.001	results	hybrid
16x16	1.003	1.000	*	hybrid

Clamped Corners, Edge W,n=0:

Moment normalized w.r.t. 3.585 $qL^2/100$				
Grid	A C M	Hybrid	Bi.MPT	most accurate
2x2	0.775	0.505	*	A C M
4x4	1.035	1.075	erratic	A C M
8x8	1.016	1.004	results	hybrid
16x16	1.004	1.001	*	hybrid

Table 3.5 Normalized Moment Comparisons for Uniform Loading.

Simply Supported Edges:

Moment normalized w.r.t. 6.0953 P /100				
Grid	A C M	Hybrid	Bi.MPT	most accurate
2x2	1.150	0.946	1.172	hybrid
4x4	1.057	1.064	1.122	A C M
8x8	1.019	1.016	1.033	hybrid
16x16	1.005	1.004	1.007	hybrid

Clamped Edges:

Moment normalized w.r.t. 12.57 P /100				
Grid	A C M	Hybrid	Bi.MPT	most accurate
2x2	1.130	1.152	0.0	A C M
4x4	0.937	1.022	0.617	hybrid
8x8	0.981	1.003	0.729	hybrid
16x16	0.994	1.000	0.839	hybrid

Simply Supported Corners :

Moment normalized w.r.t. 20.25 P /100				
Grid	A C M	Hybrid	Bi.MPT	most accurate
2x2	1.035	1.000	*	hybrid
4x4	0.981	1.030	erratic	A C M
8x8	1.004	1.008	results	A C M
16x16	1.002	1.004	*	A C M

Clamped Corners, Edge W,n=0:

Moment normalized w.r.t. 6.095 P /100				
Grid	A C M	Hybrid	Bi.MPT	most accurate
2x2	1.435	1.436	*	A C M
4x4	0.987	1.118	erratic	A C M
8x8	1.009	1.030	results	A C M
16x16	1.003	1.008	*	A C M

Table 3.6 Normalized Moment Comparisons for Point Load.

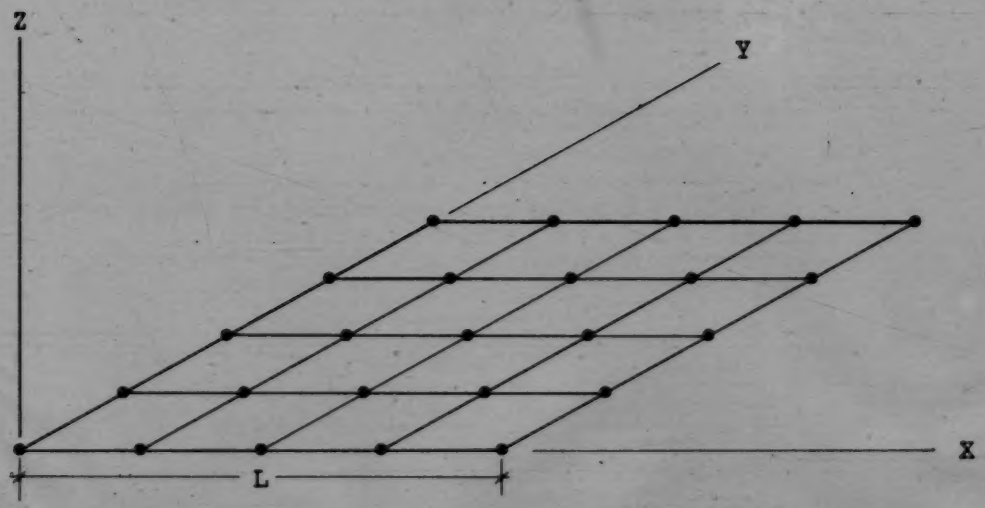

Figure 3.1 Square Test Plate with Typical 4×4 Grid.

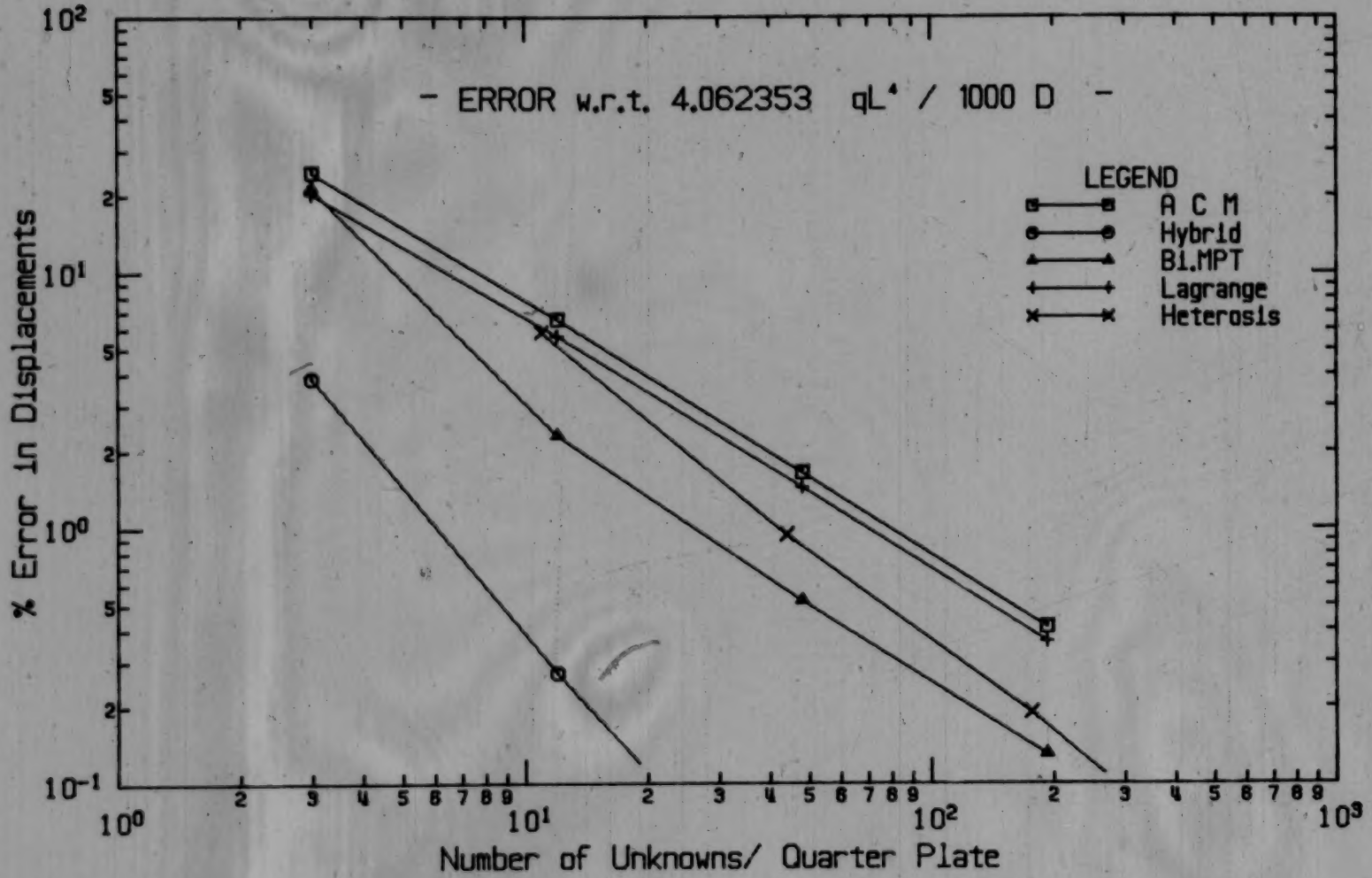

Figure 3.2 Plate Deflections: Uniform Load, Simply Supported Edges.

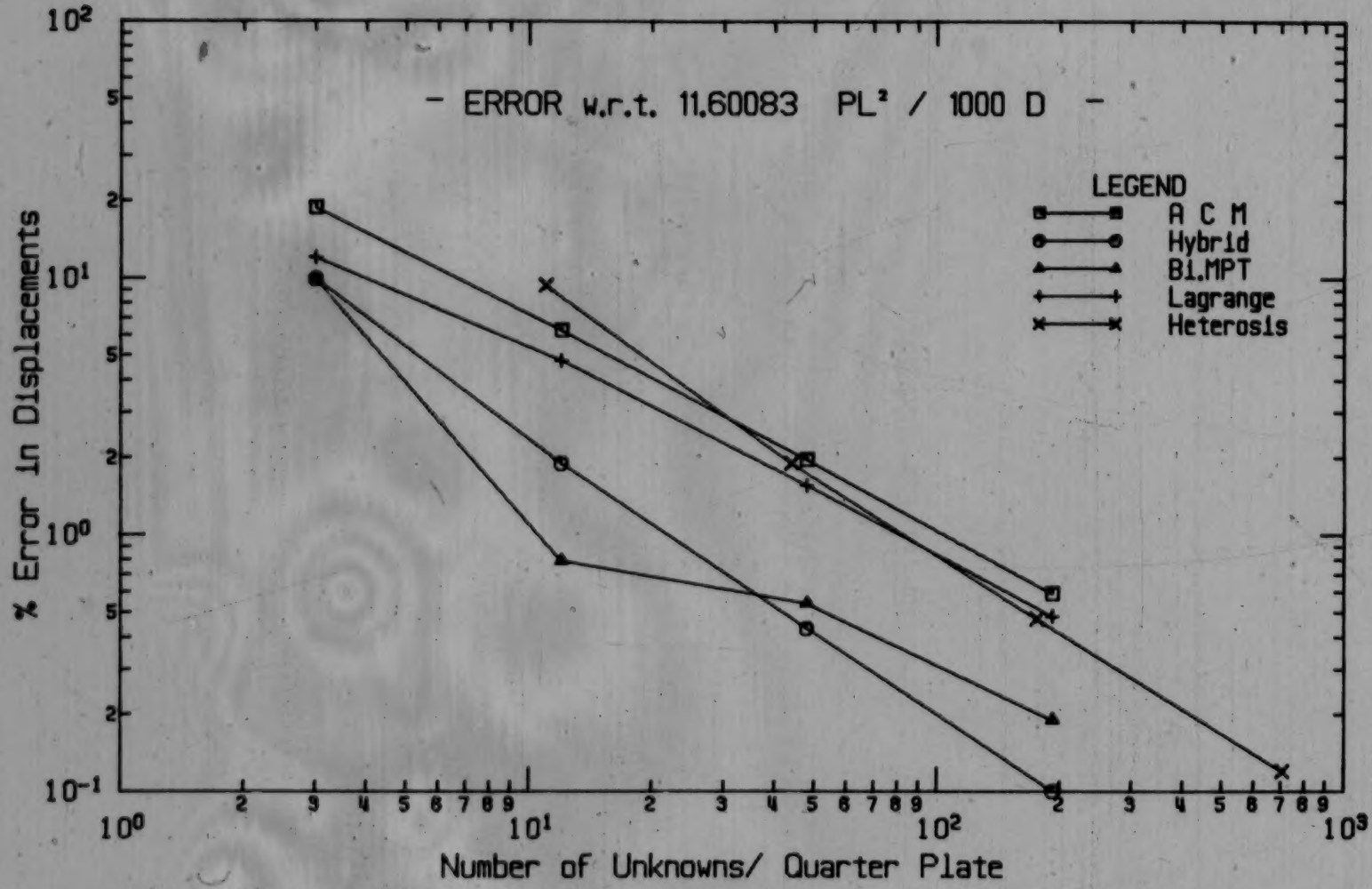

Figure 3.3 Plate Deflections: Point Load, Simply Supported Edges.

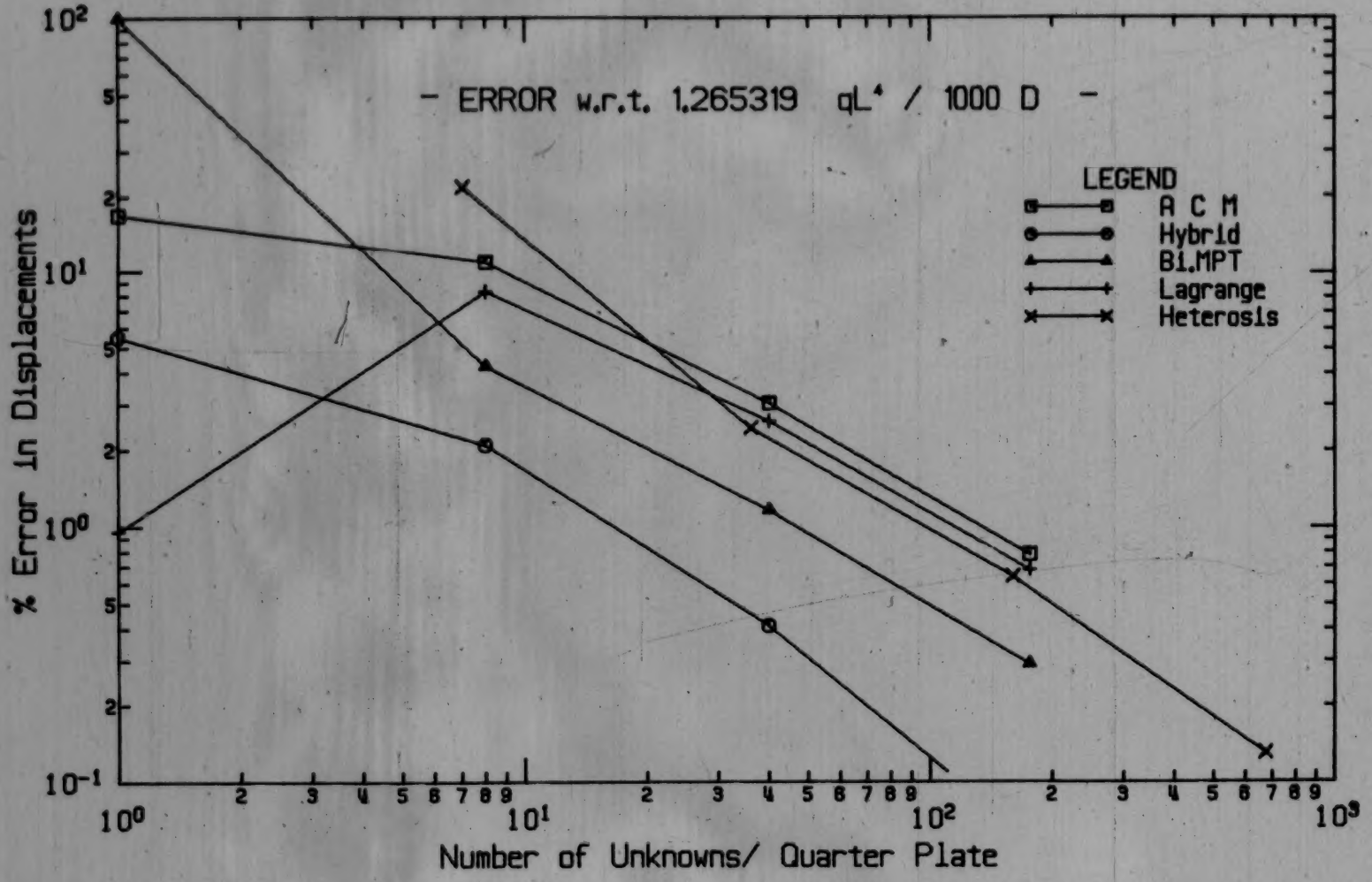

Figure 3.4 Plate Deflections: Uniform Load, Clamped Edges.

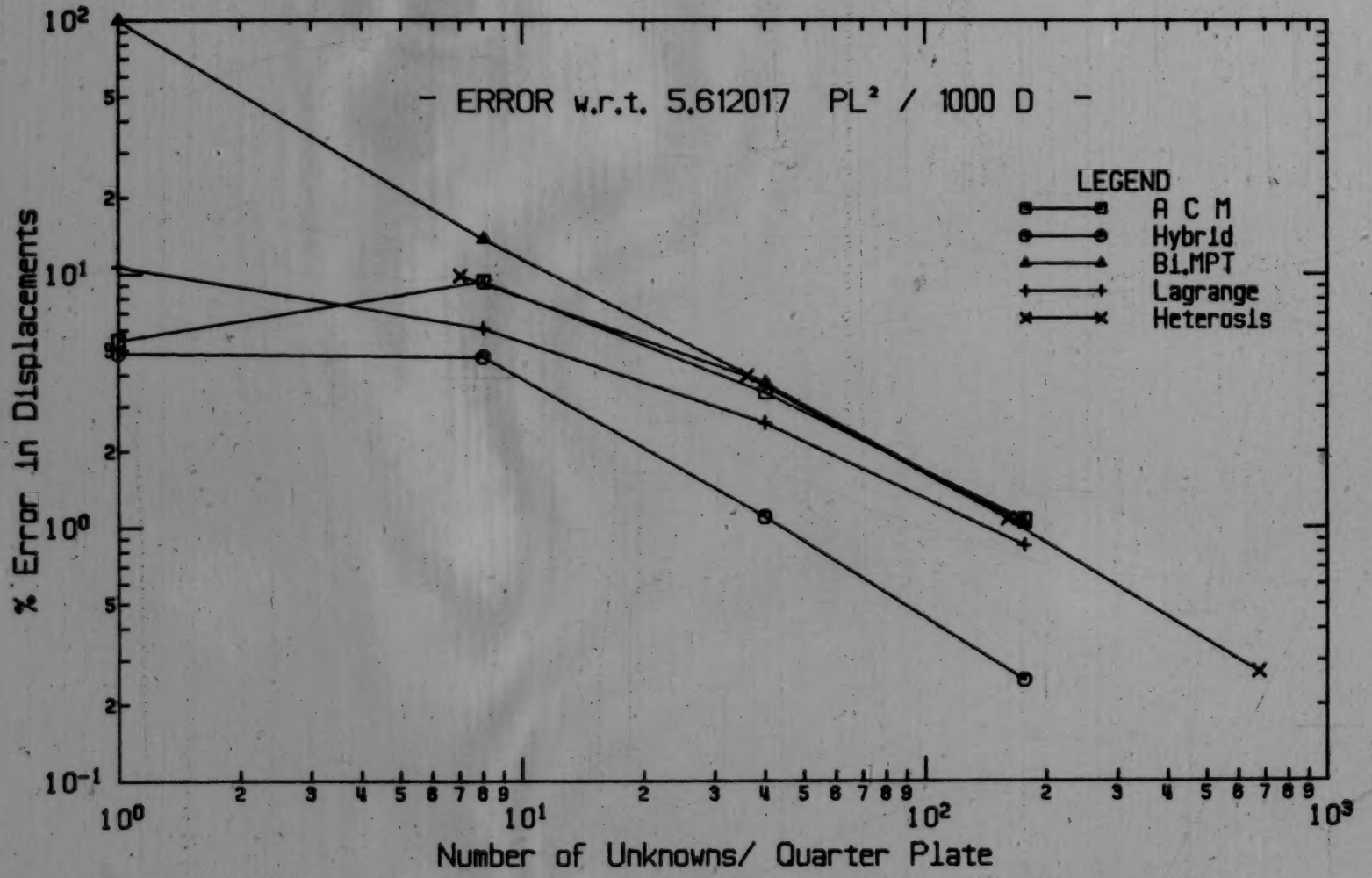

Figure 3.5 Plate Deflections: Point Load, Clamped Edges.

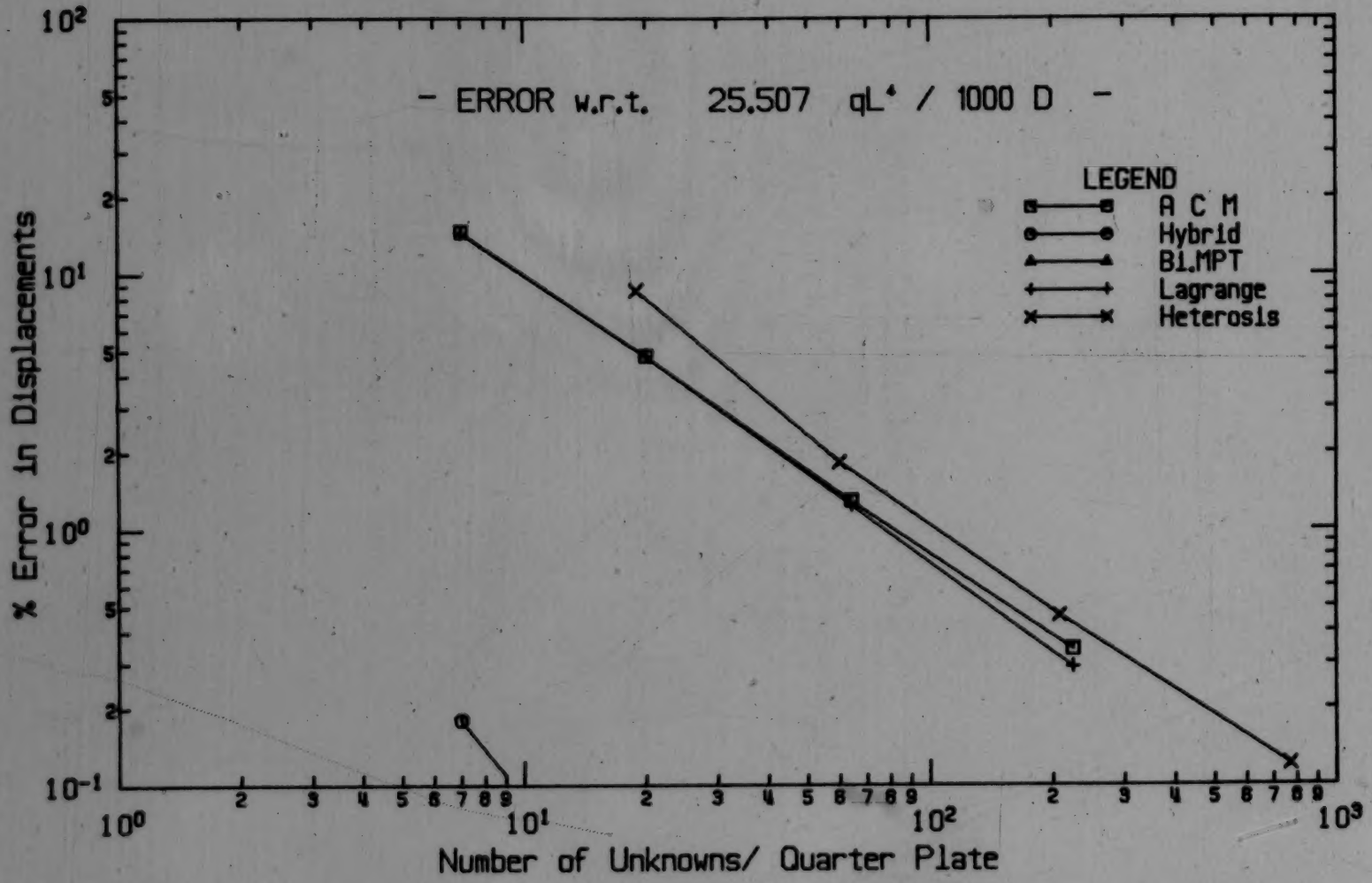

Figure 3.6 Plate Deflections: Uniform Load, Corners Simply Supported.

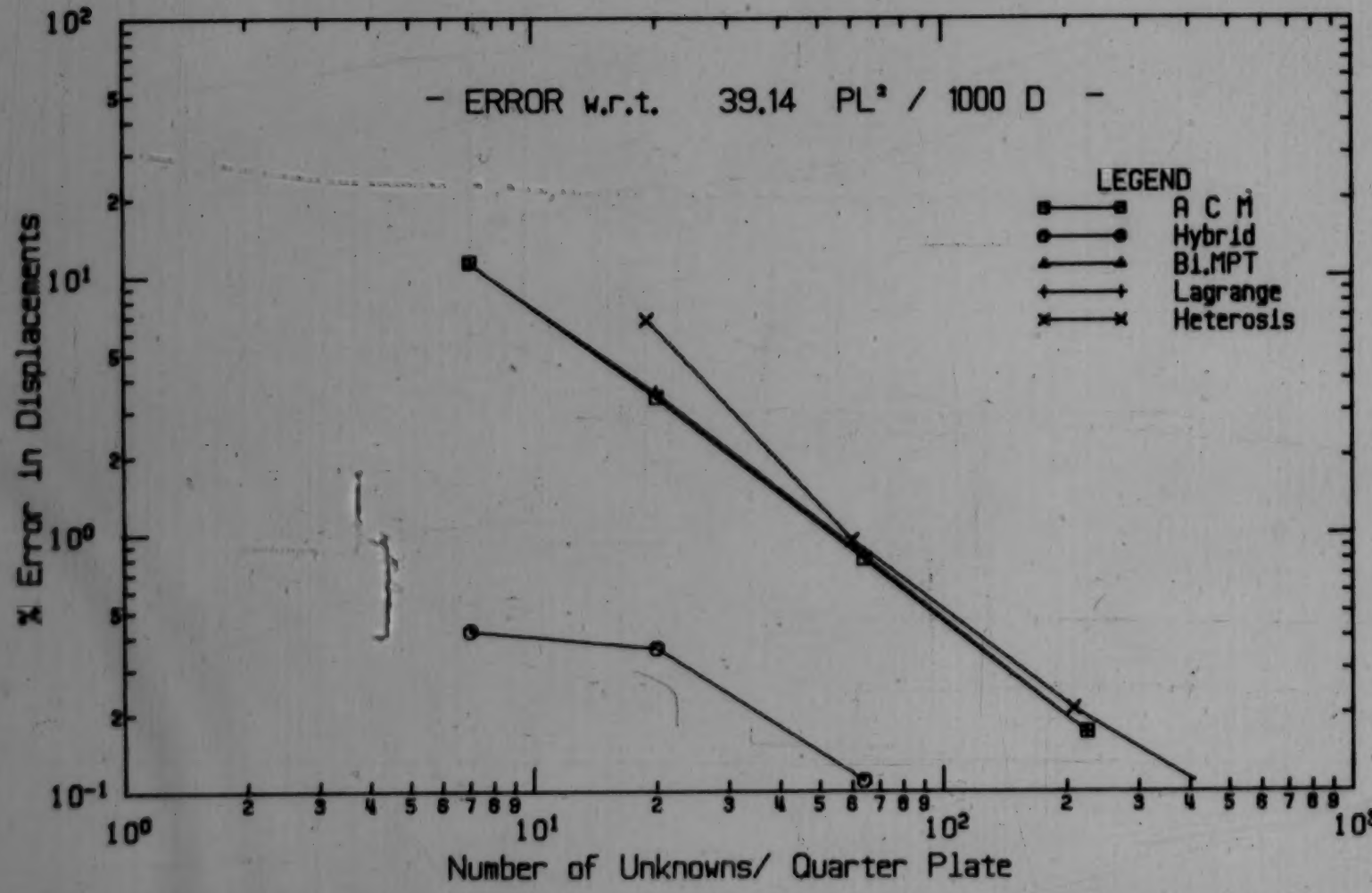

Figure 3.7 Plate Deflections: Point Load, Corners Simply Supported.

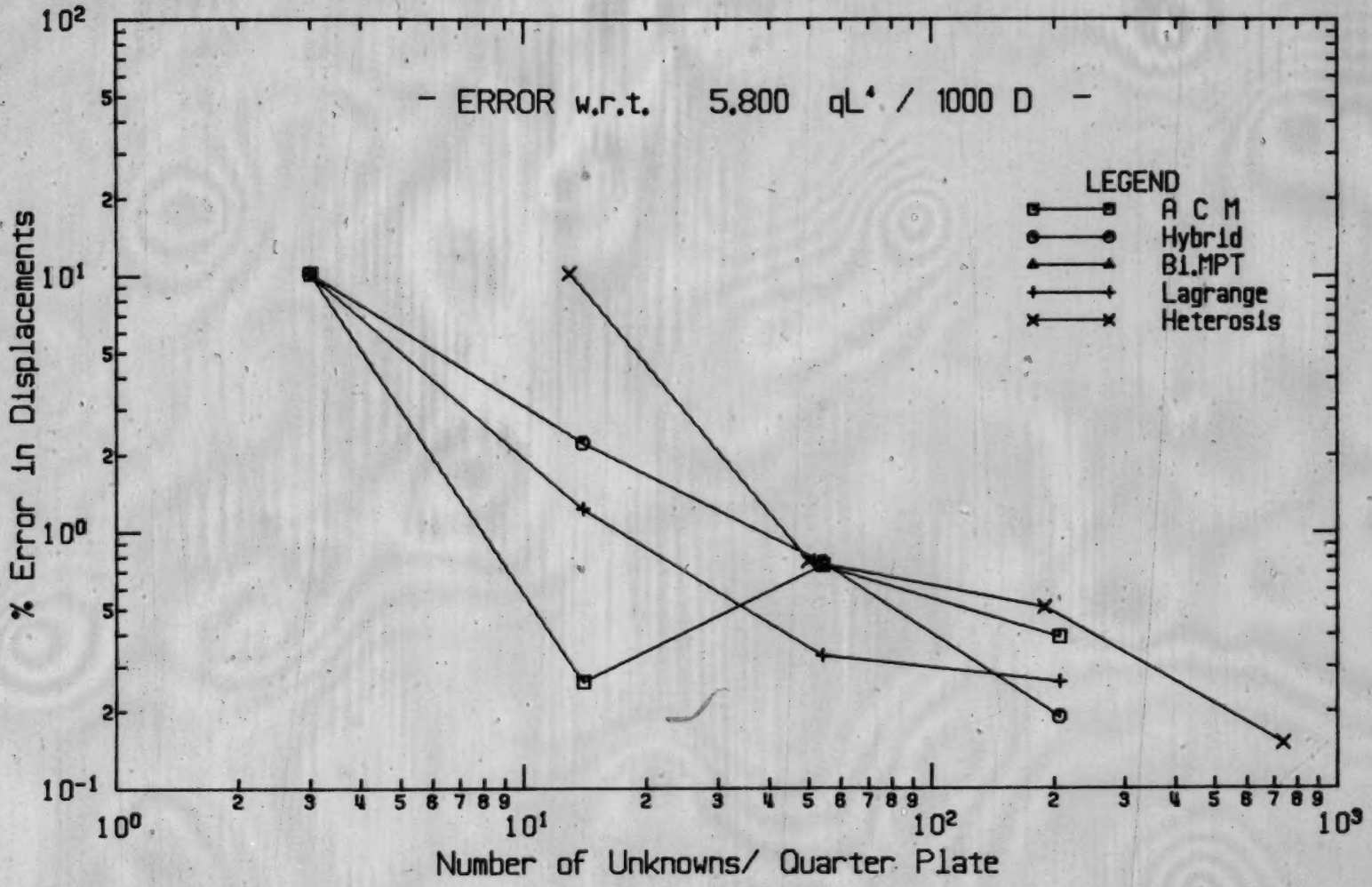

Figure 3.8 Plate Deflections: Uniform Load, Corners Clamped, Edge W,n=0.

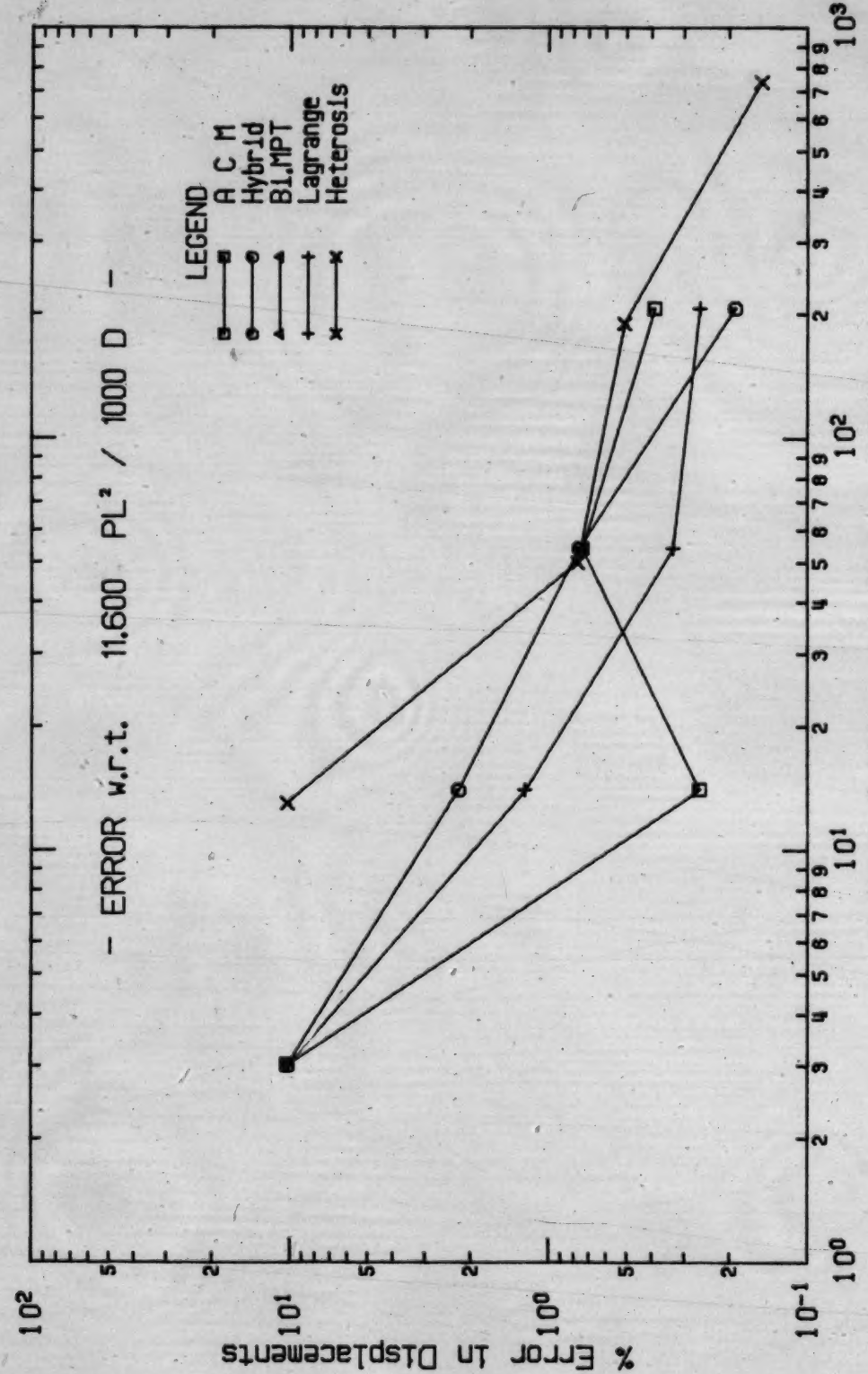

Figure 3.9 Plate Deflections: Point Load, Corners Clamped, Edge W,n=0.

Chapter 4

THE HYBRID STRESS METHOD

4.1 Theory of The Hybrid Stress Method

A complete derivation of the hybrid stress method along with its proof of convergence was given in the late 1960's by Pian and Tong[52,54]. The method as proposed by Pian and Tong requires that a set of stress functions be chosen to describe the stress field inside the element. A second set of independent functions is required to describe the displacement field along the element boundaries and to provide interelement displacement compatibility.

The presentation given in this section is an extension of Pian and Tong's work to include the effects of stress singularities. Although this type of approach has been used for in-plane problems to determine stresses at the tips of sharp cracks[53], to the best of the author's knowledge, it has not as yet been used for plate bending problems.

The presentation will proceed by describing the energy functional on which the hybrid stress method is based. Then the components of this functional, namely the the strain energy of the element and the elastic potential of the edge tractions, will be considered. These expressions will then be used to obtain an element stiffness matrix.

The Variational Principle:

The energy functional from which the hybrid stress method is obtained is a modified version of the principle of minimum complementary potential energy. This has been described in detail by Pian and Tong[52]. For the purposes of review and to provide a base for future discussion some of the main points of their derivation are given here.

The principle of minimum complementary potential energy for a structure may be written as:

$$\prod c = 1/2 \int_V \sigma ij \; Cijkl \; \sigma kl \; dV - \int_{Su} Ti \; \bar{U}i \; dSu \qquad (4.1)$$

where,

σij = stress tensor which must satisfy the differential equations of equilibrium over the volume 'V', and the prescribed boundary tractions over the region Sv,

$Cijkl$ = constitutive matrix of elastic constants which relates the stress and strain tensors,

V = volume of the structure,

Su = surfaces with prescribed displacements,

Ti = traction field on the surfaces Su, as derived from the stress tensor σij,

and,

$\bar{U}i$ = prescribed displacements on the surfaces Su.

In applying the finite element method, $\prod c$ of Equation 4.1 is evaluated on a subregion or by a piecewise approach as shown in Equation 4.2 below.

$$\prod c = \sum_n (1/2 \int_{V_n} \sigma ij \; Cijkl \; \sigma kl \; dV - \int_{Su_n} Ti \; \bar{U}i \; dSu) \qquad (4.2)$$

where,

n = the element under consideration.

Furthermore, in using the hybrid stress formulation, the choice is made to specify stress functions independently

for each element. This means that the stresses will be single-valued within the element and along its boundaries, but the boundary values of two adjoining elements will not necessarily be the same at the common boundary. However, for equilibrium to be satisfied it is necessary that the tractions across interelement boundaries be continuous. As well, the element must remain in equilibrium in the presence of the prescribed tractions. Since these equilibrium conditions are difficult to satisfy exactly on a pointwise basis, an alternate and approximate approach is used where only overall equilibrium of the element is enforced. A convenient way of implementing this approach is to regard the interelement equilibrium conditions as constraint equations and to impose these constraints by using Lagrangian multipliers. This has been done by Pian and Tong, and the Lagrangian multipliers have been identified as being the displacements along element boundaries. The energy functional is now in a modified or augmented form because $\prod c$ includes the constraint equations and can be written as:

$$\prod mc = \sum_n \left(1/2 \int_{V_n} \sigma ij \; Cijkl \; \sigma kl \; dV - \int_{Su_n} Ti \; \bar{U}i \; dSu - \int_{Si_n} Ti \; Ui \; dSi \right)$$

$$= \sum_n \left(1/2 \int_{V_n} \sigma ij \; Cijkl \; \sigma kl \; dV - \int_{S_n} Ti \; Ui \; dS + \int_{Sv_n} \bar{T}i \; Ui \; dSv \right) \qquad (4.3)$$

where,
n = the element being considered,
S = Su + Sv + Si = total surface,

and,
Su = surfaces with prescribed displacement,
Sσ = surfaces with prescribed tractions,
Si = surfaces between elements.

Whereas the original complementary energy functional involved only the stress components as unknowns, the modified complementary energy functional of Equation 4.3 has both stresses and displacements as variables. In using the hybrid stress method separate functions are used to describe each set of variables. Proof that a finite element analysis based on such an approach would converge was presented in 1969 by Tong and Pian[***].

Equation 4.3 will be used later to derive the element and global stiffness matrices. A discussion of the individual integrals follows.

Strain Energy, $\mathfrak{E}$:

For an elastic structure, there exists a scalar function known as the strain energy or elastic potential which can be calculated from the components of the stress and strain tensors as shown below in Equation 4.4.

$$\mathfrak{E} = 1/2 \int_V \sigma_{ij} \epsilon_{ij} \, dV$$

$$= 1/2 \int_V \sigma_{ij} C_{ijkl} \sigma_{kl} \, dV \qquad (4.4)$$

where,
$\mathfrak{E}$ = strain energy,
σ_{ij} = stress tensor,
ϵ_{ij} = strain tensor,
V = volume of integration.

At this point in the derivation it is convenient to regard the equilibrium stress field as consisting of a superposition of three stress fields as described below:

(1) The stress from the homogeneous or complementary solution. This solution must satisfy the homogeneous equations of equilibrium for the element. It is not necessary for this solution to satisfy any of the prescribed traction boundary conditions.

(2) The stress from the particular solution. The particular solution must satisfy the equations of equilibrium with the prescribed body forces acting and it must also satisfy the prescribed traction boundary conditions. This solution includes all the known stress parameters while the homogeneous solution includes the unknowns.

(3) The stress from the singularity solution. This solution like the homogeneous solution must satisfy the equations of equilibrium in the absence of any loading, but unlike the homogeneous solution it must give rise to stresses which may be caused by the geometry of the element.

For convenience, the singularity solution has been separated from the homogeneous part so that the homogeneous solution does not contain any singularity terms.

In equation form the stress field may be written as:

$$\sigma_{ij} = \overset{h}{\sigma}_{ij} + \overset{p}{\sigma}_{ij} + \overset{s}{\sigma}_{ij} \qquad (4.5)$$

where,

$\overset{h}{\sigma}_{ij}$ = stress from the homogeneous solution,

$\overset{p}{\sigma}_{ij}$ = stress from the particular solution,

$\overset{s}{\sigma}_{ij}$ = stress from the singularity solution.

It is not essential that any of the above solutions satisfy kinematic boundary conditions. These will be enforced on a global level when the structure's stiffness matrix is being

assembled.

By substituting Equations 4.5 into Equation 4.4, the following expression can be obtained for the strain energy:

$$\begin{aligned}\Phi = {} & 1/2 \int_V \overset{h}{\sigma}_{ij}\, C_{ijkl}\, \overset{h}{\sigma}_{kl}\, dV + 1/2 \int_V \overset{p}{\sigma}_{ij}\, C_{ijkl}\, \overset{p}{\sigma}_{kl}\, dV \\ & + 1/2 \int_V \overset{s}{\sigma}_{ij}\, C_{ijkl}\, \overset{s}{\sigma}_{kl}\, dV + \int_V \overset{h}{\sigma}_{ij}\, C_{ijkl}\, \overset{p}{\sigma}_{kl}\, dV \\ & + \int_V \overset{h}{\sigma}_{ij}\, C_{ijkl}\, \overset{s}{\sigma}_{kl}\, dV + \int_V \overset{p}{\sigma}_{ij}\, C_{ijkl}\, \overset{s}{\sigma}_{kl}\, dV \end{aligned} \tag{4.6a}$$

(or, in matrix notation)

$$\begin{aligned}\Phi = {} & 1/2 \int_V \langle \underset{h}{\sigma} \rangle\, [C]\, \{ \underset{h}{\sigma} \}\, dV + 1/2 \int_V \langle \underset{p}{\sigma} \rangle\, [C]\, \{ \underset{p}{\sigma} \}\, dV \\ & + 1/2 \int_V \langle \underset{s}{\sigma} \rangle\, [C]\, \{ \underset{s}{\sigma} \}\, dV + \int_V \langle \underset{h}{\sigma} \rangle\, [C]\, \{ \underset{p}{\sigma} \}\, dV \\ & + \int_V \langle \underset{h}{\sigma} \rangle\, [C]\, \{ \underset{s}{\sigma} \}\, dV + \int_V \langle \underset{p}{\sigma} \rangle\, [C]\, \{ \underset{s}{\sigma} \}\, dV \end{aligned} \tag{4.6b}$$

The second assumption is that each of the stress fields of Equation 4.4 can be adequately represented by the type of expressions shown in the following equations:

$$\begin{aligned} \{ \underset{h}{\sigma} \} &= [Ph]\, \{\beta h\} \\ \{ \underset{p}{\sigma} \} &= [Pp]\, \{\beta p\} \\ \{ \underset{s}{\sigma} \} &= [Ps]\, \{\beta s\} \end{aligned} \tag{4.7}$$

In the above set of equations, the $[P_\cdot]$ matrices contain polynomial or trigonometric expressions in terms of spatial coordinates. The unknown or free parameters are the $\{\beta\}$

terms. The values of $\{\beta p\}$ can be assigned as soon as the loading is known. The components of $\{\beta h\}$ and $\{\beta s\}$ can only be determined after the set of global equations is solved.

By substituting Equation set 4.7 into Equation 4.6b, the final form of Φ can be obtained as:

$$\begin{aligned}\Phi = {} & 1/2 \langle \beta h \rangle [Hhh] \{\beta h\} + 1/2 \langle \beta p \rangle [Hpp] \{\beta p\} \\ & + 1/2 \langle \beta s \rangle [Hss] \{\beta s\} + \langle \beta h \rangle [Hhp] \{\beta p\} \\ & + \langle \beta h \rangle [Hhs] \{\beta s\} + \langle \beta p \rangle [Hps] \{\beta s\} \end{aligned} \qquad (4.8)$$

where,

$$[Hhh] = \int_V [Ph]^T [C] [Ph] \, dV$$

$$[Hpp] = \int_V [Pp]^T [C] [Pp] \, dV$$

$$[Hss] = \int_V [Ps]^T [C] [Ps] \, dV$$

$$[Hhp] = \int_V [Ph]^T [C] [Pp] \, dV$$

$$[Hhs] = \int_V [Ph]^T [C] [Ps] \, dV$$

$$[Hps] = \int_V [Pp]^T [C] [Ps] \, dV$$

The remaining terms of the Πmc functional of Equation 4.3 involve the '$Ti\ \bar{U}i$' and '$Ti\ Ui$' terms. These will be discussed next.

Potential of Edge Tractions:

The second integral of Equation 4.3 involves the quantity '*Ti Ui*' over the entire surface. Integrals of the '*Ti Ui*' quantities will be referred to as the potential of edge tractions.

The tractions, *Ti*, on any surface can be calculated from:

$$Ti = \sigma ji \quad nj \tag{4.9}$$

where,

nj = components of an outward unit vector normal to the surface.

By using Equation 4.9 and the expressions $\{\sigma\} = [P]\{\beta\}$ from Equation 4.7, the tractions may be rewritten in matrix form as:

$$\{T\} = [NPh]\{\beta h\} + [NPp]\{\beta p\} + [NPs]\{\beta s\} \tag{4.10}$$

The explicit forms of the [*NP*] matrices are described in detail in later sections.

The displacements, *Ui*, of the integral term involving '*Ti Ui*' have been identified earlier as being displacements along the edges of the element. Although it may be possible to obtain a displacement field by integrating the stress functions, the amount of effort required for nonrectangular shapes is prohibitive; furthermore, this type of approach is not necessary. In the hybrid stress method, the element displacement functions and the stress functions are chosen separately. Because this is done, the hybrid stress method is sometimes referred to as a 'two-field approach'.

The assumed displacement functions which relate edge displacements to nodal displacements must be chosen to be compatible between elements and can be represented by Equation 4.11 as shown below.

$$\{U\} = [L]\ \{\underline{U}\} \tag{4.11}$$

where,

U = displacements along element edges,
L = displacement interpolating functions,
$\underline{U}$ = element nodal displacements.

Equation 4.11 can be used with Equation 4.10 to obtain the following expression:

$$\int_S Ti\ Ui\ dS =$$

$$<\beta h>[Ghh]\{\underline{U}\} + <\beta p>[Gpp]\{\underline{U}\} + <\beta s>[Gss]\{\underline{U}\}$$

where, (4.12)

$$[Ghh] = \int_S [NPh]^T\ [L]\ dS$$

$$[Gpp] = \int_S [NPp]^T\ [L]\ dS$$

$$[Gss] = \int_S [NPs]^T\ [L]\ dS$$

The last integral term of Equation 4.3 is '$\bar{T}i\ Ui$'. This can be rewritten in a matrix form similar to Equation 4.12 as:

$$\int_{S\sigma} \bar{T}i\ Ui\ dS\sigma$$

$$= \int_{S\sigma} <\bar{T}>\ [L]\ dS\sigma\ \ \{\underline{U}\}$$

$$= <\Phi>\ \{\underline{U}\} \tag{4.13}$$

The Stiffness Matrix:

The final form of $\prod mc$ can be obtained by substituting Equations 4.8, 4.12 and 4.13 into Equation 4.3 to get:

$$\begin{aligned}\prod mc = {} & 1/2 \langle \beta h \rangle [Hhh] \{\beta h\} + 1/2 \langle \beta p \rangle [Hpp] \{\beta p\} \\ & + 1/2 \langle \beta s \rangle [Hss] \{\beta s\} + \langle \beta h \rangle [Hhp] \{\beta p\} \\ & + \langle \beta h \rangle [Hhs] \{\beta s\} + \langle \beta p \rangle [Hps] \{\beta s\} \\ & - \langle \beta h \rangle [Ghh] \{\underline{U}\} - \langle \beta p \rangle [Gpp] \{\underline{U}\} - \langle \beta s \rangle [Gss] \{\underline{U}\} \\ & + \langle \Psi \rangle \{\underline{U}\} \end{aligned} \qquad (4.14)$$

The only unknown quantities of Equation 4.14 are $\{\beta h\}$, $\{\beta s\}$ and $\{\underline{U}\}$. The terms of $\{\beta p\}$ are known because the applied loading and prescribed tractions are specified. To obtain a stiffness matrix from Equation 4.14, the functional $\prod mc$ is minimized with respect to the parameters contained in the two unknown $\{\beta\}$ vectors and the terms of the $\{\underline{U}\}$ displacement vector. This is necessary because $\{\beta\}$ and $\{\underline{U}\}$ are independent vectors and the stationary value of $\prod mc$ can only be obtained if it is minimized with respect to both sets of variables.

The minimization with respect to the $\{\beta h\}$ and $\{\beta s\}$ vectors eliminates all the stress fields for which $\prod c$ does not have a stationary value. The minimization with respect to $\{\underline{U}\}$ is discussed later.

The result of the minimization of $\prod mc$ with respect to $\{\beta h\}$ and $\{\beta s\}$ vectors respectively results in the following set of equations:

$$[Hhh]\{\beta h\} + [Hhp]\{\beta p\} + [Hhs]\{\beta s\} - [Ghh]\{\underline{U}\} = \{o\}$$

$$[Hss]\{\beta s\} + [Hsh]\{\beta h\} + [Hsp]\{\beta p\} - [Gss]\{\underline{U}\} = \{o\}$$

where, (4.15)

$$[Hph] = [Hhp]^T$$

$$[Hsh] = [Hhs]^T$$

$$[Hsp] = [Hps]^T$$

and the matrices $[Hhh]$, $[Hpp]$ and $[Hss]$ are symmetrical.

Equation 4.15 can be substituted into Equation 4.14 and the functional $\prod mc$ can be rewritten so that the only unknowns are $\{\underline{U}\}$. To accomplish this, it is necessary to solve the equations in 4.15 for $\{\beta h\}$ and $\{\beta s\}$. This task is simplified if the two unknown vectors $\{\beta h\}$ and $\{\beta s\}$ are combined into a single vector $\{\beta hs\}$. After this is done, Equation 4.15 can be rewritten as:

$$[Hhhss]\{\beta hs\} = [Ghhss]\{\underline{U}\} - [Hhsp]\{\beta p\}$$

$$\{\beta hs\} = [Hhhss]^{-1} ([Ghhss]\{\underline{U}\} - [Hhsp]\{\beta p\})$$

where, (4.16)

$$\{\beta hs\} = \begin{Bmatrix} \{\beta h\} \\ \{\beta s\} \end{Bmatrix}$$

$$[Hhhss] = \begin{array}{|c|c|} \hline [Hhh] & [Hhs] \\ \hline [Hsh] & [Hss] \\ \hline \end{array}$$

$$[Hhsp] = \begin{array}{|c|} \hline [Hhp] \\ \hline [Hsp] \\ \hline \end{array}$$

$$[Ghhss] = \begin{array}{|c|} \hline [Ghh] \\ \hline [Gss] \\ \hline \end{array}$$

With the above expressions, $\prod mc$ of Equation 4.14 can be

rewritten as:

$$\prod mc = 1/2 \langle \beta hs \rangle [Hhhss] \{\beta hs\} + \langle \beta hs \rangle [Hhsp] \{\beta p\} + 1/2 \langle \beta p \rangle [Hpp] \{\beta p\} - \langle \beta hs \rangle [Ghhss] \{\underline{U}\} - \langle \beta p \rangle [Gpp] \{\underline{U}\} + \langle \Psi \rangle \{\underline{U}\} \quad (4.17)$$

Equation 4.16 can also be obtained by minimizing $\prod mc$ of Equation 4.17 with respect to $\{\beta hs\}$. After eliminating $\{\beta hs\}$ and combining like terms, the following equation can be written:

$$\prod mc = \sum (-1/2 \langle \underline{U} \rangle [GHG] \{\underline{U}\} + \langle Peq \rangle \{\underline{U}\} + Co) \quad (4.18)$$

where,

$$[GHG] = [Ghhss]^T [Hhhss]^{-1} [Ghhss]$$

$$\langle Peq \rangle = \langle \beta p \rangle ([Hhsp]^T [Hhhss]^{-1} [Ghhss] - [Gpp]) + \langle \Psi \rangle$$

and,

$$Co = \langle \beta p \rangle (1/2[Hpp] - [Hhsp]^T [Hhhss]^{-1} [Hhsp]) \{\beta p\}$$

$$= \text{a constant.}$$

The next step is to minimize Equation 4.18 with respect to $\{\underline{U}\}$. The $\{\underline{U}\}$ vector contains the second set of independent variables which were earlier derived from the Lagrangian multipliers. The Lagrangian multipliers are required to ensure that the elements remain in equilibrium. Therefore upon minimizing $\prod mc$ of Equation 4.18 with respect to $\{\underline{U}\}$ the following set of equilibrium equations is obtained:

$$\sum [GHG] \{\underline{U}\} = \sum \{Peq\} \quad (4.19)$$

From this point on, with [GHG] as a stiffness matrix, and {Peq} as a load vector, the hybrid stress method is identical in format to the standard displacement method.

In the remaining sections of this chapter, element stiffness matrices are derived for the following four cases:

(1) A plane stress element without body forces and without stress singularities. The element shape can range from a triangle to a six-sided irregular polygon.

(2) A plate bending element with body forces but without stress singularities. The element shape can range from a triangle to a six-sided irregular polygon.

(3) An L-shaped plate bending element with the stress singularity included. The two sides which meet at the reentrant corner have 'free edge' boundary conditions.

(4) An L-shaped plate bending element with the stress singularity included. The two sides which meet at the reentrant corner have 'fixed edge' boundary conditions.

Before proceeding with the derivations, some guidelines and requirements pertaining to the selection of stress functions are discussed. Although many choices are possible for the stress functions, it is necessary to satisfy two important requirements.

First, it is essential that the number of independent $\{\beta\}$ parameters must not be less then the displacement rank of the element stiffness matrix. The displacement rank of an element stiffness matrix is equal to the total number of element degrees of freedom minus the number of rigid body modes. It is the number of linearly independent rows in the element stiffness matrix. If this condition is not met, then the element stiffness matrix will be rank deficient[7,8].

Although this is a necessary condition, it is not sufficient to guarantee that spurious energy modes do not appear. Some researchers[30,32] have encountered extraneous zero-valued eigenvalues when using linear stress functions. In each case, these energy modes were successfully eliminated by the addition of some quadratic terms. Therefore, it is recommended that linear stress functions not be used without checking the number of zero eigenvalues in the stiffness matrix.

At the same time, an excess of $\{\beta\}$ parameters tends to overstiffen the element and should be avoided. Work on the subject of optimum number of $\{\beta\}$ parameters has been done by Henshell[34] and Pian[31]. Although no exact equation is given, the consensus is that the order of the stress functions should be compatible with the order of the displacement functions and that neither set should be changed without a corresponding change in the other. Henshell[34] also recommends that the number of $\{\beta\}$ parameters approximately equals the displacement rank of the stiffness matrix.

The second important requirement is that the stress functions satisfy the differential equations of equilibrium as given by, $\sigma ji,j + Fi = 0$.

These requirements and guidelines will be followed in the derivations of element stiffness matrices which follow in Sections 4.2 to 4.4.

4.2 Polygonal Element In-Plane Matrices

This section contains the derivation of in-plane stiffness matrices for plane stress elements with three to six sides. These stiffness matrices are required to model plates with in-plane displacements caused by eccentric stiffners. Because of the intended use of these elements, the body forces and prescribed tractions can be neglected. As well it is assumed that stress singularities do not have to be considered.† Therefore only the [*H*hh] and [*G*hh] matrices are needed to obtain the stiffness matrix.

[*H*hh]:

In order to obtain [*H*hh] it is necessary to assume stress functions for σx, σy, and σxy. A set of partial quadratic stress functions were chosen to describe the stress field inside the element. These functions are shown below in Equation 4.20 and satisfy the equilibrium and rank requirements discussed at the end of Section 4.1.

$$\begin{aligned} \sigma x &= \beta_1 + x\beta_2 + y\beta_3 + xy\beta_4 \\ \sigma y &= \beta_5 + x\beta_6 + y\beta_7 + xy\beta_8 \\ \sigma xy &= -y\beta_2 - 0.5y^2\beta_4 - x\beta_7 - 0.5x^2\beta_8 + \beta_9 \end{aligned} \tag{4.20}$$

In matrix form this can be written as stated earlier in Equation 4.7:

$$\underset{3x1}{\{\sigma\}} = \underset{3x9}{[Ph]}\ \underset{9x1}{\{\beta h\}} \tag{4.21}$$

---

† The situations where stress singularities do occur are not common and details of these cases are discussed by Morley[32] and Williams[98].

where,

$$\{\sigma\} = \begin{Bmatrix} \sigma_x \\ \sigma_y \\ \sigma_{xy} \end{Bmatrix} .$$

Since the above stress polynomials are not complete, coordinate invariance for rectangular shapes can only be guaranteed if the polynomials are evaluated in a local coordinate system which remains parallel to the sides of the rectangle. Although this type of invariance is a desirable property, it is not essential.

The constitutive matrix is assumed to be of the form:

$$[C] = \begin{array}{|c|c|c|} \hline C_1 & C_3 & . \\ \hline C_3 & C_2 & . \\ \hline . & . & C_4 \\ \hline \end{array} \qquad (4.22)$$

The matrix [*H*hh] can now be calculated from the expression in Equation 4.8 which is repeated below:

$$[Hhh] = \int_V [Ph]^T [C] [Ph] \, dV$$

$$= t \int_A [Ph]^T [C] [Ph] \, dA \qquad (4.23)$$

where,
t = thickness of the element.

Since any polygonal element can be constructed from an assemblage of triangular and trapezoidal shapes, it was decided to evaluate the explicit form of [*H*hh] for a trapezoidal region. Triangular shapes are defined as a trapezoid with one of the parallel sides equal to zero. The explicit form is then used in the computer program *HYBSLAB* and [*H*hh] for the element as a whole is obtained from a summation of [*H*hh]'s from the trapezoids. Additional

details of this procedure are provided in the next chapter.

[*G*hh]:

The matrix [*G*hh] is obtained from the expression in Equation 4.12 which is shown below:

$$[Ghh] = \int_S [NPh]^T [L] \, dS$$

$$= t \int_{\pounds} [NPh]^T [L] \, d\pounds \qquad (4.24)$$

where,
t = thickness of the element,
£ = length along the element's perimeter.

The [*NP*h] matrix is obtained from '*T*i *U*i' and for a plane stress element its form can be determined as indicated below in Equation 4.25. In this equation, n_1 and n_2 are the components of an outward unit normal vector located at a point on the element's boundary. The matrix {*U*} consists of '*U*' and '*V*' which are the in-plane x and y displacements of the point. As well, the set of indices '$_1$' and '$_2$', are used interchangeably with the set 'x' and 'y'. The following steps in Equation 4.25 indicate how [*NP*h] is obtained from '*T*i *U*i':

$$\int_S Ti \; Ui \, dS$$

$$= t \int_{\pounds} Ti \; Ui \, d\pounds$$

$$= t \int_{\pounds} (\sigma ji \; nj \; Ui) \, d\pounds$$

(and, in matrix form)

$$= t \int_{\ell} \langle \sigma_x \; , \; \sigma_y \; , \; \sigma_{xy} \rangle \begin{bmatrix} n_1 & \cdot \\ \cdot & n_2 \\ n_2 & n_1 \end{bmatrix} \begin{Bmatrix} U \\ V \end{Bmatrix} d\ell$$

(or)

$$= t \int_{\ell} \langle \sigma \rangle \; [N]^T \; \{U\} \; d\ell$$

$$= t \underset{1x9}{\langle \beta h \rangle} \int_{\ell} \underset{9x3}{[Ph]^T} \; \underset{3x2}{[N]^T} \; \underset{2x4}{[L]} \; d\ell \; \underset{4x1}{\{U\}}$$

$$= t \underset{1x9}{\langle \beta h \rangle} \int_{\ell} \underset{9x2}{[NPh]^T} \; \underset{2x4}{[L]} \; d\ell \; \underset{4x1}{\{U\}} \qquad (4.25)$$

As indicated in the last two steps of the above equation, $[NPh]$ is the product of the $[N]$ and $[Ph]$ matrices. At this time it is noted that Equation 4.25 requires integration along the element sides only. This means that $[Ghh]$ can be calculated in a step-by-step manner by considering one side at a time. The explicit form of $[NPh]$ for one side is a (2x9) matrix which can be written as:

$[NPh]$ =

n_1	$n_1 x$ $-n_2 y$	$n_1 y$	$n_1 xy$ $-n_2 y^2/2$	$\cdot$	$\cdot$	$-n_2 x$	$-n_2 x^2/2$	n_2
$\cdot$	$-n_1 y$	$\cdot$	$-n_1 y^2/2$	n_2	$n_2 x$	$n_2 y$ $-n_1 x$	$n_2 xy$ $-n_1 x^2/2$	n_1

(4.26)

The next step is to choose the shape functions of the matrix $[L]$ which relates edge displacements to nodal displacements. For an element side, defined by nodes 1 and 2, a suitable set of displacement functions is the linear set shown below in Equation 4.27.

$$\{U\} = [L]\ \{\underline{U}\}$$

(or)

$$\begin{Bmatrix} U \\ V \end{Bmatrix} = \begin{bmatrix} 1-\rho & . & \rho & . \\ . & 1-\rho & . & \rho \end{bmatrix} \begin{Bmatrix} \underline{U}_1 \\ \underline{V}_1 \\ \underline{U}_2 \\ \underline{V}_2 \end{Bmatrix} \qquad (4.27)$$

where,

U = in-plane X displacement along the element side,
V = in-plane Y displacement along the element side,
ρ = non-dimensional coordinate measured along the element side from node 1 to node 2.

The matrix product of [*NP*h] [*L*] is integrated to form a resultant matrix which will be called [*G*hh]$_\circ$, where the subscript '$_\circ$' indicates that only one side has been considered. The [*G*hh] matrix is formed by a direct entry and summation procedure of the [*G*hh]$_\circ$ matrices.

The element stiffness matrix [GHG] is evaluated from Equation 4.28 as shown below:

$$\underset{mxm}{[GHG]} = \underset{mx9}{[Ghh]^T}\ \underset{9x9}{[Hhh]^{-1}}\ \underset{9xm}{[Ghh]} \qquad (4.28)$$

where, m = number of element degrees of freedom $\leq$ 12

If any external in-plane loads exist they can be proportioned directly to the nodes.

At this time it is again pointed out that the chosen stress functions have only nine independent β parameters and therefore the element cannot have more than six nodes.

Details of the computer subroutine which is used to calculate the stiffness matrix can be found in the program *HYBSLAB* which is discussed in Chapter 5.

4.3 Polygonal Element Flexural Matrices

This section contains the derivation of flexural stiffness matrices for plate elements with three to six sides. The derivation is based on the following assumptions and conditions:

(1) Classical Kirchhoff plate theory is used to describe the behavior of the plate.

(2) Body forces are included but prescribed tractions are not considered. These assumptions are discussed in more detail in the paragraphs which follow.

(3) Stress singularities are not considered in the derivation.

Disregarding the prescribed tractions means, that in the Πmc functional of Equation 4.3, '$\bar{T}i$' is assumed to be zero-valued. This assumption is true where elements share a common boundary and the equation, $Ti = \sigma ji\ nj$, gives the correct values of edge tractions. However, it is not valid for cases where the edge tractions are specified beforehand. A common example is the free edge condition.

For a free edge, only in the limit will the the assumed stress functions provide a stress-free condition. This problem is not unique to the hybrid formulation and similar statements can be made for the displacement and mixed methods. In the hybrid stress method the situation may be rectified in one of two ways. The first approach was introduced by Pian and Tong[5] and requires a reformulation of the [*NP*h] matrix so that the stress functions do reproduce the desired traction conditions. The second

approach consists of adding corrective T_i values to those calculated from $T_j = \sigma_{ij} n_i$ in such a manner that the desired boundary conditions are obtained. Since neither approach is easily implemented and because good results were obtained in the previous chapter without making any corrections, it was decided to formulate the stiffness matrix for a typical interior element only.

This stiffness matrix is to be used for all elements regardless of edge conditions. In doing so, no serious problems are expected, because the error decreases with element size and although the rate of convergence may be changed, the values to which the solution converges remain unchanged.

From Equations 4.16 to 4.18 it can be seen that the matrices which are required to calculate a stiffness matrix are: [H_{hh}], [H_{hp}], [H_{pp}], [G_{hh}], and [G_{pp}]. Before considering the functions required for these matrices, the equations of Section 4.1 will be modified so that moments and curvatures appear in place of stresses and strains.

The term 'moment' is being used in the context of plate bending and denotes a stress resultant which has the units of 'force × distance/ distance'. In equation form this moment, denoted by 'M_{ij}', is defined as:

$$M_{ij} = \int z \, \sigma_{ij} \, dz \qquad (4.29)$$

where,

z= distance from the plates's midsurface to the fibre being considered, measured along the +Z coordinate direction.

Using Kirchhoff plate theory the strain tensor, ϵij, may be written in terms of curvatures, W,ij, as shown below in Equation 4.30. Partial differentiation is indicated by using the comma notation.

$$\epsilon ij = - z \; W,ij \tag{4.30}$$

where,

W = transverse displacement of the midsurface of the plate and is a function of the X and and Y coordinates only.

As well, it is assumed that there are constitutive tensors, $Dijkl$ and $Eijkl$, which relate the moment and curvature tensors according to:

$$W,ij = - Dijkl \; Mkl \quad \text{(or)} \quad Mij = - Eijkl \; W,kl \tag{4.31}$$

With the above three equations, the expression for '$\sigma ij \; \epsilon ij$' may be rewritten to get the following equation:

$$\int_V \sigma ij \; \epsilon ij \; dV$$

$$= \int_V (\sigma ij) \; (-z \; W,ij) \; dz \; dA$$

$$= - \int_A Mij \; W,ij \; dA$$

$$= + \int_A Mij \; Dijkl \; Mkl \; dA \tag{4.32}$$

(or, in matrix notation)

$$= + \int_A \langle M \rangle \; [D] \; \{M\} \; dA$$

where,

$$\langle M \rangle = \langle\, Mx\ My\ Mxy \,\rangle$$

and,

A = midsurface area of the element as defined by the X and Y coordinates.

By following through Equations 4.4 to 4.8 and replacing the stress and strain tensors by moment and curvature tensors the following sets of equations can be obtained:

$$\begin{aligned} \{M\}_h &= [Ph]\,\{\beta h\} \\ \{M\}_p &= [Pp]\,\{\beta p\} \\ \{M\}_s &= [Ph]\,\{\beta s\} \end{aligned} \qquad (4.33)$$

(and)

$$\begin{aligned} [Hhh] &= \int_A [Ph]^T\,[D]\,[Ph]\,dA \\ [Hpp] &= \int_A [Pp]^T\,[D]\,[Pp]\,dA \\ [Hss] &= \int_A [Ps]^T\,[D]\,[Ps]\,dA \\ [Hhp] &= \int_A [Ph]^T\,[D]\,[Pp]\,dA \\ [Hhs] &= \int_A [Ph]^T\,[D]\,[Ps]\,dA \\ [Hps] &= \int_A [Pp]^T\,[D]\,[Ps]\,dA \end{aligned} \qquad (4.34)$$

The individual matrices [Hhh], [Hhp], [Hpp] are discussed in the following paragraphs.

[*H*hh]:

To describe the moment field inside the element, it is necessary to assume functions for *M*x, *M*y, and *M*xy . A set of complete quadratic moment functions were chosen. These functions are shown below in Equation 4.35 and satisfy the equilibrium and rank requirements discussed at the end of Section 4.1.

$$Mx = \beta_1 + x\beta_2 + y\beta_3 + x^2\beta_4 + xy\beta_5 + y^2\beta_6$$

$$My = \beta_7 + x\beta_8 + y\beta_9 + x^2\beta_{10} + xy\beta_{11} + y^2\beta_{12} \qquad (4.35)$$

$$Mxy = -xy\beta_4 - xy\beta_{12} + \beta_{13} + x\beta_{14} + y\beta_{15} + x^2\beta_{16} + y^2\beta_{17}$$

In matrix form, the above can be written as:

$$\{M\}_h = [Ph]\ \{\beta h\} \qquad (4.36)$$

The moment functions of Equation 4.35 have a total of seventeen independent β parameters. The plate bending elements have as nodal degrees of freedom $< W , \theta x , \theta y >$, where:

W = transverse displacement in the +Z direction,
θx = rotation about the +X axis (= *W*,y),
θy = rotation about the -Y axis (= *W*,x).

Hence, the moment functions of Equation 4.35 can be used to formulate stiffness matrices for any plate element with six nodes or less.

The constitutive matrix is assumed to be of the form:

$$[D] = \begin{bmatrix} d_1 & d_3 & . \\ d_3 & d_2 & . \\ . & . & d_4 \end{bmatrix} \qquad (4.37)$$

The matrix [*H*hh] can now be calculated from the expression in Equation 4.34 which is repeated below:

$$[Hhh] = \int_A \underset{17x3}{[Ph]^T} \; \underset{3x3}{[D]} \; \underset{3x17}{[Ph]} \; dA$$

[*H*pp]:

The matrix [*H*pp] is calculated from the moment functions of the particular solution. Although many such solutions exist, Tong and Pian[10] have shown that the introduction of body forces does not change the stiffness matrix at all. This statement can be verified by examining Equation 4.18. However, as can also be seen from Equation 4.18, the form of the equivalent load vector {Peq} is very much dependent on the particular solution. Therefore, one might expect that the finite element solution would depend on the choice of particular solution, but Tong and Pian[10] have proved that this is not so if a certain requirement is met. The requirement is: if all the terms of the different [*P*p]{βp} particular solutions appear in the polynomials of the homogeneous solution [*P*h]{βh} then the finite element solution is independent of the choice of particular solution.

In keeping with the above requirement, if a uniform load, q_o, is to be accommodated then the [*P*h] polynomials must be at least complete quadratics. The moment functions of Equation 4.35 satisfy this requirement. The various

particular solutions, which can be chosen, contain only quadratic and lesser order terms. The quadratic terms satisfy the equilibrium equation:

$$Mx,xx + 2\,Mxy,xy + My,yy = -\,q_o$$

while the constant and linear terms drop out upon double differentiation.

Some possible particular solutions are:

$$(1)\quad \langle M \rangle_p = \langle -x^2/2,\ o\ ,\ o \rangle\, q_o$$

$$(2)\quad \langle M \rangle_p = \langle o\ ,\ -y^2/2,\ o \rangle\, q_o \qquad (4.38)$$

$$(3)\quad \langle M \rangle_p = \langle o\ ,\ o\ ,\ -xy/2 \rangle\, q_o$$

An infinite number of other particular solutions can be obtained from combinations of the above three solutions. The last two solutions were used at different times in the *HYBSLAB* program to confirm that the displacements and stresses were not dependent on the choice of particular solution.

The last particular solution shown in Equation 4.38 will be used in this chapter. The matrix [*H*pp] can be calculated from the second expression of Equation 4.34 which is repeated below:

$$[Hpp] = \int_A \underset{1x3}{[Pp]^T}\ \underset{3x3}{[D]}\ \underset{3x1}{[Pp]}\ dA$$

where,

$$[Pp]^T = \langle o\ ,\ o\ ,\ -xy/2 \rangle$$

and,

$$\{\beta p\} = q_o$$

[*H*hp]:

The matrix [*H*hp] is calculated from the homogeneous and particular solutions according to the following expression of Equation 4.34:

$$[Hhp] = \int_A \underset{17x3}{[Ph]^T} \; \underset{3x3}{[D]} \; \underset{3x1}{[Pp]} \; dA$$

The explicit forms of [*H*hh], [*H*hp] and [*H*pp] were evaluated for a trapezoidal region as described earlier and used in the computer program *HYBSLAB*.

[*G*hh] and [*G*pp]:

The matrices [*G*hh] and [*G*pp] are obtained from the following expressions of Equation 4.12:

$$[Ghh] = \int_S [NPh]^T \; [L] \; dS$$

$$[Gpp] = \int_S [NPp]^T \; [L] \; dS$$

The [*NP*] matrices are obtained from '*T*i *U*i' and for a plate bending element their form can be determined as indicated below in Equation 4.39. In this equation, n_1 and n_2 are the components of an outward unit normal vector located at a point on the element's boundary, and '*M*n' and '*M*nt' denote the normal and twisting moments at this same point. The ordinary transverse shear is denoted by '*Q*', (Kirchhoff's shear will be denoted by '*V*'). The indices ',' and ',', are used interchangeably with 'x' and 'y'.

$$\int_S Ti\ Ui\ dS$$

$$= \int_{\pounds} (-Mn\ W,n - Mnt\ W,t + Qn\ W)\ d\pounds$$

(or)

$$= \int_{\pounds} (-Mji\ nj\ W,i + Qi\ ni\ W)\ d\pounds$$

$$= \int_{\pounds} \{-(Mx\ n_1 + Myx\ n_2)(\theta y) - (Mxy\ n_1 + My\ n_2)(\theta x) + (Mx,x + Myx,y)(n_1)(W) + (Mxy,x + My,y)(n_2)(W)\}\ d\pounds$$

(and, in matrix operator form:)

$$= \int_{\pounds} \langle Mx\ ,\ My\ ,\ Mxy \rangle \begin{bmatrix} n_1\ (\ )_{,1} & \cdot & -n_1 \\ n_2\ (\ )_{,2} & -n_2 & \cdot \\ n_1\ (\ )_{,2} + n_2\ (\ )_{,1} & -n_1 & -n_2 \end{bmatrix} \begin{Bmatrix} W \\ \theta x \\ \theta y \end{Bmatrix} d\pounds$$

(or)

$$= \int_{\pounds} \underset{1x3}{\langle M \rangle}\ \underset{3x3}{[N]}^T\ \underset{3x1}{\{U\}}\ d\pounds \qquad (4.39)$$

(if $\langle M \rangle$ of the homogeneous solution is considered then;)

$$= \underset{1x17}{\langle \beta h \rangle} \int_{\pounds} \underset{17x3}{[Ph]}^T\ \underset{3x3}{[N]}^T\ \underset{3x6}{[L]}\ d\pounds\ \underset{6x1}{\{\underline{U}\}}$$

$$= \underset{1x17}{\langle \beta h \rangle} \int_{\pounds} \underset{17x3}{[NPh]}^T\ \underset{3x6}{[L]}\ d\pounds\ \underset{6x1}{\{\underline{U}\}} \qquad (4.40)$$

As indicated in the above equation, the product of [*N*] from Equation 4.39 and [*P*h] from Equation 4.35, provides the [*NP*h] matrix. The explicit form of [*NP*h] for one side of an element can be determined as:

$$[NPh]^T =$$

.	.	$-n_1$	β_1
$+n_1$	.	$-n_1x$	β_2
.	.	$-n_1y$	β_3
$n_1x - n_2y$	n_1xy	$-n_1x^2 + n_2xy$	β_4
n_1y	.	$-n_1xy$	β_5
.	.	$-n_1y^2$	β_6
.	$-n_2$	.	β_7
.	$-n_2x$	.	β_8
n_2	$-n_2y$	.	β_9
.	$-n_2x^2$	.	β_{10}
n_2x	$-n_2xy$	.	β_{11}
$-n_1x + n_2y$	$+n_1xy - n_2y^2$	n_2xy	β_{12}
.	$-n_1$	$-n_2$	β_{13}
n_2	$-n_1x$	$-n_2x$	β_{14}
n_1	$-n_1y$	$-n_2y$	β_{15}
$2\,n_2x$	$-n_1x^2$	$-n_2x^2$	β_{16}
$2\,n_1y$	$-n_1y^2$	$-n_2y^2$	β_{17}

(4.41)

Likewise, the form of $[NPp]$ can be calculated as:

$$[NPp]^T = \langle -(n_1x+n_2y)/2,\ +n_1xy/2,\ +n_2xy/2 \rangle \qquad (4.42)$$

The next step is to choose the shape functions of the matrix $[L]$ which relate edge displacements to nodal displacements. For an element side, defined by nodes 1 and 2, and orientation specified by n_1 and n_2, the Hermitian interpolation functions shown in Equation 4.43 were used. According to these interpolation functions, W and θt have a cubic variation between nodes, while θn varies linearly.

$$\underset{3x1}{\{U\}} = \underset{3x6}{[L]} \quad \underset{6x1}{\{\underline{U}\}} \qquad (4.43)$$

where,

$$\{U\} = \begin{Bmatrix} W \\ \theta x \\ \theta y \end{Bmatrix}, \quad \text{and} \quad \{\underline{U}\} = \begin{Bmatrix} W_1 \\ \theta x_1 \\ \theta y_1 \\ --- \\ W_2 \\ \theta x_2 \\ \theta y_2 \end{Bmatrix}$$

and,

$[L]$ =

$H^1_{0,1}$	$n_1\ H^1_{1,1}$	$-n_2\ H^1_{1,1}$	$H^1_{0,2}$	$n_1\ H^1_{1,2}$	$-n_2\ H^1_{1,2}$
$n_1\ dH^1_{0,1}$	$n_2^2\ H^0_{0,1}$ $+n_1^2\ dH^1_{1,1}$	$n_1 n_2 H^0_{0,1}$ $-n_1 n_2 dH^1_{1,1}$	$n_1\ dH^1_{0,2}$	$n_2^2\ H^0_{0,2}$ $+n_1^2\ dH^1_{1,2}$	$n_1 n_2 H^0_{0,2}$ $-n_1 n_2 dH^1_{1,2}$
$-n_2\ dH^1_{0,1}$	$n_1 n_2\ H^0_{0,1}$ $-n_1 n_2 dH^1_{1,1}$	$n_1^2\ H^0_{0,1}$ $+n_2^2\ dH^1_{1,1}$	$-n_2\ dH^1_{0,2}$	$n_1 n_2\ H^0_{0,2}$ $-n_1 n_2 dH^1_{1,2}$	$n_1^2\ H^0_{0,2}$ $+n_2^2\ dH^1_{1,2}$

where,

$H^0_{0,1} = 1 - \rho$

$H^0_{0,2} = \rho$

$H^1_{0,1} = 1 - 3\rho^2 + 2\rho^3$

$H^1_{0,2} = 3\rho^2 - 2\rho^3$

$H^1_{1,1} = £(\rho - 2\rho^2 + \rho^3)$

$H^1_{1,2} = £(-\rho^2 + \rho^3)$

$dH^1_{0,1} = 6(-\rho + \rho^2)/£$

$dH^1_{0,2} = 6(\rho - \rho^2)/£$

$dH^1_{1,1} = (1 - 4\rho + 3\rho^2)$

$dH^1_{1,2} = (-2\rho + 3\rho^2)$

and,

ρ = non-dimensional coordinate measured along the element side from node 1 to node 2

$£$ = length of the element side from node 1 to node 2.

To form the [Ghh] matrix, the matrix product of [*NP*h] [*L*] is integrated and the resultant matrix is called $[Ghh]_e$. The [Ghh] matrix is formed by a direct entry and summation procedure of the individual $[Ghh]_e$ matrices.

The procedure is repeated with the [*NP*p] and [*L*] matrices to obtain [Gpp].

[GHG]:

The stiffness matrix [GHG] and the equivalent load vector {Peq} can now be calculated from the set of equations shown below:

$$[GHG]_{mxm} = [Ghh]^T_{mx17}\ [Hhh]^{-1}_{17x17}\ [Ghh]_{17xm} \qquad (4.45)$$

(and)

$$\underset{1xm}{\langle Peq \rangle} = \underset{1x1}{\langle \beta p \rangle} \left(\underset{1x17}{[Hhp]^T} \underset{17x17}{[Hhh]^{-1}} \underset{17xm}{[Ghh]} - \underset{1xm}{[Gpp]} \right)$$

where, m = number of element degrees of freedom ≤ 18.

The procedure described in this section and the previous one has been used in a subroutine called 'STIFFS' of the program *HYBSLAB* to generate the in-plane and flexural stiffness matrices for the various shaped elements.

4.4 L-Shaped Singularity Elements

In this section, the effects of stress singularities at the reentrant corner of an L-shaped element are included in the formulation of the flexural stiffness matrix. It is assumed that the plate material is isotropic. Two types of elements are considered. The distinction between the two types is made on the basis of the boundary conditions along the two sides which meet at the reentrant corner. The first element type has 'free edge' conditions along these edges while the second type has 'fixed' or clamped edges.

The various matrices which are required to obtain a stiffness matrix are shown in Equations 4.16 and 4.18 of Section 4.1. The matrices [*H*hh], [*H*hp], [*H*pp], [*G*hh] and [*G*pp] have been dealt with in the previous section and can be reused without any changes. The remaining matrices [*H*ss], [*H*sh], [*H*sp], and [*G*ss] are still required and this section deals solely with these four matrices.

The formulation is based on a singularity deflection function, W_s. The form of this function was established and verified by Williams'[7] in the early 1950's. It consists of a trigonometric series and in terms of polar coordinates† it may be written as:

$$W_s = r^{(\lambda+1)} (F) (\beta_o) \qquad (4.46)$$

where,

$$F = C_1\sin(\lambda+1)\alpha + C_2\cos(\lambda+1)\alpha + C_3\sin(\lambda-1)\alpha + C_4\cos(\lambda-1)\alpha$$

r = radius from the reentrant corner to some point in the element (see Fig. 4.1),
λ = an eigenvalue determined from a characteristic equation,
C_i = $(i=1,2,3,4)$, constants of 'W_s' to be determined from the boundary conditions along the reentrant edges,
α = an in-plane angle defining the position of 'r' and serving as the rotational polar coordinate (see Fig. 4.1),
β_o = a 'stress singularity factor' which indicates the intensity of the singularity.

A sketch of a typical L-shaped element and its coordinate systems is shown in Figure 4.1. The derivation which will be presented in this section is valid for any orientation of the element. In Figure 4.1, point 1 is the reentrant corner and sides 'a' and 'f' which meet at point 1 will be referred to as the reentrant sides.

With the aid of the deflection function, W_s, the intended meaning of the term 'singularity' will now be explained. The type of singularity being considered here is

---

† Polar coordinates are most often represented by 'r' and 'θ', but since 'θ' is already being used for rotation of the midsurface, the polar coordinates will be denoted by 'r' and 'α'.

often referred to as a singularity of the 'first type''[3]. In this type of singularity the prime variable remains finite-valued or 'non-singular' but its derivatives can become unbounded or 'singular'. For the plate bending problem being considered here, one can be more specific and state that neither the prime variable, W_s, nor its first derivative are singular but that its second and third derivatives may become unbounded. The second derivatives are required to calculate moments while the third derivatives are needed to calculate shears, hence the terminology 'stress singularities'. All singularities referred to in this study are stress singularities. Also, unless otherwise noted, all moments and shears in this section will be those calculated from W_s of Equation 4.46.

Referring to Figure 4.1, along each of the reentrant sides 'a' and 'f' there exist two boundary conditions. From these conditions a set of four simultaneous equations can be obtained with the unknowns C_1, C_2, C_3, C_4 and λ. For both the free-free case and the fixed-fixed case, the boundary conditions are such that the set of equations is homogeneous; that is, the right hand side is a null vector. For these types of equation sets, a non-trivial solution can only be obtained for certain characteristic values or 'eigenvalues' of λ. The eigenvalues are obtained by setting the determinant of the coefficient matrix equal to zero and then solving for λ.

a) L-Shaped Element with Free Edge Conditions:

The derivation of the stiffness matrix [GHG] for the free edge element will begin by obtaining the λ values.

For both sides, 'a' and 'f', the free edge conditions are:

(1) the normal moment, $M\alpha = 0$.

(2) the Kirchhoff shear, $V = 0$.

In equation form, the zero moment condition can be written as:

$$M\alpha = -D\,[\, r^{(-2)}\, Ws,\alpha\alpha \;+\; r^{(-1)}\, Ws,r \;+\; \nu\, Ws,rr]$$

$$= -D\;\; r^{(\lambda-1)}\;\; [\; (\lambda+1)(1+\nu\lambda)\; F \;+\; \ddot{F}\;]$$

(and, for $M\alpha = 0$)

$$(\lambda+1)(1+\nu\lambda)\; F \;+\; \ddot{F} \;=\; 0 \qquad (4.47)$$

The Kirchhoff shear condition can be written as shown below, where $\nabla^2 W = W,rr + r^{(-1)}W,r + r^{(-2)}W,\alpha\alpha$.

$$V = -D\,[\, r^{(-1)}(\nabla^2 W),\alpha \;+\; (1-\nu)(r^{(-1)}Ws,r\alpha - r^{(-2)}Ws,\alpha),r]$$

$$= -D\;\; r^{(\lambda-2)}\;\; [\; ((\lambda+1)^2 + \lambda(1-\nu)(\lambda-1))\; \dot{F} \;+\; \dddot{F}\;]$$

(and, for $V = 0$)

$$[(\lambda+1)^2 + \lambda(1-\nu)(\lambda-1)]\; \dot{F} \;+\; \dddot{F} \;=\; 0 \qquad (4.48)$$

where,
(from Eq. 4.46)

$$F = C_1\sin(\lambda+1)\alpha + C_2\cos(\lambda+1)\alpha + C_3\sin(\lambda-1)\alpha + C_4\cos(\lambda-1)\alpha$$

and,

$$\dot{F} = F,\alpha = (\lambda+1)\,[C_1\cos(\lambda+1)\alpha - C_2\sin(\lambda+1)\alpha] + (\lambda-1)\,[C_3\cos(\lambda-1)\alpha - C_4\sin(\lambda-1)\alpha]$$

$$\ddot{F} = F,\alpha\alpha = (\lambda+1)^2\,[-C_1\sin(\lambda+1)\alpha - C_2\cos(\lambda+1)\alpha] + (\lambda-1)^2\,[-C_3\sin(\lambda-1)\alpha - C_4\cos(\lambda-1)\alpha]$$

$$\ddot{F} = F,_{\alpha\alpha\alpha} = (\lambda+1)^2 [-C_1\cos(\lambda+1)\alpha + C_2\sin(\lambda+1)\alpha] + (\lambda-1)^2 [-C_3\cos(\lambda-1)\alpha + C_4\sin(\lambda-1)\alpha]$$

and,

D = flexural rigidity of the plate

$$= E\,t^3/[12(1-\nu^2)]$$

By substituting the values of α for the two sides 'a' and 'f' into Equations 4.47 and 4.48, the set of four equations discussed earlier can be obtained. These equations are shown below:

$$\begin{bmatrix} a_1\sin(\lambda+1)a & +a_1\cos(\lambda+1)a & a_2\sin(\lambda-1)a & +a_2\cos(\lambda-1)a \\ a_3\cos(\lambda+1)a & -a_3\sin(\lambda+1)a & a_4\cos(\lambda-1)a & -a_4\sin(\lambda-1)a \\ a_1\sin(\lambda+1)f & +a_1\cos(\lambda+1)f & a_2\sin(\lambda-1)f & +a_2\cos(\lambda-1)f \\ a_3\cos(\lambda+1)f & -a_3\sin(\lambda+1)f & a_4\cos(\lambda-1)f & -a_4\sin(\lambda-1)f \end{bmatrix} \begin{Bmatrix} C_1 \\ C_2 \\ C_3 \\ C_4 \end{Bmatrix} = \begin{Bmatrix} 0 \\ 0 \\ 0 \\ 0 \end{Bmatrix} \quad (4.49)$$

where,

$a_1 = (\lambda+1)(1+\nu\lambda) - (\lambda+1)^2$

$a_2 = (\lambda+1)(1+\nu\lambda) - (\lambda-1)^2$

$a_3 = (\lambda+1)(1-\nu)(\lambda)(\lambda-1)$

$a_4 = (\lambda-1)[(\lambda+1)^2 + (1-\nu)(\lambda)(\lambda-1) - (\lambda-1)^2]$

and,

a = α value of side 'a'

f = α value of side 'f'

The characteristic equation from the above set of equations has trigonometric terms and there exist an infinite number of characteristic values which satisfy it. However, the eigenvalues required for this study are those between 0.0 and 2.0. The reasons for using this range are based on the behavior of the plate at the reentrant corner (r=0).

From a physical point of view, negative eigenvalues are not permissible because the transverse displacement and the

slopes at the reentrant corner must remain finite. A zero eigenvalue is of no interest because it results in the trivial solution, $W_s=0$.

The need for eigenvalues above 0.0 but less than 2.0 can be explained with the aid of Equations 4.47 and 4.48. Values between 0.0 and 1.0 cause singularities in both the moment and shear at the reentrant corner. Eigenvalues starting at 1.0 but less than 2.0 cause singularities in the shear only.

From the characteristic equation(4.49) the following five real eigenvalues were calculated:

$$\{\lambda\} = \begin{Bmatrix} 0.637865868034631 \\ 0.698211827331357 \\ 1.27520788054242 \\ 1.39718494820201 \\ 1.91141012573973 \end{Bmatrix}$$

There are no complex eigenvalues for this case.

To obtain the constants C_i (i=1,2,3,4), only three of the four equations of 4.49 are independent and a solution can only be obtained in terms of one of the C_i constants. The remaining equation can be used to check the accuracy of the computations. In this study, the equations were normalized with respect to C_4 and a large number of digits for the λ values were required to satisfy the 'checking' equation. This was especially true for the second and third eigenvalues.

With λ and the C_i constants evaluated, the deflection function, W_s, now contains only the three unknowns 'r', 'α',

and 'β_o'. In the process of evaluating the Πmc functional, values are assigned to the polar coordinates and therefore the only unknown which remains is 'β_o'.

Since Ws is available, it is advantageous to express the strain energy in terms of line integrals rather than area integrals. This can be done by using Gauss' theorem as shown below:

$$\int_A Mij\ Dijkl\ Mkl\ dA$$

$$= \int W,ij\ Eijkl\ W,kl\ dA$$

$$= \int (W,i\ Eijkl\ W,kl),j\ dA - \int (W\ Eijkl\ W,jkl),i\ dA + \int (W\ Eijkl\ W,ijkl)\ dA$$

$$= -\oint (Mji\ nj\ W,i)\ d\pounds + \oint (Qi\ ni\ W)\ d\pounds - \int q\ W\ dA$$

$$= \oint \langle Qi\ ni,\ -M_{i2}\ ni,\ -M_{i1}\ ni \rangle \begin{Bmatrix} W \\ W,_2=\theta x \\ W,_1=\theta y \end{Bmatrix} d\pounds - \int q\ W\ dA \qquad (4.50)$$

where,
$q = q(x,y)$ = transverse loading on the plate.

There are a number of reasons for making the above conversion and some of these are discussed below.

First, when using numerical integration to integrate non-polynomial expressions it is usually computationally more efficient to evaluate the line integrals than an area integral. This is especially true when the integrand involves a trigonometric series and the value of the integral can only be approximated.

Second, since [*H*ss], [*H*sh] and [*H*sp] can now be evaluated by either an area integral or a line integral, this provides a convenient means of checking the computations of a computer program. This was done in the program which was used to obtain the stiffness matrices for the singularity example problems of Chapter 6.

The third reason may be the most important of all. In some circumstances, even though the area integral itself is finite-valued, its integrand may at times be singular. For such cases, the change from an area to a line integral may eliminate this problem.

[*H*hs], [*H*ps], and [*H*ss]:

The expression '(-*M*ji *n*j *W*,i) + (*Q*i *n*i *W*)' appears in both Equations 4.50 and 4.39 and is the product of two vectors. One vector is '<*Q*i *n*i, $-M_{i_2}$ *n*i, $-M_{i_1}$ *n*i>' and it was shown in Equations 4.39 and 4.40 that it could be rewritten as a matrix product '<β >[*NP*]'.

The other vector, as indicated in Equation 4.50, consists of *W* and its first derivatives. If this vector is rewritten in the form '[*Bw*]{βs}' then [*H*hs], [*H*ps], and [*H*ss] can be written directly from Equation 4.50 as:

$$\int {}^{h}_{Mij}\, D_{ijkl}\, {}^{s}_{Mkl}\, dA = \underset{1x17}{\langle \beta h \rangle} \int \underset{17x3}{[NPh]^{T}} \underset{3xe}{[Bw]}\, d\pounds \underset{ex1}{\{\beta s\}} \qquad (4.51a)$$

$$= \langle \beta h \rangle\, [Hhs]\, \{\beta s\}$$

$$\int {}^{p}_{}M_{ij}\, D_{ijkl}\, {}^{s}_{}M_{kl}\, dA = \underset{1x1}{\langle \beta p \rangle} \int \underset{1x3}{[NPp]^{T}} \underset{3xe}{[Bw]}\, d\pounds \underset{ex1}{\{\beta s\}} - \int \underset{1xe}{q\langle \bar{W}s \rangle} dA \underset{ex1}{\{\beta s\}}$$

$$= \langle \beta p \rangle\, [Hps]\, \{\beta s\} \qquad (4.51b)$$

$$\int {}^{s}_{}M_{ij}\, D_{ijkl}\, {}^{s}_{}M_{kl}\, dA = \underset{1xe}{\langle \beta s \rangle} \int \underset{ex3}{[NPs]^{T}} \underset{3xe}{[Bw]}\, d\pounds \underset{ex1}{\{\beta s\}}$$

$$= \langle \beta s \rangle\, [Hss]\, \{\beta s\} \qquad (4.51c)$$

where,

e = number of eigenvalues being considered,

$\bar{W}s$ = set of Ws displacement functions but with the β_s factors omitted.

The only matrices in the above equations which have not been explained as yet are $[NPs]$ and $[Bw]$. This will be done now.

The $[NPs]$ matrix could be calculated from the product of $[N]$ and $[Ps]$ in the manner described earlier for $[NPh]$. This time however, rather than working with a $[Ps]$ matrix, $[NPs]$ will be obtained directly from Equation 4.50 by expanding the vector $\langle Qi\,ni,\ -M_{i,2}\,ni,\ -M_{i,1}\,ni \rangle$. Each term of this vector can be written as:

$$Qi\ ni = (Mx,x + Myx,y)\ n_1 + (Mxy,x + My,y)\ n_2 \qquad (4.52a)$$

$$-M_{i,2}\ ni = -Mxy\ n_1 - My\ n_2 \qquad (4.52b)$$

$$-M_{i,1}\ ni = -Mx\ n_1 - Myx\ n_2 \qquad (4.52c)$$

where,

$$Mx,x = \cos\alpha\ Mx,r - r^{(-1)} \sin\alpha\ Mx,\alpha$$

$$Myx,y = \sin\alpha\ Myx,r + r^{(-1)} \cos\alpha\ Myx,\alpha$$

$$Mxy,x = \cos\alpha\ Mxy,r - r^{(-1)} \sin\alpha\ Mxy,\alpha$$

$$My,y = \sin\alpha\ My,r + r^{(-1)} \cos\alpha\ My,\alpha$$

and,

$$\cdots\cdots\cdots\cdots\cdots\cdots\cdots\cdots$$

$$Mx = -D\ r^{(\lambda-1)}\ G_1\ \beta_0$$

$$Mx,r = -D\ r^{(\lambda-2)}\ (\lambda-1)\ G_1\ \beta_0$$

$$Mx,\alpha = -D\ r^{(\lambda-1)}\ \dot{G}_1\ \beta_0$$

where,

$$G_1 = [(\cos\alpha^2+\nu\sin\alpha^2)(\lambda^2+\lambda) + (\sin\alpha^2+\nu\cos\alpha^2)(\lambda+1)]\ F - 2(\cos\alpha\ \sin\alpha)(1-\nu)(\lambda)\ \dot{F} + (\sin\alpha^2+\nu\cos\alpha^2)\ \ddot{F}$$

$$\dot{G}_1 = -2(\cos\alpha\ \sin\alpha)(1-\nu)(\lambda^2-1)\ F + [-2(\cos\alpha^2-\sin\alpha^2)(1-\nu)\lambda + (\cos\alpha^2+\nu\sin\alpha^2)(\lambda^2+\lambda) + (\sin\alpha^2+\nu\cos\alpha^2)(\lambda+1)]\ \dot{F} + 2(\cos\alpha\ \sin\alpha)(1-\nu)(1-\lambda)\ \ddot{F} + (\sin\alpha^2+\nu\cos\alpha^2)\ \dddot{F}$$

$$\cdots\cdots\cdots\cdots\cdots\cdots\cdots\cdots$$

$$My = -D\ r^{(\lambda-1)}\ G_2\ \beta_0$$

$$My,r = -D\ r^{(\lambda-2)}\ (\lambda-1)\ G_2\ \beta_0$$

$$My,\alpha = -D\ r^{(\lambda-1)}\ \dot{G}_2\ \beta_0$$

where,

$$G_2 = [(\sin\alpha^2+\nu\cos\alpha^2)(\lambda^2+\lambda) + (\cos\alpha^2+\nu\sin\alpha^2)(\lambda+1)]\ F + 2(\cos\alpha\ \sin\alpha)(1-\nu)(\lambda)\ \dot{F} + (\cos\alpha^2+\nu\sin\alpha^2)\ \ddot{F}$$

$$\dot{G}_2 = 2(\cos\alpha\ \sin\alpha)(1-\nu)(\lambda^2-1)\ F + [2(\cos\alpha^2-\sin\alpha^2)(1-\nu)\lambda + (\sin\alpha^2+\nu\cos\alpha^2)(\lambda^2+\lambda) + (\cos\alpha^2+\nu\sin\alpha^2)(\lambda+1)]\ \dot{F} + 2(\cos\alpha\ \sin\alpha)(1-\nu)(\lambda-1)\ \ddot{F} + (\cos\alpha^2+\nu\sin\alpha^2)\ \dddot{F}$$

$$\cdots\cdots\cdots\cdots\cdots\cdots\cdots\cdots$$

$$Mxy = -D\ r^{(\lambda-1)}\ (1-\nu)\ G_3\ \beta_0$$

$$My,r = -D\ r^{(\lambda-2)}\ (1-\nu)\ (\lambda-1)\ G_3\ \beta_o$$

$$My,\alpha = -D\ r^{(\lambda-1)}\ (1-\nu)\ \dot{G}_3\ \beta_o$$

where,

$$G_3 = (\cos\alpha\ \sin\alpha)(\lambda^2-1)\ F + (\lambda)(\cos\alpha^2-\sin\alpha^2)\ \dot{F} - (\cos\alpha\ \sin\alpha)\ \ddot{F}$$

$$\dot{G}_3 = (\cos\alpha^2-\sin\alpha^2)(\lambda^2-1)\ F + (\cos\alpha\ \sin\alpha)[-4\lambda + (\lambda^2-1)]\ \dot{F} + (\cos\alpha^2-\sin\alpha^2)(\lambda-1)\ \ddot{F} - (\cos\alpha\ \sin\alpha)\ \dddot{F}$$

.....

The matrix [*NP*s] can now be written as:

$$[NPs]\ \{\beta s\} =$$

$Qi\ ni/\ \beta_{o,1}$	<-----//------->
$-M_{i,2}\ ni/\ \beta_{o,1}$	repeat for each
$-M_{i,1}\ ni/\ \beta_{o,1}$	eigenvalue

(3xe)

$$\begin{Bmatrix} \beta_{o,1} \\ \beta_{o,2} \\ \cdot \\ \cdot \\ \cdot \\ \beta_{o,e} \end{Bmatrix}$$

(ex1)

(4.53)

The '$/\ \beta_{o,1}$' term simply indicates that [*NP*s] consists of the expressions given in Equations 4.52a) to 4.52c) but with the unknown term 'β_o' factored out. Therefore [*NP*s] contains only known quantities and can be calculated from the information given in Equations 4.52.

Equation set 4.52 also contains all the information required to calculate [*H*sh], [*H*sp], [*H*ss] from area integrals. To evaluate these same matrices by using the

line integral approach the [Bw] matrix is still required.

The [Bw] matrix is calculated from Ws and its first derivatives according to:

$[Bw]\ \{\beta s\} =$

$$\begin{array}{|l|l|} \hline Ws/\ \beta_{o,1} & \text{<-----//-------->} \\ \hline -Ws_{,2}/\ \beta_{o,1} & \text{repeat for each} \\ \hline -Ws_{,1}/\ \beta_{o,1} & \text{eigenvalue} \\ \hline \end{array} \quad \begin{Bmatrix} \beta_{o,1} \\ \beta_{o,2} \\ \cdot \\ \cdot \\ \cdot \\ \beta_{o,e} \end{Bmatrix}$$

(3xe) (ex1) (4.54)

where,

$$Ws = r^{(\lambda+1)}\ F\ \beta_o$$

$$Ws_{,2} = \sin\alpha\ Ws,r + r^{(-1)} \cos\alpha\ Ws,\alpha$$

$$= r^{(\lambda)} [(\lambda+1) \sin\alpha\ F + \cos\alpha\ \dot{F}]\ \beta_o$$

$$Ws_{,1} = \cos\alpha\ Ws,r - r^{(-1)} \sin\alpha\ Ws,\alpha$$

$$= r^{(\lambda)} [(\lambda+1) \cos\alpha\ F - \sin\alpha\ \dot{F}]\ \beta_o$$

[Gss]:

The only remaining matrix which has not been discussed thus far is [Gss]. This matrix is calculated from the following expression of Equation 4.12.

$$[Gss] = \int_{\ell} [NPs]^T\ [L]\ d\ell$$

Since [NPs] has just been discussed, and [L] was given in Equation 4.27 of the previous section, [Gss] can be calculated by the procedure described in the last section.

[GHG]:

The stiffness matrix [GHG] can now be obtained from the expressions of Equation 4.18 which are repeated below:

$$[GHG]_{18x18} = [Ghhss]^{T}_{18xf}\,[Hhhss]^{-1}_{fxf}\,[Ghhss]_{fx18}$$

and,

$$\langle Peq \rangle_{18x1} = \langle \beta p \rangle_{1x1}\,([Hhsp]_{1xf}\,[Hhhss]^{-1}_{fxf}\,[Ghhss]_{fx18} - [Gpp]_{1x18})$$

where,
f = 17 + e, (e = the number of eigenvalues).

Before proceeding with the next element, a problem which was encountered at the reentrant corner will be discussed. In evaluating the singularity line integrals for [Gss] along element sides 'a' and 'f', problems were encountered with the terms '$r^{(\lambda-1)}$' and '$r^{(\lambda-2)}$' at the reentrant corner (r=0). To overcome this problem the expression '$(-Mn\,W,n - Mnt\,W,t + Qn\,W)\,d\pounds$' from Equation 4.39 was rewritten as:

$$\int_{\pounds} (-Mn\,W,n - Mnt\,W,t + Qn\,W)\,d\pounds$$

$$= \int_{\pounds} [-(Mn\,W,n) - (Mnt\,W),t + (Mnt,t\,W) + (Qn\,W)]\,d\pounds$$

(and, when integrated from point 1 to point 2)

$$= -(Mnt\,W)]_{1}^{2} + \int [-(Mn\,W,n) + (Mnt,t + Qn)(W)]\,d\pounds \qquad (4.55)$$

For the following reasons the integrand in the above

equation is zero. The quantity '(*M*n *W*,n)' is zero because the normal moment, *M*n, is zero along the free edges. The remaining part of the integrand is zero because the quantity '(*M*nt,t + *Q*n)' is the Kirchhoff shear and it also is zero along free edges.

Therefore, the '*T*i *U*i' contribution of the two free edges to the [*G*ss] matrix simply consists of the quantity '(*M*nt *W*)]' evaluated at corners 1,2, and 6 of the element shown in Figure 4.1. Since the contributions of sides 'a' and 'f' at point 1 are equal but opposite, only points 2 and 6 have to be considered.

b) L-Shaped Element with Fixed Edge Conditions:

The stiffness matrix for an L-shaped element with clamped reentrant edges is described in this part. For this case, the eigenvalues of interest consist of one real number and a conjugate pair of complex numbers.

After the real eigenvalue and related C_i constants have been determined, then the procedure outlined in part a) of this section can be used without any modifications.

In order to include the complex eigenvalues considerable revision is required to most of the presentation given thus far in this section. Because substantially more work is still required and because of the time factor involved, these values were not included in this study. Assessing the importance of the complex eigenvalues in the formulation of

the stiffness matrix is left as a subject for future research.

The remainder of this section deals with the calculation of the eigenvalues for the case where edges 'a' and 'f' are assumed to be clamped. Along these two edges the boundary conditions are:

(1) the transverse displacement, $W_s = 0.$

(2) the normal rotation, $W_{s,\alpha} = 0.$

In equation form, the zero transverse displacement condition can be written as:

$$W_s = -D\ r^{(\lambda+1)}\ F\ \beta_o = 0.$$

(and, for $r^{(\lambda+1)} \neq 0$, $\beta_o \neq 0$)

$$F = 0. \qquad (4.56)$$

(or)

$$C_1\sin(\lambda+1)\alpha + C_2\cos(\lambda+1)\alpha + C_3\sin(\lambda-1)\alpha + C_4\cos(\lambda-1)\alpha = 0$$

The zero normal slope condition can be written as:

$$W_{s,\alpha} = -D\ r^{(\lambda+1)}\ \dot{F}\ \beta_o = 0.$$

(and, for $r^{(\lambda+1)} \neq 0$, $\beta_o \neq 0$)

$$\dot{F} = 0. \qquad (4.57)$$

(or)

$$(\lambda+1)\ [C_1\cos(\lambda+1)\alpha - C_2\sin(\lambda+1)\alpha] + (\lambda-1)\ [C_3\cos(\lambda-1)\alpha - C_4\sin(\lambda-1)\alpha] = 0.$$

By substituting the values of α for the two sides 'a' and 'f' into Equations 4.56 and 4.57, the set of four

equations can be obtained. These equations are shown below:

$$\begin{bmatrix} \sin(\lambda+1)a & \cos(\lambda+1)a & \sin(\lambda-1)a & \cos(\lambda-1)a \\ a_1\cos(\lambda+1)a & -a_1\sin(\lambda+1)a & a_2\cos(\lambda-1)a & -a_2\sin(\lambda-1)a \\ \sin(\lambda+1)f & \cos(\lambda+1)f & \sin(\lambda-1)f & \cos(\lambda-1)f \\ a_1\cos(\lambda+1)f & -a_1\sin(\lambda+1)f & a_2\cos(\lambda-1)f & -a_2\sin(\lambda-1)f \end{bmatrix} \begin{Bmatrix} C_1 \\ C_2 \\ C_3 \\ C_4 \end{Bmatrix} = \begin{Bmatrix} 0 \\ 0 \\ 0 \\ 0 \end{Bmatrix} \tag{4.58}$$

where,

$a_1 = (\lambda+1)$

$a_2 = (\lambda-1)$

and,

α_1 = α value of side 'a'

α_2 = α value of side 'f'

As discussed earlier, the only eigenvalues of interest for this study are those between 0.0 and 2.0. From the characteristic equation of 4.58 the following eigenvalues were calculated:

$$\{\lambda\} = \begin{Bmatrix} 0.54448 \\ 1.62925 \pm 0.23125\ i \end{Bmatrix}$$

For the real eigenvalue, a stiffness matrix was calculated according to the procedure described in Part a) of this section. This stiffness matrix was then used for an example problem in Chapter 6.

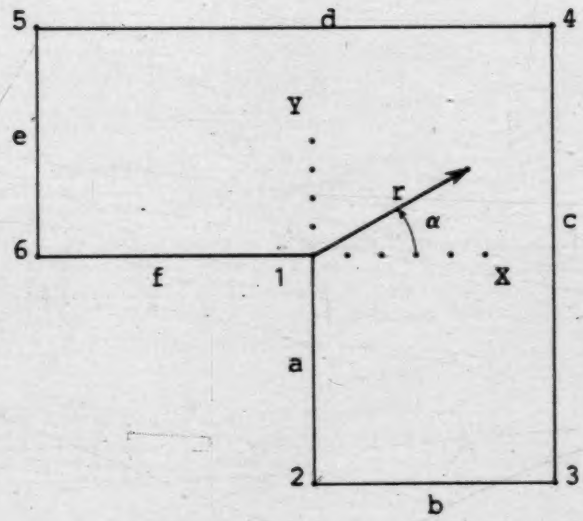

Figure 4.1 Typical L-Shaped Element and Coordinate Systems.

Chapter 5

THE COMPUTER PROGRAM '*HYBSLAB*'

5.1 Introduction

The hybrid stress finite element method as described in the previous chapter was used as the basis for a Fortran IV computer program called *HYBSLAB*. The program was written for the elastic analysis of flat plate structures with the intent that it could be used for analysing the type of floor systems typically found in buildings.

From a technical point of view, for a program to serve such a purpose it must not only be capable of providing stiffness matrices for a variety of element shapes but it must also be capable of modelling beams which are eccentric to the plate. As well, in certain situations it may be desirable to model the columns not only as point supports but also as finite-sized members.

From a practical point of view, any program intended for design office use must be cost-competitive. This means that the time spent in the preparation and checking of input data and the interpretation of the output must be kept to a minimum. As well, the cost of 'running' the program must not be unreasonable.

In addition to the time factor and the data checking demands, the user of a finite element program is also faced with the challenge of choosing a gridwork which will provide

values suitable for the design phase. The choosing of gridworks is best learned through repeated use of the finite element method, but it is hoped that the test cases of Chapter 3 and the example problems of the next chapter may provide some guidelines.

There are very few programs available which have the features and capabilities discussed thus far, and none of these are based on the hybrid stress method. The remainder of this chapter is devoted to explaining how the program *HYBSLAB* has been written to meet the technical and practical requirements discussed so far. The presentation consists of a general description of the program in the next section, followed by two more sections which deal with the modelling of beams and columns.

5.2 General Description

The program *HYBSLAB* is based on the hybrid stress method and the stress functions and related matrices as presented in the previous chapter. The calculation of stiffness matrices for the L-shaped singularity elements has not been included directly in the program. However, these matrices and the associated load vectors are available from another program and can be accessed by *HYBSLAB*.

The derivation of flexural stiffness matrices for quadrilateral and polygonal shapes by the hybrid stress method is relatively easy when compared to the other

methods. Therefore, the focal point of technical interest is probably the subroutine 'STIFFS' which calculates the in-plane and flexural stiffness matrices for the various shaped elements. As mentioned earlier, the element shapes may vary from a triangle to a polygon with six nodes or less. Some possible element configurations are shown in Figure 5.1.

In the subroutine 'STIFFS' the strain energy of the element is evaluated in a piecewise manner by explicit integration of the stress polynomials over trapezoidal regions. The individual [*H*hh], [*H*hp] and [*H*pp] matrices are then summed to obtain the corresponding matrices for the element as a whole. The orientation of a typical trapezoid and the limits of integration are shown in Figure 5.2.

In the present version of *HYBSLAB*, the local coordinates axes of an element may be placed at any location relative to the global axes but the two sets must remain parallel. As discussed in Section 4.2, the lack of complete order expressions for the in-plane stress polynomials suggests a potential problem with lack of invariance. To assess the significance of the lack of complete quadratic expressions, tests were conducted where rectangular grids were rotated in the X-Y plane. The tests consisted of a rectangular 2x2 grid with minimal support provided at two corners and a point load applied at a third corner. The tests indicated that, even though the grids were rotated, the displacements at all nodes remained invariant. This

appears to suggest that the contribution from the quadratic terms is insignificant.

The potential of edge tractions as described in the previous chapter requires the evaluation of line integrals necessary for the calculation of the [Ghh] and [Gpp] matrices. In the current version of the program these integrals are evaluated by using a Gaussian numerical integration procedure. This completes the discussion of the subroutine 'STIFFS'. The program has a number of other technical features which may be of interest.

Provisions have been made in the program to accommodate the singularity elements and other elements for which *HYBSLAB* cannot generate a stiffness matrix and load vector. For example, the stiffness matrix and load vector for the singularity elements are generated by the singularity program and are stored in a file which is later accessed by *HYBSLAB*. This file is separate from the file which contains the data for the main problem and will be referred to as an auxiliary file.

To model eccentric stiffeners, the user can use either beam elements or other plate elements which have midsurfaces offset from the midsurface of the main plate. Details of this procedure are given in the next section.

The effects of columns may be lumped at a single node or the finite dimensions of the column cross section may be represented. A more detailed discussion of this topic is contained in the last section.

The program has a number of special features that may be required for certain problems. For example, the user may specify non-zero values for any degree of freedom or constrain two or more degrees of freedom to have the same value. As well, additional stiffness may be added to the diagonal term associated with any degree of freedom.

The solution for nodal displacements is obtained by using an in-core banded Gaussian elimination routine. The problem size that may be solved with the present version on the AMDAHL 470/V8 is 1500 unknowns with a semi-band of 80. These values may be varied subject to the condition that their product must be compatible with the in-core storage limits of the computer facility being used.

The following measures have been taken to assist the user with the practical aspects of time and cost, and error detection.

The input data may be specified in one of three ways, which will be referred to as 'automatic', 'semi-automatic' and 'manual'. The automatic data generating subroutine, called 'RECDAT', is specifically intended for rectangular element gridworks and requires very little input from the user. The semi-automatic data generating subroutine, called 'LINDAT', operates from 2 two-dimensional integer matrices, one of which contains the joint numbers of the structure while the other contains the element numbers. The input required for this subroutine basically consists of specifying the rows of the matrices, but with provisions

made to automatically generate subsequent rows from any given row and numbers within a row. The third method is to manually specify the input data, element by element. This is the most inefficient and time-consuming way to prepare the data and should only be used when no other option is available. To provide the user with added flexibility in data preparation, all three methods may be used at the same time in a given problem.

To reduce computational costs, elements with identical stiffness matrices are placed in the same group so that only one element stiffness matrix needs to be calculated.

After the input data has been prepared, the user can run the program without calculating any stiffness matrices and create an auxiliary data file. This data file can then be used to produce a drawing of the structure complete with node and element numbers. This type of graphical display provides a quick and easy means of detecting errors in the connectivity data of the structure.

The program output for each load case consists of the nodal displacements and rotations, element nodal and centre point stress values, and internal nodal forces. As well, at each node, stresses averaged from the values associated with the adjoining elements are printed along with the principal flexural stresses.

The solution output may also be obtained in a graphical form. In the current version of the program, two auxiliary files are required to store output data for contour plots.

The first of these files contains the nodal values of the transverse displacement, while the second file contains the averaged nodal values of *Mx*, *My*, *Mxy*, *Mp*, and Mp_2, where *Mp*, and Mp_2 are the principal moments. For example, in the design of reinforced concrete slabs if the reinforcing is to be placed in the X and Y coordinate directions, then contour plots of the orthogonal moments *Mx* and *My* would be most useful. If these plots are done to the same scale as the working drawings, then the designer can do the steel layout directly on the contour drawings. Examples of such moment plots are provided in Chapter 7.

5.3 Modelling of Eccentric Stiffeners

When a plate is stiffened by a beam which has its centroidal axis in a plane not coinciding with the plate's midsurface, then in-plane or membrane strains are introduced into the structure. The applied loads are carried jointly by flexural action and membrane action in proportion to the relative rigidities of the plate and the beam and the amount of eccentricity. In order to analyse these types of structures it is necesary to consider not only the geometric degrees of freedom, $< W , \theta x , \theta y >$, but also, the in-plane displacements, $< U , V >$. Before describing the method used in *HYBSLAB*, a brief discussion will be given of some of the more common methods used in the past.

Prior to the finite element era, three general methods were used to analyse plates with integral stiffeners. The first method was to replace the plate and beam structure with an equivalent grillage. The second method was to apply orthotropic plate theory to the problem and replace the beam and plate system by an equivalent orthotropic plate. The third approach ignores the interface shear between the beam and the plate but then adjusts the flexural stiffness of the beam to compensate for the composite action. All three approaches have the disadvantage of requiring considerable engineering judgement in assigning equivalent properties. As well, the final results are for an equivalent member from which it may be impossible to separate the beam forces.

In the finite element method, the use of beam elements with plate elements appears to have started in the late 1960's with the work of Zienkiewicz and co-workers[20],[42],[5]. In one of these publications, Davies, Parekh, and Zienkiewicz[5] compared finite element analysis against test results from perspex models for plates with concentric and eccentric edges beams. They modelled the eccentric beams both by vertical plate elements and by an equivalent concentric beam which had its moment of inertia calculated from the composite cross section. They found that the more accurate approach was to use the equivalent concentric beam. The advantage of the concentric beam approach is that in-plane degrees of freedom are not required. The disadvantage is that an effective flange width must be

assumed in order to locate the neutral axis of the composite section.

An alternative to the equivalent concentric beam approach is to calculate the stiffness matrix of a rectangular beam about its own centroid and then transfer it to the midsurface of the plate. The transfer is done by pre- and post-multiplying the beam matrix by a linear transformation matrix. In essence, the transformation matrix relates the nodal actions by attaching the beam node to the plate node by a rigid bar. This is equivalent to specifying that plane sections remain plane. Even though this method introduces additional unknowns in the form of in-plane degrees of freedom, it has become quite popular because it does away with estimating the location of the neutral axis in the composite section. This approach has been used in the SAP4 computer program and will also be used in *HYBSLAB*. In this study it will be referred to as the 'coupling' approach. However, before proceeding with the details of the transformation matrix, it is necessary to draw attention to an error introduced by this method.

The nature of the error was identified in 1977 by Gupta and Ma''. The error arises from a conflict in describing the axial displacement field of the beam element. If plane sections are assumed to remain plane, then a rotation at a node in the plate causes the axial displacements in the beam to vary according to the plate functions. The plate functions are usually quadratic or higher order and the

conflict arises because a linear function was used to derive the beam's axial stiffness. The magnitude of the error is problem dependent and is discussed in more detail in the next chapter. It is important to note that published articles tend to exaggerate the error by not using the overall height of the beam. This is illustrated in the next chapter and measures which can be taken to reduce the error are discussed.

An obvious solution to the problem is to eliminate the error entirely by adding intermediate axial displacement degrees of freedom to the beam element. Such a solution was published in 1980 by Miller[39], but it has the drawback that the additional degrees of freedom cannot be eliminated until after the beam matrix has been combined with the plate matrices.

The stiffness matrix for the beam element and the linear transformation matrix which were used in *HYBSLAB* will now be presented. The beam axis is initially assumed to be parallel to the global X axis. To obtain the stiffness matrix of the beam in terms of the global coordinates, it is necessary to pre- and post-multiply the centroidal matrix by a transformation matrix. Since the beam's centroidal 10x10 stiffness matrix consists of four very similar submatrices, it is necessary to consider only one of the submatrices. The 5x5 submatrices have terms which are identical except for the signs and each submatrix is of the form:

$$[\underline{K}] = \begin{bmatrix} k_1 & . & k_4 & . & . \\ . & k_2 & . & . & . \\ k_7 & . & k_3 & . & . \\ . & . & . & k_4 & . \\ . & . & . & . & k_5 \end{bmatrix} \qquad (5.1)$$

The stiffness submatrix in the global X-Y plane is $[Te]^T[\underline{K}][Te]$ where the terms of of [Te] are given below in Equation 5.2. In this matrix, the offsets between the beam and the plate node are e_1 and e_2, where e_1 is measured in the +Y direction and e_2 along the +Z direction.

$$[Te] = \begin{bmatrix} 1.0 & -e_1 & . & . & . \\ . & 1.0 & . & . & . \\ . & . & 1.0 & . & . \\ . & . & +e_2 & 1.0 & . \\ . & +e_2 & . & . & 1.0 \end{bmatrix} \qquad (5.2)$$

where,

e_1 = Y(plate) - Y(beam)
e_2 = Z(plate) - Z(beam)

If the beam is to be rotated in plan (X-Y plane) then it is also necessary to pre- and post-multiply by a rotational transformation matrix [Tr]. The final form of the beam submatrix in the global system will be denoted as [Kb] and can be written as:

$$[Kb] = [Tr]^T[Te]^T[\underline{K}][Te][Tr] \qquad (5.3)$$

where,

$$[Tr] = \begin{bmatrix} 1.0 & . & . & . & . \\ . & +c & +s & . & . \\ . & -s & +c & . & . \\ . & . & . & +c & -s \\ . & . & . & +s & +c \end{bmatrix}$$

and,

c = cos(γ),
s = sin(γ),
γ = the angle between the global X axis and the beam's longitudinal axis (positive counterclockwise).

In explicit form [Kb] can be written as:

[Kb]=

$+k_1$	$-ce_1k_1 + sk_4$	$+se_1k_1 + ck_4$	.	.
$-ce_1k_1$ $+sk_7$	$c^2e_1^2k_1-cse_1k_4$ $+c^2k_2-cse_1k_7$ $+s^2k_3+s^2e_2^2k_4$ $+c^2e_2^2k_5$	$-cse_1^2k_1-csk_2+$ $s^2e_1k_7-c^2e_1k_4$ $+csk_3+cse_2^2k_4$ $-cse_2^2k_5$	$+cse_2k_4$ $-cse_2k_5$	$+s^2e_2k_4$ $+c^2e_2k_5$
$+se_1k_1$ $+ck_7$	$-cse_1^2k_1-csk_2+$ $s^2e_1k_4-c^2e_1k_7$ $+csk_3+cse_2^2k_4$ $-cse_2^2k_5$	$s^2e_1^2k_1+cse_1k_4$ $+s^2k_2+cse_1k_7$ $+c^2k_3+c^2e_2^2k_4$ $+s^2e_2^2k_5$	$+c^2e_2k_4$ $+s^2e_2k_5$	$+cse_2k_4$ $-cse_2k_5$
.	$+cse_2k_4$ $-cse_2k_5$	$+c^2e_2k_4$ $+s^2e_2k_5$	$+c^2k_4$ $+s^2k_5$	$+csk_4$ $-csk_5$
.	$+s^2e_2k_4$ $+c^2e_2k_5$	$+cse_2k_4$ $-cse_2k_5$	$+csk_4$ $-csk_5$	$+s^2k_4$ $+c^2k_5$

(5.4)

where,

$k_1 = 12\ E\ Ix/\ L^3$
$k_2 = G\ J/\ L$
$k_3 = 4\ E\ Ix/\ L$
$k_4 = E\ A/\ L$
$k_5 = 12\ E\ Iy/\ L^3$
$k_6 = 6\ E\ Ix/\ L^2$
$k_7 = 6\ E\ Ix/\ L^2$

Signs for Submatrix:

(1,1)	(2,2)	(1,2)
+	+	-
+	+	-
+	+	+
+	+	-
+	+	-
+	-	+
+	-	-

and,

E = modulus of elasticity,
G = shear modulus,
Ix = moment of inertia resisting *W* displacements,
Iy = moment of inertia resisting *V* displacements,
J = St. Venant's uniform torque constant,
L = length of the beam.

The matrix shown above in Equation 5.4 was used in the program *HYBSLAB*.

The process described thus far has dealt with the representation of eccentric line beams. Provisions have also been made to allow the user to model the finite width of a beam. When this option is used the beam will be referred to as a wide beam.

To model wide beams, thick plate elements are used and the stiffness matrix which is calculated at the midsurface of the thick plate is transferred to the global midsurface by pre- and post-multiplying it by a transformation matrix. The transformation matrix consists of diagonal submatrices obtained from [Te] of Equation 5.2 but with $e_i=0$.

5.4 Modelling of Columns

Typically, floor systems of buildings are supported either by columns or by load bearing walls or a combination of the two. The column support dimensions are usually of the same order of magnitude as the plate or slab thickness and are considerably less than the span dimensions. For these cases it is customary to assume that the plate is resting on point supports. In making this assumption, a concern immediately arises because, according to plate theory, even though the deflections at a point support remain finite the bending moments and shears become infinite. Because of this stress singularity, it is not clear if a numerical method such as the finite element method can provide meaningful stress results in the vicinity

of the column. This problem was investigated in connection with slab bridges by Cheung, King and Zienkiewicz[12] in 1968. By comparing moment contours from the finite element method against those from an exact solution, they concluded that despite the singularity even the coarsest subdivision (a 4x4 triangular grid / quarter plate) illustrated the trend accurately and gave values suitable for engineering design.

In the program *HYBSLAB* provisions have been made to allow the designer to use either point-sized or finite-sized columns. To use either type of column, the program requires as input the column's axial and flexural stiffnesses at the location where the column and the midsurface of the plate meet. Since these values are very much dependent on the far end conditions, the material properties of the column, and the joint connection detail, the assigning of these values is left solely to the discretion of the engineer. The remaining input consists of the X and Y coordinates for the column centroid and the joint numbers to which the centroidal stiffnesses are to be distributed.

For finite-sized columns, the joints to which the distribution is made are those which lie on the perimeter of the column. The distribution is done in such a manner that two conditions are satisfied. The first is that the centroid of the column and the joints on the column's perimeter define an X-Y region which can undergo rigid body motions only. This region will be referred to as a 'column head' and the following constraint equations are assumed to

apply in this region:

$$W_i = W_o + (y_i - y_o)\,\theta x_o + (x_i - x_o)\,\theta y_o$$
$$\theta x_i = \theta x_o \qquad (5.5)$$
$$\theta y_i = \theta y_o$$

where, the subscript '$_o$' denotes the column centroid,
and '$_i$' denotes a joint in the rigid body region.

The second condition is that the substitute system of distributed stiffnesses at the perimeter joints contributes the same strain energy to the structure as the original system. An alternate view of this method is that rigid bars have been used to attach each perimeter joint to the centroid of the column.

For point-sized columns the same method is used but only one finite element joint is usually involved. The advantage of using this method for point supports is that the centroid of the column and a joint of the finite element model do not have to coincide. This permits the user to use more rectangles when doing the grid layout. However, the transfer distances between the two points should be kept small so that the constraints in Equation 5.5 still apply.

To implement the constraint equations for finite-sized columns two separate approaches were tried. The first approach involved the use of substructuring around the column head. The second approach was to use artificially thick elements to represent the column head.

The substructuring approach was considered because it is more economical to impose the constraint equations on an individual column head at a substructure level than on a global level. The procedure consists of forming the stiffness matrix for the entire substructure and then imposing the constraint equations to eliminate the dependent degrees of freedom. All the degrees of freedom on the perimeter of the column can be eliminated, while the degrees of freedom at the centroid of the column are retained. The resulting stiffness matrix and load vector can now be partitioned and the interior degrees of freedom eliminated according to the standard method of substructures[3,8].

If no interior joints are present in the substructure, then further savings in computational effort can be realised because a number of operations involving the partitioning, inverting and multiplying of matrices are not required. The geometry in the vicinity of the column head is such that it can be represented by a substructure which has only boundary joints, joints on the perimeter of the column, and a joint at the centroid of the column. After the substructure matrix has been formed and modified by the constraint equations, the only degrees of freedom which remain are those of the boundary joints and the joint at the centroid of the column. This matrix can now be entered directly into the global stiffness matrix. After the complete set of equations for the structure have been solved, all the displacements within the substructure can be calculated

directly from the constraint equations; it is not necessary to recalculate the stiffness matrix of the substructure.

The substructuring approach satisfies the constraint equations exactly but it has the disadvantages of increasing the complexity of the program and widening the semi-band width of the problem. Therefore, an alternate approach was tried wherein the constraint equations were satisfied only approximately.

The alternate approach consists of using artificially thick elements to provide the rigid body behavior described by Equation 5.5. The accuracy of such an approach can only be assessed by considering specific problems. One such problem which was considered involved an 8.0 inch slab spanning 20.0 feet and supported by 24.0 inch square columns 11.5 feet in length. In representing the column heads, 800.0 inch thick elements were used and a comparison of nodal rotations and transverse displacements between this method and the substructuring method indicated agreement of the first four digits. It appears that the thick element approach can be made as accurate as desired for practical usage. Therefore, in the *HYBSLAB* program, the more involved substructuring approach was abandoned in favor of the thick element approach. No additional comparisons were done because when using the program, the designer can always determine the extent of column head 'mushrooming' by looking at the displacement output for the column head.

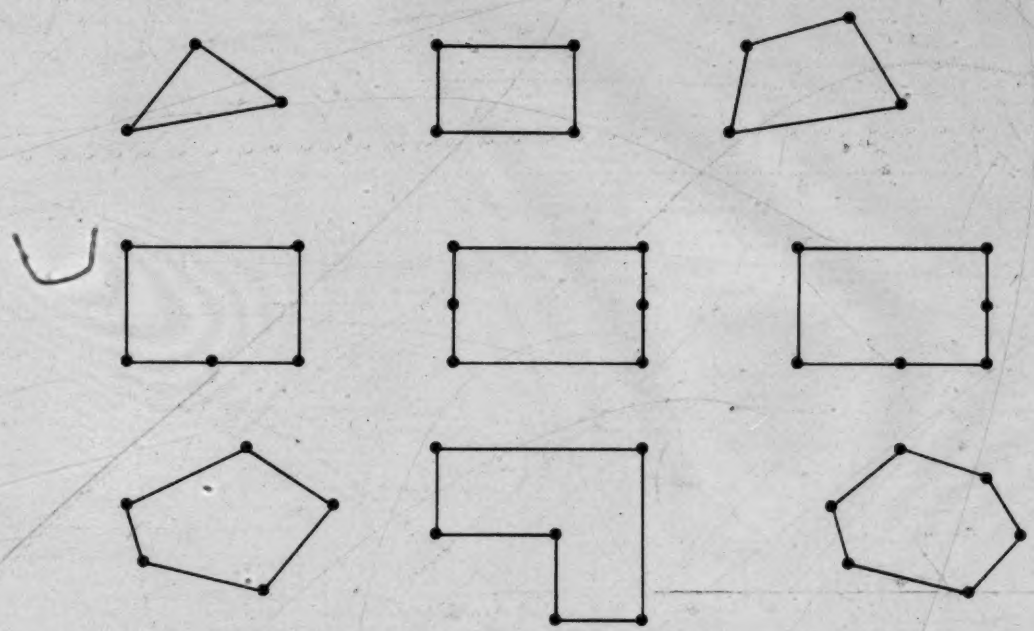

Figure 5.1 Some Possible Element Configurations.

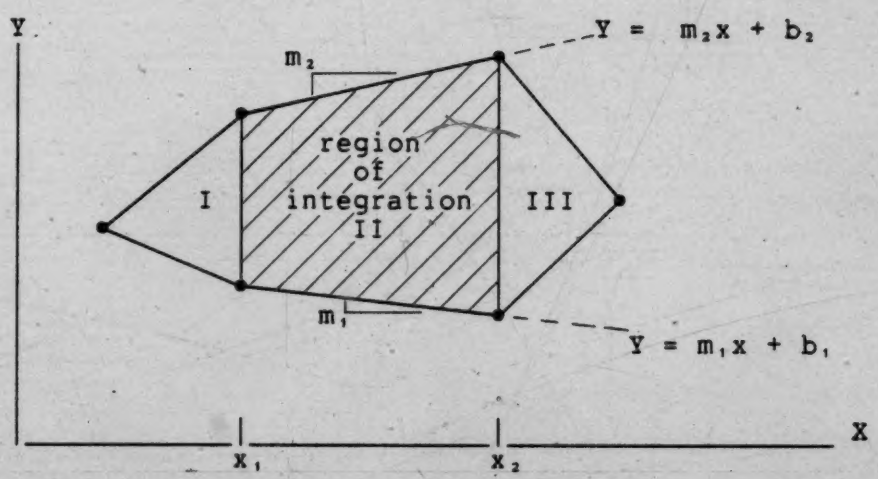

Figure 5.2 Regions for Evaluating [*H*hh], [*H*hp] and [*H*pp].

Chapter 6

VERIFICATION OF ELEMENT MATRICES

6.1 Introduction

In this chapter the program *HYBSLAB* is used to solve a wide range of test problems. The problems involve a variety of element shapes and were chosen to check the program and to verify the matrices given in Chapter 4. The next chapter will deal with the analysis of actual floor systems, but before analysing such structures it is necessary to verify that the elements, when assembled, are able to represent the constant strain states. As well, for modelling floors with eccentric stiffeners, it is necessary to know the magnitude of the error caused by coupling such stiffeners to the plate.

The importance of representing the constant strain (or constant stress states) was discussed in Chapter 2. For the individual elements, no tests are required because each of the polynomial stress functions in Chapter 4 contains a constant β term. Therefore each of the constant stress states has been included. As an assemblage, the elements are required to pass the 'patch test'. The nature and the role of the patch test were described in Chapter 2. If the elements can meet these two requirements, then one can be certain that as the gridwork is refined the results will converge to the correct values.

In this chapter the testing of the hybrid elements is done through the use of simple test problems. The nature of some of the constant strain tests is such that they can be labelled as patch tests. Section 6.2 contains the constant strain tests for the in-plane stiffness matrices while Section 6.3 deals with the constant curvature states for the flexural matrices. As well, some simple test structures are included to compare the convergence characteristics of the various element shapes.

In Section 6.4 two stress singularity problems are considered. The first problem uses the free edge singularity element, while the second problem uses the fixed edge element developed in Section 4.4.

Some numerical results are presented in Section 6.5 for the error introduced when coupling eccentric beam elements to a plate. The error was identified earlier in Section 5.3 and some example problems are done in Section 6.5 to illustrate how it can be reduced.

6.2 Plane Stress Problems

This section contains the test problems used to verify that the in-plane stiffness matrices are able to represent the constant strain states for ϵx, ϵy, and ϵxy. The gridworks and element shapes which were used are shown in Figures 6.1 and 6.2.

In addition to these tests, similar elements shapes are used to analyse a cantilever beam supporting a point load at its free end. This test case was included to compare the accuracy and convergence characteristics for the different element shapes. The results for the cantilever beam are presented after dealing with the constant strain cases.

For the test cases shown in Figure 6.1, the patch test for constant strains was applied in the following manner. The in-plane displacements, *U* and *V*, were prescribed at the perimeter nodes of each group of elements according to the equations shown below.

$$U = a_1 + a_2 x + a_3 y$$
$$V = a_4 + a_5 x + a_6 y \qquad (6.1)$$

From this set of equations, the following expressions for stresses and strains can be obtained.

$$\epsilon x = a_2$$
$$\epsilon y = a_6$$
$$\epsilon xy = (a_3 + a_5)/2$$

and,

$$\sigma x = \frac{E}{(1-\nu^2)} (a_2 + \nu a_6)$$
$$\sigma y = \frac{E}{(1-\nu^2)} (\nu a_2 + a_6) \qquad (6.2)$$
$$\sigma xy = \frac{E}{2(1+\nu)} (a_3 + a_5)$$

To use the program *HYBSLAB* it is necessary to assign numerical values to the a_i coefficients. Since the choice of these coefficients is arbitrary, it was decided to assign to each coefficient the value of its subscript, that is,

a_1=1, a_2=2, ..., a_4=6. With these values and E=27.300 ksi, ν=0.3, and t=0.1 inches, the following results were obtained.

For all interior points of the element groups in Figure 6.1, the *U* and *V* displacements were output to 7 digits of accuracy and agreed exactly with the values calculated from Equation 6.1. The stresses at all nodal points, both on the perimeter and on the interior, were σ_x=+114.0 ksi, σ_y=+198.0 ksi, and σ_{xy}=+84.00 ksi. These numbers are identical to the values calculated from Equation 6.2.

Based on the above results, it can be concluded that the hybrid in-plane matrices are capable of representing the constant strain states and that rigid body motion does not cause straining of the element. However, it was decided to do some additional testing on these element groups by analysing them as supported structures subjected to nodal loads. The primary reasons for doing this was to provide additional checking of the *HYBSLAB* program and to determine if the unsymmetrical gridworks could still provide accurate results with only a minimum number of constrained joints. The nature of the load cases was such that they would cause constant strain conditions in the structure. Values of E=27300 ksi, ν=0.3, and t=0.1 inches were used for each case. Three separate cases were considered.

For the first case, the structures of Figure 6.1 were supported at X=0 and loaded at X=20 inches with loads of Px=100 kips. The resulting X displacements for the loaded

nodes were U=0.07326007 inches, and the stresses at all nodal points were σx=+100.0 ksi, σy=0.0 ksi, and σxy=0.0 ksi.

For the second case, the same structures were supported at Y=0, and loads of Py=+100 kips were applied at Y=10 inches. The resulting Y displacements of the loaded nodes were V=0.01831502 inches, and the stresses at all nodal points were σx=0.0 ksi, σy=+50.00 ksi, and σxy=0.0 ksi.

For the third case, that of pure shear, the groups of elements shown in Figure 6.2 were used. In each of these structures, the node at X=0,Y=0 was prevented from moving, while the node at X=20 inches was permitted to move in the X direction only. The loads were calculated from a pure shear of 10.0 ksi, acting along the sides of the structure. The calculated displacements from *HYBSLAB* at X=20 inches were U=0.009523810 inches, and the stresses at all nodal points were σx=+10.00 ksi, σy=-10.00 ksi, and σxy=0.0 ksi. In all three of the above test cases, the values from the *HYBSLAB* program were identical to the expected values.

The results from these three cases and the patch tests done earlier indicate that the in-plane stiffness matrices, as generated by *HYBSLAB*, are capable of providing an exact analysis of constant strain structures. The importance of this capability is that, in the limit, exact results can be obtained for any structure.

To get an indication of the convergence characteristics for the different shaped elements, a cantilever beam was

analysed. A sketch of the beam and the gridworks are shown in Figure 6.3. The (x,y,z) dimensions of the beam are (20.0,2.0,1.2), where the length is 20.0 inches and the depth is 2.0 inches. Only a single rectangular element was used to model the depth, while gridworks based on 1, 4, and 10 equal rectangular subdivisions were used along the length of the beam. The loading condition consisted of an end load of Py=-100 kips.

The results of the analyses are shown as normalized values in Table 6.1. As well, the results from a bilinear conforming displacement element have also been included.

From these results it can be concluded that, with the exception of the triangular elements, all of the element shapes perform reasonably well. The excessive stiffness displayed by the triangular elements can be attributed to the relatively large number of β parameters in comparison to the low order of the displacement functions and the low displacement rank of the triangular stiffness matrix. This was discussed earlier in Section 4.1.

6.3 Pure Bending Problems

In this section test cases are presented to determine if the hybrid flexural matrices are capable of representing the constant curvature states W,xx , W,yy , and W,xy . The gridworks and element shapes used for the test cases are the same as those used in the previous section and are shown

in Figures 6.1 and 6.2.

In addition to the above, two more test cases were added to investigate the convergence characteristics of the different element shapes. The first of these cases is the cantilever beam used in the previous section. The second is a clamped square plate subjected to uniform and point loading. The results of these two test cases will be dealt with after the constant curvature states are discussed.

In addition to examining the various groups of elements in Fig 6.1 for the constant curvature states, it was also decided to test for linear curvatures. To achieve this, the following equation was used for W .

$$W = a_1 + a_2x + a_3y + a_4x^2 + a_5xy + a_6y^2 + a_7x^3 + a_8x^2y + a_9xy^2 + a_{10}y^3 \qquad (6.3)$$

From Equation 6.3 the following expressions can be obtained.

$$\begin{aligned} \theta x &= a_3 + a_5x + 2a_6y + a_8x^2 + 2a_9xy + 3a_{10}y^2 \\ \theta y &= a_2 + 2a_4x + a_5y + 3a_7x^2 + 2a_8xy + a_9y^2 \\ W,xx &= 2a_4 + 6a_7x + 2a_8y \\ W,yy &= 2a_6 + 2a_9x + 6a_{10}y \\ W,xy &= a_5 + 2a_8x + 2a_9y \end{aligned} \qquad (6.4)$$

The moments can be calculated from the above expressions as:

$$\begin{aligned} Mx &= -D\,[(2a_4 + 6a_7x + 2a_8y) + \nu(2a_6 + 2a_9x + 6a_{10}y)] \\ My &= -D\,[\nu(2a_4 + 6a_7x + 2a_8y) + (2a_6 + 2a_9x + 6a_{10}y)] \\ Mxy &= -D\,(1-\nu)(a_5 + 2a_8x + 2a_9y) \end{aligned} \qquad (6.5)$$

As discussed earlier, the choice of the a_i coefficients is quite arbitrary, and again the value of each coefficient was assigned equal to its subscript.

The constant curvature states were considered first, and for these cases it is necessary to reset the values of a_7, a_8, a_9 and a_{10} to zero. Before running the program *HYBSLAB*, the values of W, θx, and θy were calculated from the above equations and prescribed for the perimeter nodes in Figure 6.1. Values of E=27300 ksi, ν=0.3, and t= 0.1 inches were used again.

The results of the analysis were the same for each group of elements. At all interior points, the W, θx, θy values were output to 7 digits of accuracy and agreed exactly with the values calculated from Equations 6.3 and 6.4. The moments at all nodal points, both on the perimeter and on the interior, were Mx=-29.00 kip.in/in, My=-36.00 kip.in/in, and Mxy=-8.750 kip.in/in. These values agree with those calculated from Equation 6.5.

In addition to the above test cases, another test was done for pure shear by using the element groups shown earlier in Figure 6.2. Three corners of each group were simply supported, while the fourth corner was subjected to a load of 1.0 kips in the Z direction. For each structure, with E=27300 ksi, ν= 0.3, and t=0.1, the resulting displacement at the point of loading was +57.14286 inches. At all nodes, both interior and exterior, the bending moments were Mx=-0.5000 kip.in/in, My=+0.5000 kip.in/in,

and M_{xy}=0.0 kip.in/in. These values agree well with the published results of W=0.7142858 PL^2/D and principal moment values of 0.5000 P. The output for the displacement at the centre of the plate was +14.28571 inches. This is the same value as calculated from $W=k_o\bar{x}\bar{y}$, which is the equation of the deflected surface, with k_o a constant and the $(\bar{x},\bar{y})$ coordinate system at 45 degrees to the X axis.

From the results obtained thus far, it can be stated that the hybrid flexural matrices generated by *HYBSLAB* are capable of representing the constant curvature states in a structure.

Testing of the element groups for linear curvatures can be done in the same manner as described for the constant curvature conditions. The only difference is that all ten a_i coefficients of Equation 6.3 are used to describe W . An analysis of the element groups shown in Figure 6.1 revealed that the values of W, θx and θy could not be reproduced exactly at all interior points. It was therefore concluded that linear variations of curvatures cannot be represented within a single element.

The next test case considered is the cantilever beam of Figure 6.3. This time, to cause bending about the Y axis, the free end of the cantilever was loaded with a point load of Pz=10.0 kips. The results for the same gridworks as those used in the previous section are shown in Table 6.2.

From the results presented in this table, it is interesting to note that all element shapes, even the

triangular elements, provide rather accurate values for the end displacement. The much better results for the coarser grids can be attributed to the fact that cubic functions are used to describe *W*, whereas only linear functions were used for *U* and *V* of the in-plane matrix.

Another test case which was done on the cantilever beam involved the use of the 1x1 rectangular grid and a Poisson's ratio of zero. Under these conditions, a rectangular plate element should degenerate to the classical beam element and give exactly the same results. Although seldom discussed in the literature, this is a performance test which any rectangular plate element should pass.

To do the test, a single rectangle was used to model a cantilever beam carrying a point load at its free end. Under these conditions, the curvature variation in the X direction is linear. The output from *HYBSLAB* for the free end displacement and rotation agreed with the expected values to 7 digits of accuracy. The stresses at both ends of the beam were also calculated correctly.

The last test case to be considered is a clamped plate subjected to uniform and point loading. The various gridworks which were used are shown in Figure 6.4. Values of E=27300 ksi, ν=0.3, t=0.1 inches, and q_o=-1.0 ksi were used in the analysis.

Displacement and moment results from the program *HYBSLAB* are shown in Tables 6.3 and 6.4. The results indicate that, for all element shapes, both the

displacements and moments are converging to the accepted values. The quadrilateral shapes with reentrant corners do not appear to cause any convergence problems. It is again noted that the tables only indicate accuracy versus the number of rectangular subdivisions. The total number of unknowns does not enter into the comparison. It also appears that, of all the element shapes, the rectangular shape is the most accurate. General conclusions regarding convergence rates cannot be made because many alternate choices exist for defining the nonrectangular element grids.

6.4 Singularity Problems

The singularity elements derived in Chapter 4 are used in this section for two example problems with reentrant corners. The first problem is that of a simply supported square plate with a concentric square opening as shown in Figure 6.5. The second problem uses the same plate but with all edges clamped.

For both problems the analysis was first done by using a number of gridworks with square elements only. A typical 8x8 grid is shown in Figure 6.5. This was then followed by an analysis which involved one L-shaped singularity element at the reentrant corner with the remaining elements being rectangles. Two such gridworks were considered and a typical 7x7 L-grid is shown in Figure 6.5. The plate with the square opening will be discussed first, followed by the

plate with fixed edges. The following values were used for both cases: E=27300 ksi, ν=0.3, and t=0.75 inches.

Two load conditions were considered for the plate with the square opening. The first load case was a uniform load, while the second load case consisted of four equal Pz point loads applied at the reentrant corners.

The results from the program *HYBSLAB* are presented in Tables 6.5 and 6.6. The locations of points 'a', 'b', 'c', and 'd' are shown in Figure 6.5. As discussed earlier in Section 4.4, there are five eigenvalues of interest and therefore the analysis was done with e=0,1,2,3,4, and 5, where 'e' is the number of eigenvalues. From the results it appears that for this problem the second and third eigenvalues are the most important and that the remaining three have little, if any, influence on the solution. No explanation is offered as to why the first eigenvalue does not play a more prominent role.

From the comparison of displacements in these tables, it can be concluded that, for both gridworks and for both load cases, the results with the eigenvalues are at least as accurate as those without them. As a matter of fact, with the exception of the first eigenvalue, the results with the eigenvalues are significantly better.

A comparison of moments at point 'a' indicates that when the eigenvalues are included there is only a modest increase in accuracy. This can be attributed to the fact that point 'a' is far removed from the singularity point.

A graphical comparison of moments along side 'a-b' is presented in Figure 6.6 for the uniform load and the 7x7L, 8x8, and 24x24 grids. The use of the singularity element reduces significantly the number of elements required. The 7x7L solution with a singularity element is seen to be comparable to the 24x24 solution obtained using square elements only.

The second test case to be considered is the same plate but with all edges fixed. For this case, only the real eigenvalue discussed in Section 4.4 b) was used. The same grids were used as for the previous problem, but only uniform loading was considered. Results for deflection and moments from the *HYBSLAB* program are shown in Table 6.7. As well, bending moments normal to the fixed edge are shown in graphical form in Figure 6.7.

The deflection comparisons in Table 6.7 indicate that at point 'c' the results basically remain unchanged when the singularity functions are included. This is not surprising, as point 'c' is far removed from the reentrant corner. The deflection results at point 'd' are improved significantly for the 3x3 L-grid, but there is only a modest improvement for the 7x7 L-grid. A similar statement also applies to the bending moments at point 'd'; these values are not shown in Table 6.7.

The deflection and moment values for a fixed end beam along 'a-c' are also given in Table 6.7. These values are included simply to provide an estimate of the deflection at

point 'c' and the moment at point 'a'.

In Figure 6.7 the bending moment normal to the clamped edge 'a-b' is shown for the 24x24 square grid. The values for all the other square grids fall below this curve and were omitted for clarity. From this graph, it can be seen that the rapid increase in moment does not occur until one approaches the immediate vicinity of the reentrant corner. For comparison, the data points for the 7x7 L-grid are also shown in the same figure. Although the 7x7 L-grid is less accurate along most of the edge, it appears to be as accurate as the 24x24 grid in the immediate vicinity of the reentrant corner. More detailed results cannot be presented because stresses were not calculated within the singularity element.

The results discussed thus far indicate that the grids with the singularity elements appear to provide more accurate results than those without. Additional work on this subject is still required for the clamped edge element to assess the importance of including the complex eigenvalue discussed in Section 4.4. As well, extensive testing of both elements is still required.

6.5 Errors in Modelling Eccentric Stiffeners

An error which occurs when eccentric beams are coupled to a plate was identified in 1977 by Gupta and discussed earlier in Section 5.3. Before undertaking the analysis of

actual floor systems, it was decided to obtain some additional information on the magnitude of this error. To do this, it was decided to analyse a cantilevered T-beam supporting a point load at its free end.

The beam and its cross section are shown in Figure 6.8. Also, as indicated in this figure, two choices exist for representing the flange and the stem of the cross section. The first choice, referred to as the 'layered' approach, is to regard the plate as having the same width and thickness as the overall flange and the beam being only the portion which protrudes above or below the slab. The second choice, referred to as the 'overall thickness' or 'overall height' approach, is to consider the plate as being only the overhanging portions of the T-beam flange.

To illustrate the magnitude of the error, Gupta used the layered approach and replaced the plate element with a beam element. He then derived the following expression.

$$\text{error} = \frac{A_1 A_2 e^2}{4(A_1+A_2)(I_1+I_2)} \qquad (6.6)$$

where,
A_i = area of the cross section for beam 'i',(i=1,2),
I_i = moment of inertia for beam 'i',(i=1,2),
e = the distance between the beam centroids.

Using the above equation for the T-beam shown in Figure 6.8, the error for the layered cross section can be calculated as 0.600. This means that if the entire length of the T-beam is represented by a single beam element, then

the calculated displacement will be 1.600 times the correct value. However, what Gupta fails to mention is that the same expression is valid for the overall approach and the error calculated for the overall cross section shown in Figure 6.8 is only 0.136 .

With this information, it was decided to try both the layered and the overall approaches for the T-beam with the dimensions shown in Figure 6.8. As well, it was decided not only to use beam elements as Gupta had done, but also to model each cross section by using plate elements only; the corresponding models are shown in Figure 6.9. The use of the offset plate elements to model beam stems was discussed earlier in Section 5.3.

The choice to use both a layered and an overall approach and either beam or plate elements leads to four different representations of the cross section. For each of these cross section models, it was decided to use 1,2,4,8,16, and 32 equal subdivisions in the X direction along the length of the T-beam. For the plate element models, the dimensions of the plates in the Y direction were kept equal and constant at 12.0 inches for all the gridworks. The results from the *HYBSLAB* program are given in Table 6.8. The following observations can be made for this T-beam.

For the beam models with only one subdivision along the length, the results are identical to those calculated from Gupta's expression given in Equation 6.6. For the coarser

gridworks, the overall height approach is much more accurate than the layered approach. Both the overall and the layered methods converge to the correct value.

The plate models both appear to be converging to a normalized value between 0.997 and 0.998. This slight dicrepancy can be attributed to Poisson's ratio and the modelling of the T-beam support conditions. The boundary conditions at the fixed end are suspected of causing some restraint of the Y displacement. To confirm this, the 32-subdivision gridwork was rerun with a Poisson's ratio of zero and the normalized values were found to be 1.005 for the layered approach and 1.004 for the overall approach.

Again for the plate models as for the beam models, with the coarser grids, the overall approach is much more accurate than the layered approach. Also for the coarser grids, the plate models are more accurate than their counterpart beam models.

A totally unexpected convergence trend is indicated by the values in the last column for the plate model. Here convergence begins at a value above 1.000 for the first two grids and then drops sharply and converges from below. Although in the hybrid method there is no reason to expect monotonic convergence, this type of behaviour appears to be totally out of character for a member in single curvature. For the 4-subdivision gridwork, extensive backchecking of the data and independent calculations of the stiffness matrices failed to reveal any errors and therefore it is

assumed that the results being presented are correct.

Although the results presented in Table 6.8 are for a particular cross section, the following general statements can be made. Gupta's expression as given in Equation 6.6 can be used to estimate the displacement error for both the beam and the offset plate model. The overall thickness approach is expected to be more accurate than the layered approach for both the beam and the plate models.

Cantilever Beam with Point Load, Py, at the Free End.

Y-Deflection at Free End, normalized w.r.t. $PL^3/3EI$			
GRID	1×1	4×1	10×1
Rectangles	0.02568	0.32787	0.88181
Triangles	0.01286	0.10074	0.23118
Quadrilaterals	0.02440	0.30894	0.83454
Polygons	0.21594	0.86521	0.94888
Disp. Rectangle	0.02547	0.28776	0.67323

Table 6.1 Cantilever Beam In-Plane Displacements.

Cantilever Beam with Point Load, Pz, at the Free End.

Z-Deflection at Free End, normalized w.r.t. $PL^3/3EI$			
GRID	1×1	4×1	10×1
Rectangles	0.93167	0.97861	0.98794
Triangles	0.91102	0.96235	0.98179
Quadrilaterals	0.93012	0.97694	0.98623
Polygons	0.95503	0.98357	0.98930

Table 6.2 Cantilever Beam Flexural Displacements.

Deflections for Uniform Loading:

Deflection at centre, normalized w.r.t. 0.001265319 qL^4/D				
GRID	2×2	4×4	8×8	16×16
Rectangular	1.055	0.979	0.996	0.999
Triangular	0.564	0.928	0.979	0.995
Quadrilateral	1.009	0.961	0.989	0.998
Polygonal	0.964	0.981	0.997	0.999
Transitions	1.110	0.994	0.998	1.000

Moments for Uniform Loading:

Moment at centre, normalized w.r.t. 0.02291 qL^2				
GRID	2×2	4×4	8×8	16×16
Rectangular	1.481	0.982	1.002	1.000
Triangular	0.218	0.898	0.948	0.982
Quadrilateral	1.540	0.834	0.950	0.986
Polygonal	0.940	0.970	0.990	0.997
Transitions	1.339	1.013	1.007	1.002

Table 6.3 Clamped Plate: Deflections and Moments for Various Shaped Elements (Uniform Load).

Deflections for Central Point Load:

Deflection at centre, normalized w.r.t. 0.005612017 PL^2/D				
GRID	2×2	4×4	8×8	16×16
Rectangular	0.952	0.953	0.989	0.998
Triangular	0.377	0.857	0.957	0.988
Quadrilateral	0.914	0.933	0.980	0.994
Polygonal	0.955	0.979	0.995	0.999
Transitions	1.362	1.078	1.020	1.005

Moments for Central Point Load:

Moment at midside, normalized w.r.t. 0.1257 P				
GRID	2×2	4×4	8×8	16×16
Rectangular	1.152	1.022	1.003	1.000
Triangular	0.459	0.779	0.863	0.924
Quadrilateral	1.167	0.811	0.898	0.955
Polygonal	0.780	0.877	0.930	0.965
Transitions	1.053	1.057	1.021	1.006

Table 6.4 Clamped Plate: Deflections and Moments for Various Shaped Elements (Point Load).

Uniform Load Deflections and Moments:

GRID	e	Deflection/ ($qL^4/100D$)		Moment/(qL^2)
		Point 'a'	Point 'b'	Point 'a'
2x2	-	0.30716	0.22169	0.0204
4x4	-	0.31539	0.22293	0.0239
8x8	-	0.31811	0.22749	0.0240
16x16	-	0.31915	0.22930	0.0240
24x24	-	0.31943	0.22979	0.0240
3x3 L	0	0.32726	0.24251	0.0232
3x3 L	1	0.32726	0.24251	0.0232
3x3 L	2	0.31877	0.22717	0.0236
3x3 L	3	0.31897	0.22866	0.0234
3x3 L	4	0.31897	0.22865	0.0234
3x3 L	5	0.31897	0.22866	0.0234
7x7 L	0	0.32320	0.23658	0.0236
7x7 L	1	0.32320	0.23658	0.0236
7x7 L	2	0.31965	0.23011	0.0238
7x7 L	3	0.31958	0.23018	0.0238
7x7 L	4	0.31957	0.23017	0.0238
7x7 L	5	0.31957	0.23017	0.0238

Table 6.5 Deflections and Moments for the Singularity Test Case with the Free Edge Opening (Uniform Load).

Point Load Deflections and Moments:

GRID	e	Deflection/ ($PL^2/10D$)		Moment/ P
		Point 'a'	Point 'b'	Point 'a'
2x2	-	0.30218	0.21944	0.068
4x4	-	0.31620	0.23660	0.146
8x8	-	0.32107	0.24473	0.145
16x16	-	0.32310	0.24826	0.145
24x24	-	0.32367	0.24927	0.145
3x3 L	0	0.34229	0.28702	0.108
3x3 L	1	0.34229	0.28702	0.108
3x3 L	2	0.32386	0.25371	0.117
3x3 L	3	0.32288	0.24732	0.125
3x3 L	4	0.32287	0.24732	0.125
3x3 L	5	0.32287	0.24732	0.125
7x7 L	0	0.33217	0.26521	0.138
7x7 L	1	0.33217	0.26521	0.138
7x7 L	2	0.32441	0.25104	0.143
7x7 L	3	0.32412	0.25017	0.142
7x7 L	4	0.32410	0.25016	0.142
7x7 L	5	0.32411	0.25016	0.142

Table 6.6 Deflections and Moments for the Singularity Test Case with the Free Edge Opening (Point Loads).

Uniform Load Deflections and Moments:

GRID	e	Deflection/ ($qL^4/100D$)		Moment/$100qL^2$
		Point 'c'	Point 'd'	Point 'a'
4x4	-	0.10134	0.11299	0.464
8x8	-	0.10114	0.11835	0.505
16x16	-	0.10113	0.12015	0.515
24x24	-	0.10112	0.12068	0.517
3x3 L	0	0.10140	0.14086	0.474
3x3 L	1	0.10150	0.11929	0.491
7x7 L	0	0.10102	0.12696	0.507
7x7 L	1	0.10117	0.12077	0.509
Fixed Beam	-	0.10173	-	0.521

Table 6.7 Deflections and Moments for the Singularity Test Case with the Clamped Edge Opening (Uniform Load).

Cantilever T-Beam with Point Load, Pz, at the Free End.

Z-Deflection at Free End, normalized w.r.t. $PL^3/3EI$				
Grid along X-axis	BEAM MODELS		PLATE MODELS	
	LAYERED APPROACH	OVERALL DEPTH	LAYERED APPROACH	OVERALL THICKNESS
1	1.600	1.136	1.486	1.064
2	1.150	1.034	1.106	1.001
4	1.038	1.009	1.019	0.993
8	1.009	1.002	1.002	0.995
16	1.002	1.001	0.999	0.996
32	1.001	1.000	0.998	0.997

Table 6.8 Error Comparison for Modelling of Eccentric Stiffeners.

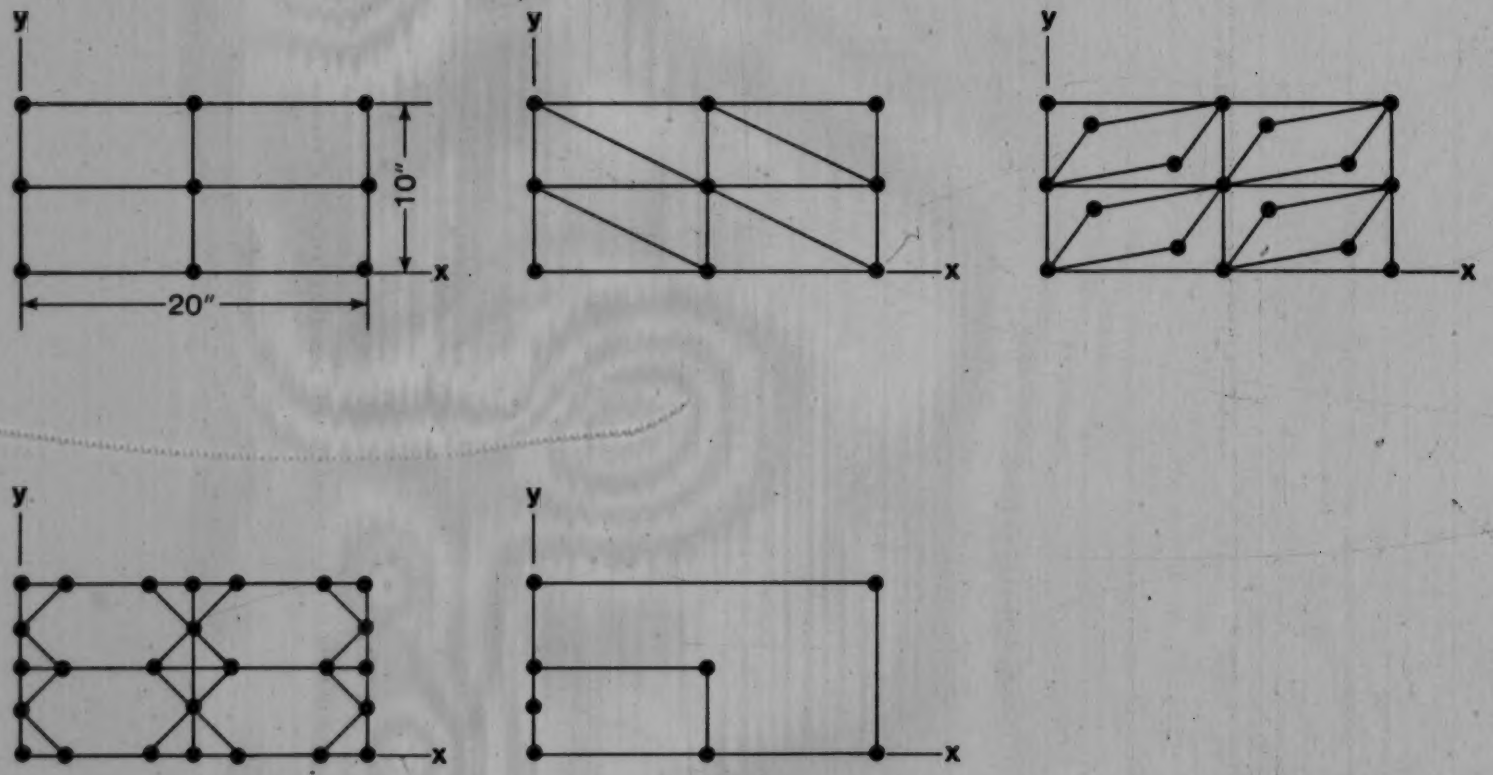

Figure 6.1 Test Cases for Constant Strains and Curvatures.

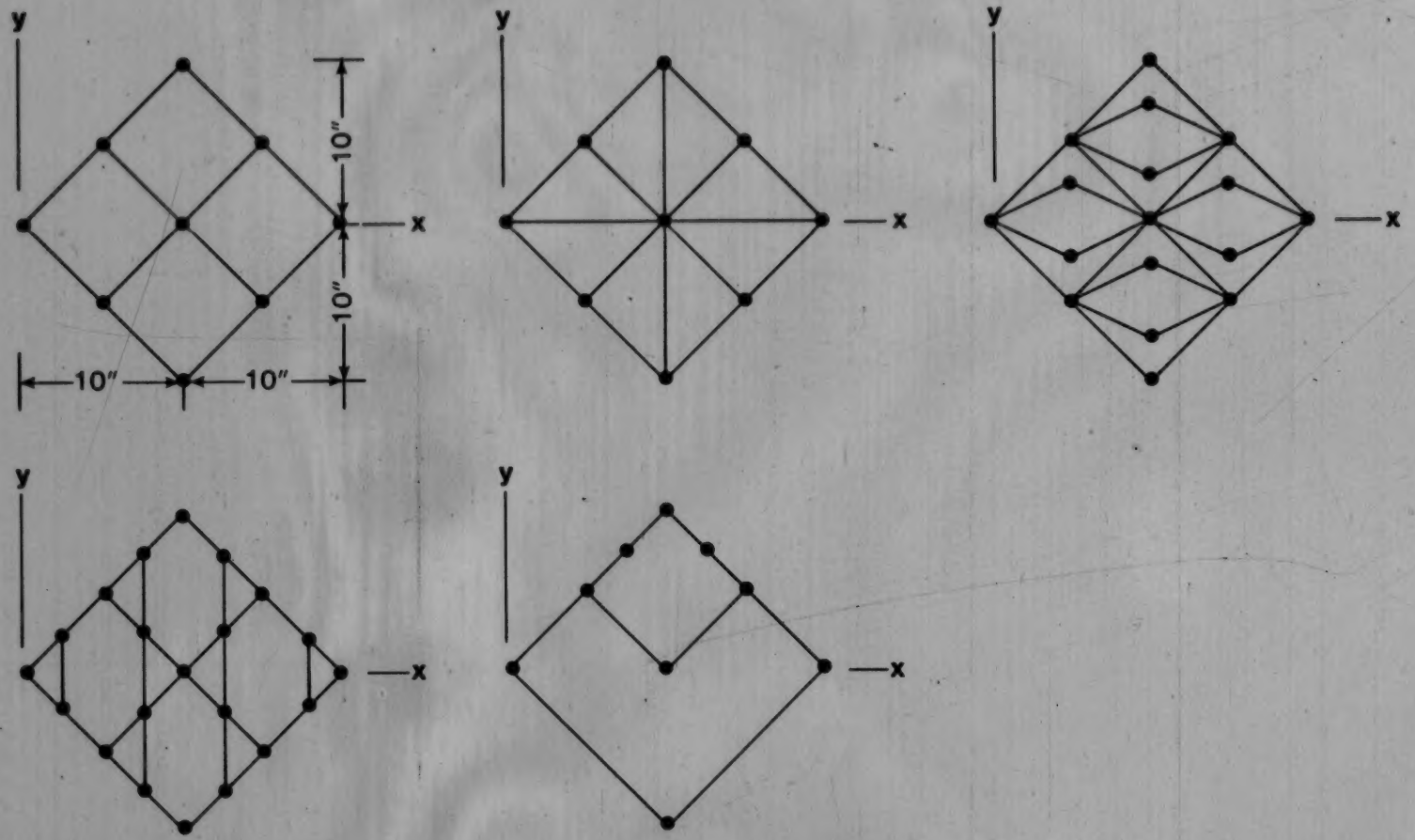

Figure 6.2 Additional Test Cases for Pure Shear and Pure Twist.

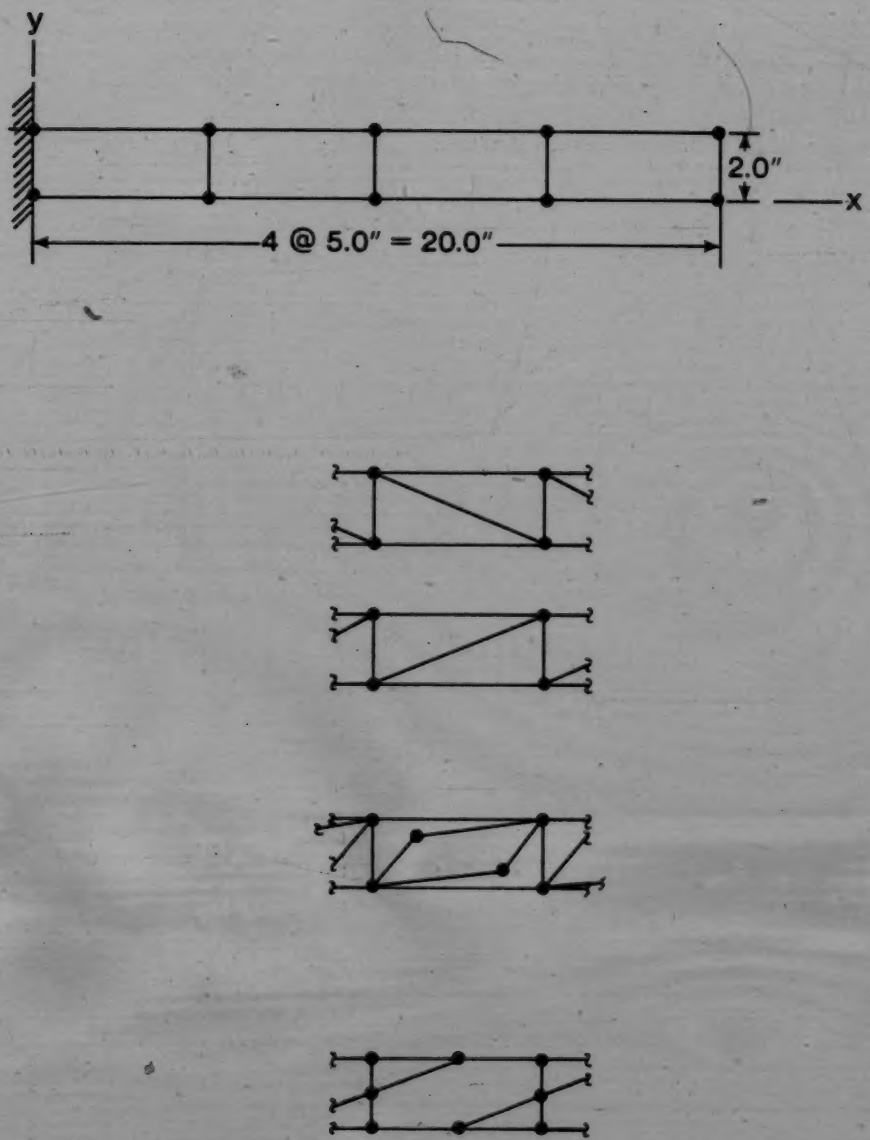

Figure 6.3 Cantilever Beam Test Case and Element Grids.

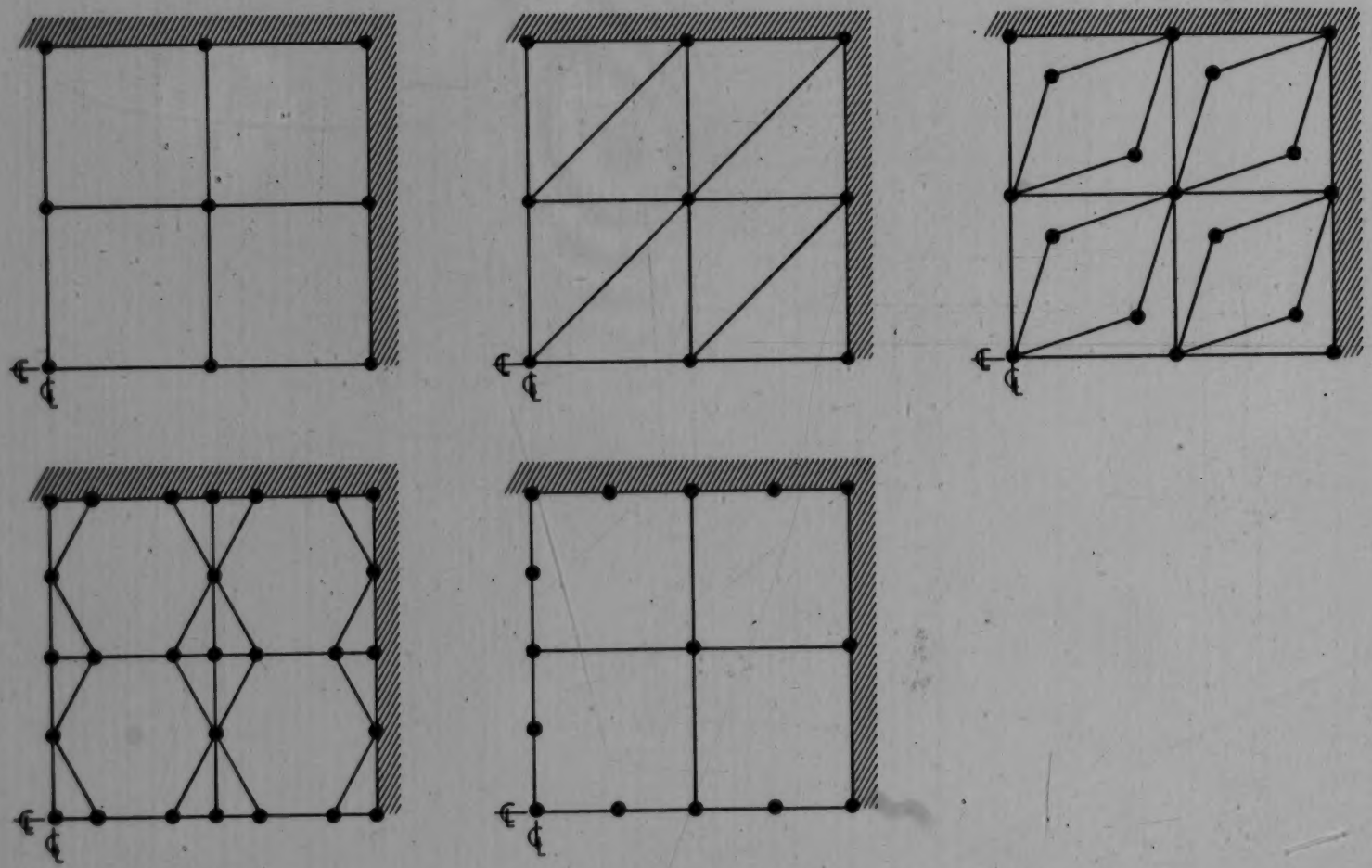

Figure 6.4 Clamped Plate Test Case and Element Grids.

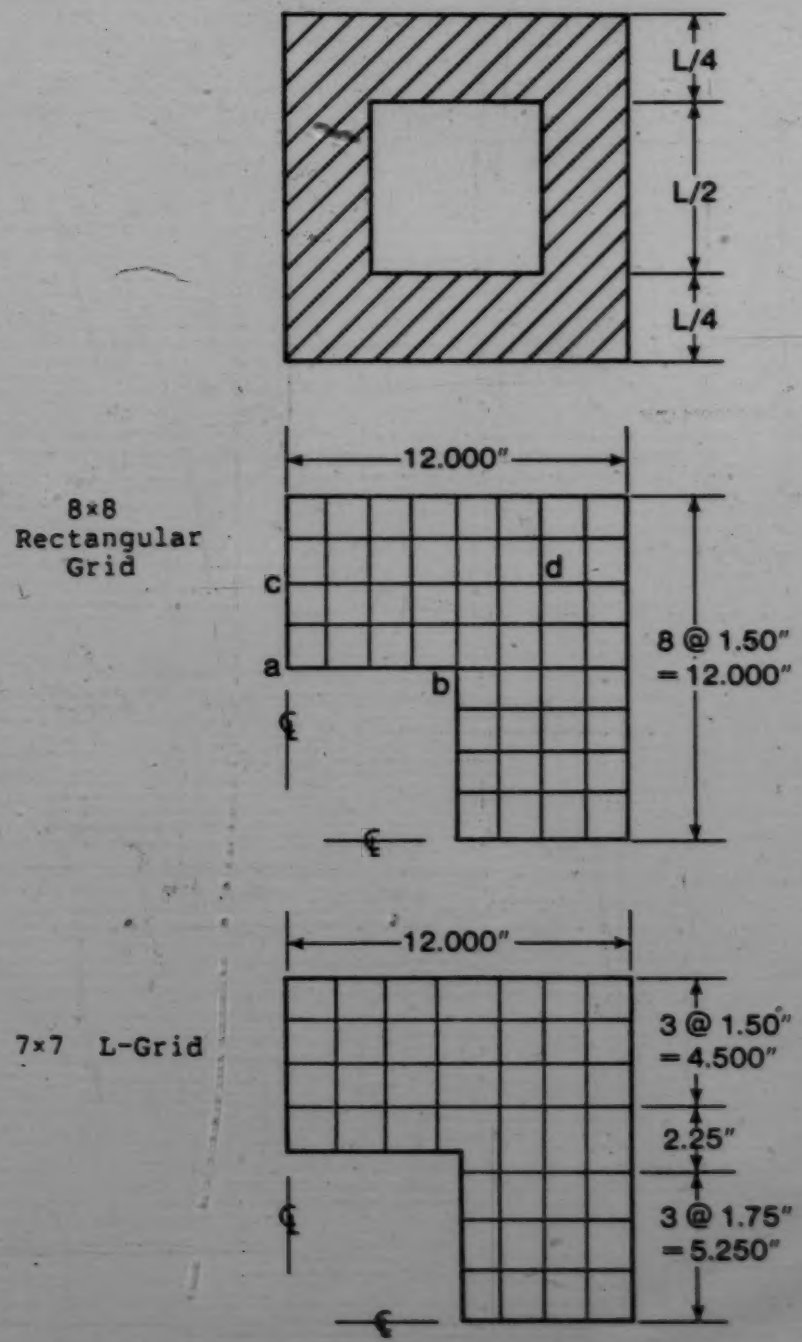

Figure 6.5 Singularity Test Plate and Element Grids.

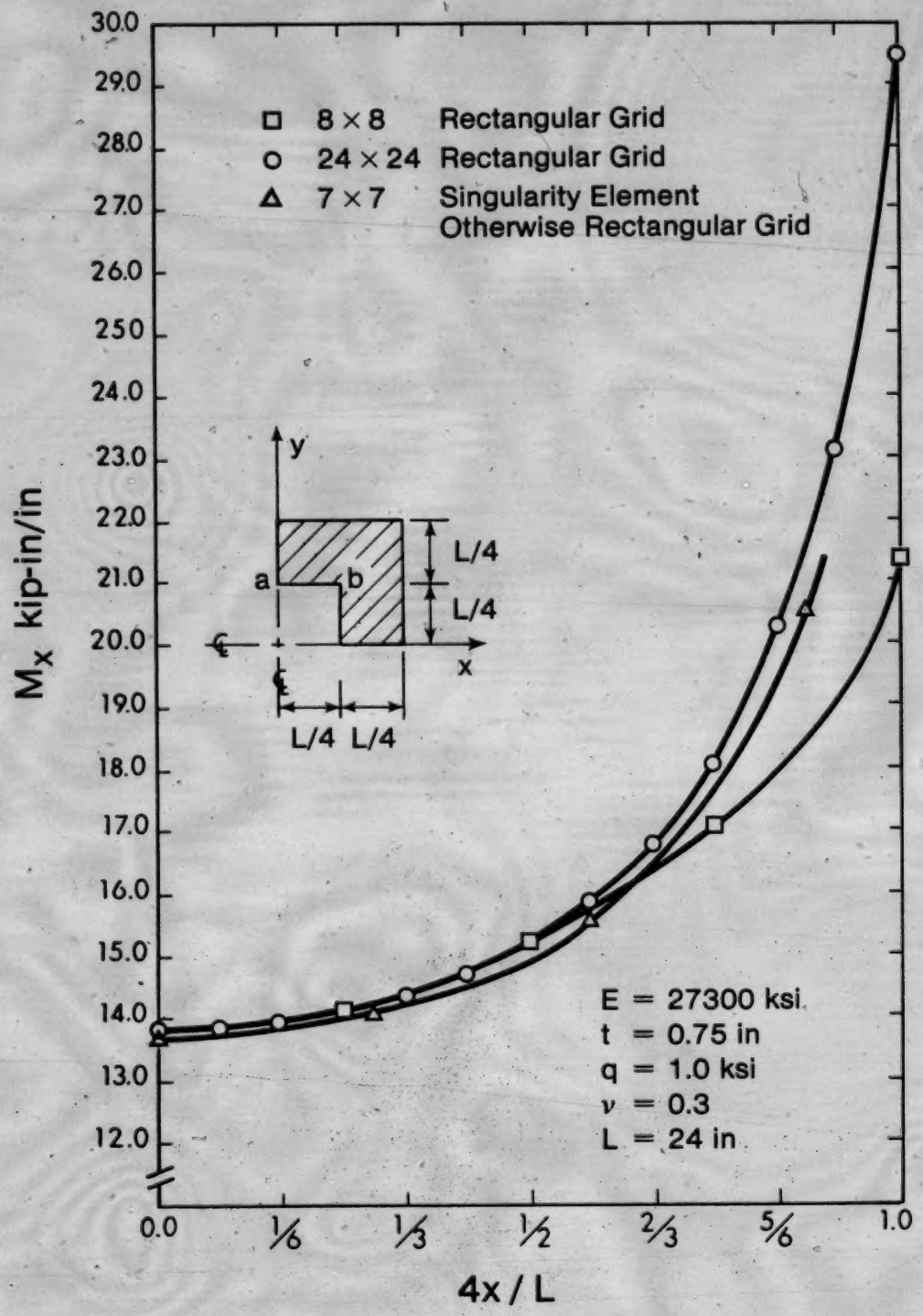

Figure 6.6 Free Edge Opening; Moments along Edge a-b.

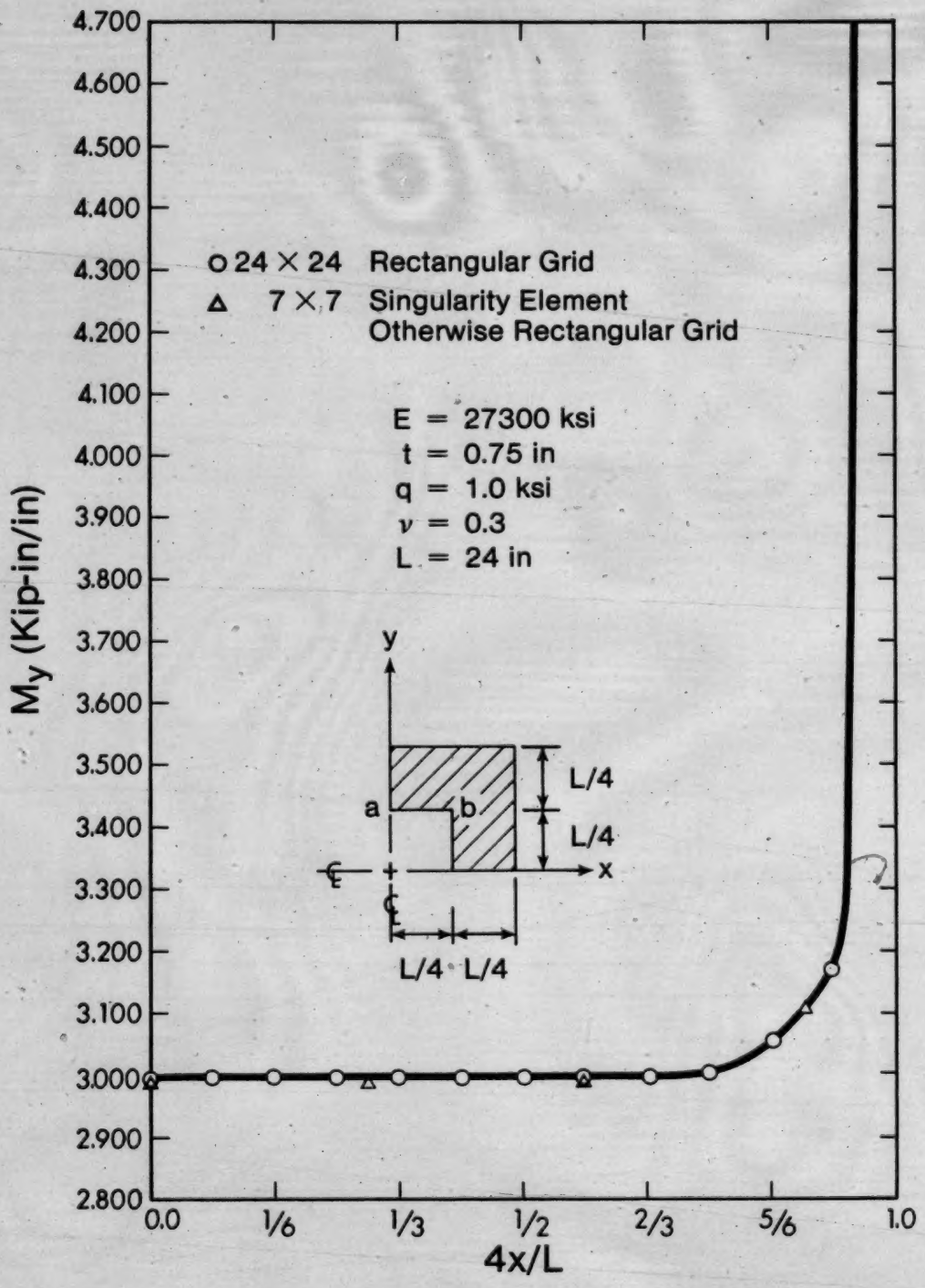

Figure 6.7 Clamped Edge Opening; Moments along Edge a-b.

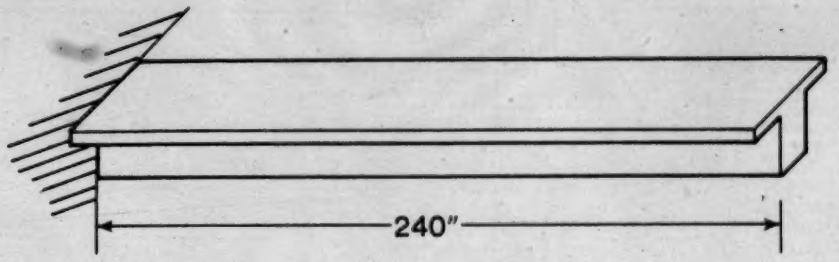

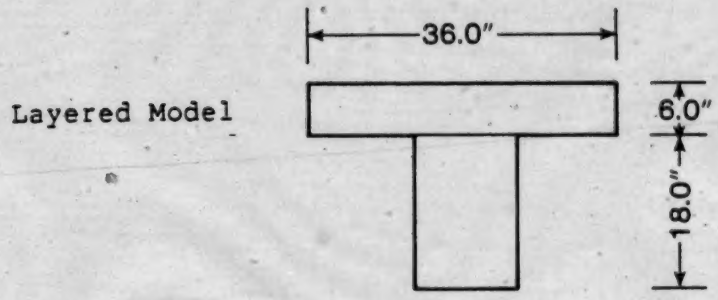

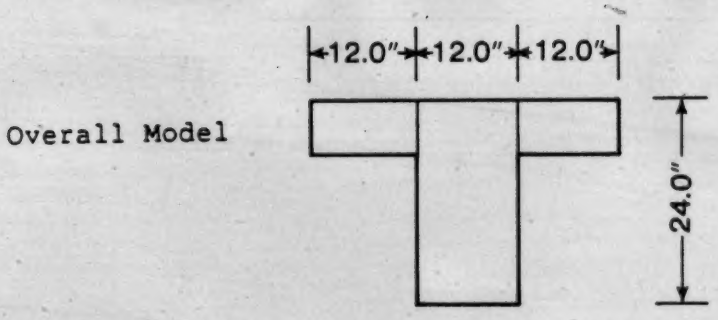

Figure 6.8 T-Beam and Representation of Cross Sections.

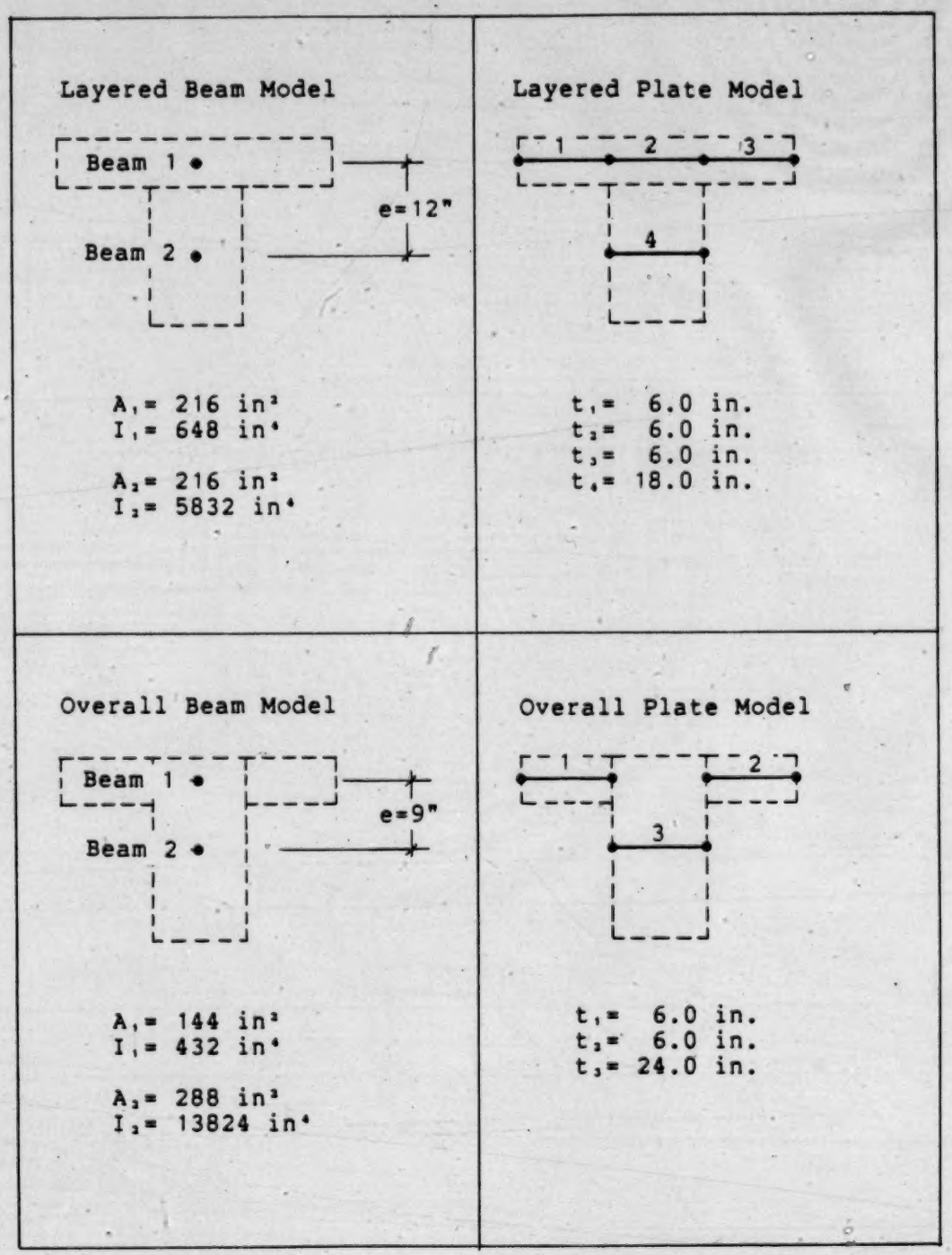

Figure 6.9 Beam and Plate Models for Eccentric Stiffeners.

Chapter 7

APPLICATIONS TO FULL-SCALE FLOOR SYSTEMS

7.1 Introduction

In this chapter the program *HYBSLAB* is used for the analysis of actual floor systems. Two reinforced concrete floors were chosen. The first is presented in Section 7.2 and is a flat plate without stiffeners. The second case is dealt with in Section 7.3 and is a plate with eccentric stiffeners. Whereas in the first case the columns are modelled as point supports, in the second case finite-sized columns are used.

For the first case, a typical floor of a high-rise building is analysed. Often in dealing with this type of structure, circumstances allow the designer to use one-dimensional beam elements and plane frame or plane grid computer programs to do the analysis. For example, the CSA and ACI building codes[1,2] for the design of reinforced concrete structures permit designers to analyse two-way slabs by an equivalent frame method. This method is satisfactory and practical for most floor systems which have columns laid out on a rectangular grid. However, as floor plans are selected to meet functional requirements, it is often necessary to move or even remove columns from a rectangular layout. The resulting column layout may become so irregular that it is virtually impossible to model the

floor system by an equivalent frame method. Similarly, the presence of large floor openings or load bearing walls can further complicate the frame analysis. It is for these situations that the finite element method is particularly suited and the use of equivalent frame methods is highly questionable.

The second floor system analysed is an experimental test slab with eccentric beams. For this floor both the finite size of the columns and the finite width of the beams is considered. This case is included not only to illustrate the use of the program but also to provide analytical data which can be correlated with experimental test data. The experimental data was obtained from a 3/4 scale test conducted in 1962 by the Portland Cement Association''. Such correlation studies are essential to verify that that an elastic finite element model can represent accurately the behavior of a real structure under service loads. The results of the data correlation are the subject of a continuing study and will not be discussed in this chapter.

7.2 Typical Floor of an Apartment Building

To illustrate the use of the program *HYBSLAB* and to demonstrate the feasibility of using this program for the analysis of real floor systems, the floor plan shown in Figure 7.1 was chosen. It is a typical floor of a recently constructed 17 story condominium apartment building. This

plan is characterized by an irregular layout of columns, large openings, cantilevered corners and load bearing walls. All of these features make it particularly difficult to choose a set of equivalent frames for analysis purposes. It is therefore the type of problem which is ideally suited for a finite element analysis. The floor plan shown in Figure 7.1 has overall plan dimensions of 109.0 feet by 81.7 feet and a slab thickness of 7.0 inches. The strength of the concrete was assumed to be 3500 psi and a single load case of 0.225 ksf was applied to the structure.

The finite element gridwork is shown in Figure 7.2. A total of 504 joints and 430 elements were used. For this gridwork, the amount of data and the number of man hours required to produce it are comparable to the data and preparation time required by an equivalent frame analysis.

Several guidelines were followed in selecting the gridwork. Rectangles were used wherever possible with an effort made to maximize the number of elements having the same dimensions. On the basis of the results from the square test plates in Chapter 3, an attempt was made to use at least four plate elements per panel side. This grid was felt to be adequate because, for the uniformly loaded square plate, the following errors in maximum positive moment were obtained: 0.80% for the simply supported plate, 1.79% for the clamped plate, 0.54% for the corner supported plate with free edges, and 7.50% for the clamped corners plate with zero normal slope along the edges.

In-plane displacements were not considered because the structure is a flat plate without any eccentric stiffeners. The chosen gridwork resulted in a problem with 1378 unknowns and a semi-band of 75. The analysis required 40.6 seconds of execution time on the AMDAHL 470/V7 computing system. At current(1981) commerical computing rates this run would cost approximately $55. This cost can be considered as insignificant compared to the cost associated with the manpower demands on a design project of this type.

To check the results from the analysis, a comparison was made between the *HYBSLAB* solution and an approximate equivalent frame method. An extensive comparison of the methods is not possible for this problem due to the difficulties in selecting suitable equivalent frames in most regions of the floor. One frame which can be chosen with some confidence is in the X direction along the row of columns located approximately midway between the edge of the building and the core. The frame is supported by the wall at nodes 5, 15 and 26, and the columns at nodes 122, 182, 262, 351, 441, and 496.

Negative moments at the columns and positive moments at or near midspans were compared and the results are shown in Table 7.1. In this table, the location of the moment is indicated by joint numbers along the section and the suffixed letters 'L' and 'R' denote the left and right side of the section. The width of the strip or section is also indicated and is the same for the equivalent frame as for

the finite element model.

The numbers in Table 7.1 indicate that from joints 26 to 397 the equivalent frame values ranged from 0.93 to 1.35 times the finite element values. From joints 441 to 496 this factor increased to 2.04. The larger discrepancy in this region can be attributed to the fact that the equivalent frame model which was used is not capable of modelling the free edges caused by the termination of the slab. The two free edges as shown in Figure 7.2 are connected by joints 436 to 441 and joints 496 to 504. The ratios of column axial loads are also shown in Table 7.1 and compare quite favorably, except for the corner column at node 496. Again the discrepancy for the corner column can be attributed to the difference in moment restraint of the two models at the free edge.

The ratios cited above are clearly dependent on the choice of the finite element gridwork and the assumed lines of zero shear which define the width of the equivalent frame. However, comparisons and cross-checking of this type are necessary for structures where no other solutions exist.

On the assumption that the reinforcing steel is to be placed in the X and Y directions, contour plots of M_x and M_y were produced and are presented in Figures 7.3 and 7.4. It is felt that plots of this type are particularly useful to a designer. Qualitatively, they provide a means of observing the overall behavior of the structure and detecting gross errors in the analysis. As well, the contour plots provide

a means of identifying potential areas of cracking, since unexpected tension zones can be readily detected. Quantitatively, they contain sufficient information so that, when drawn to the same scale as the working drawings, the steel layout can be done directly on the contour plots. The zero moment contours or lines of contraflexure are useful in avoiding unintentional termination of reinforcing in a tension zone.

The contour plots shown in Figures 7.3 and 7.4 were produced from the finite element solution by using the SURFACE2 plotter package. Some minor problems have been experienced with this process. The solution data supplied to the plotting routine is for element node points. In some regions, the combination of node spacing and the changes in the data between nodes may be such that the plotting routine has difficulty in producing the true contours. In these regions, contours have been found to touch or cross over. As well, the plotting routine has difficulty in plotting the contours along supporting walls and in representing the normal moments along free and simply supported edges. The latter problem is due in part to the fact that the finite element solution produces zero normal moments along free edges only in the limit as the gridwork is refined. Although these free edge moments are sufficiently small for design purposes, they do tend to distort the contour plots. The situation can be rectified prior to plotting by editing the auxiliary data file which contains the moment values.

The more serious problems with SURFACE2 are the method in which openings inside the plot areas are handled and the cost of running the program. It is felt that a simple plotting program can be developed which draws the contour lines for one element at a time. This would overcome the problems associated with irregular geometry and openings in the floor plan. As well, it would be more economical and would provide more meaningful plots because the data at the nodal points would be used directly. This would eliminate the costly and approximate operation in SURFACE2 of transferring the nodal data to rectangular grid points. The two main disadvantages of this simple approach are that the contour lines would appear as a series of straight line segments and also it may be difficult to label the contours. The development of such a plotting program was not undertaken in this study, but it is felt that it would be a worthwhile project.

7.3 Experimental Test Floor

The second floor chosen to test the *HYBSLAB* program is the experimental test floor with eccentric beams. One of the main reasons for using this floor is to illustrate the use of the computer program for plates supported by beams and finite-sized columns. The floor plan is shown in Figure 7.5 and has overall dimensions of 46.0 feet × 46.0 feet with a slab thickness of 5.25 inches. Two different sizes of

edge beams are present in the structure. Along the edge at X=0 and the edge at Y=45 feet, the edge beams are 12 inches wide and have an overall depth of 8.25 inches. Along the other two edges, the beams are 6.0 inches wide and have an overall depth of 15.75 inches. These members will be called the 'narrow' beams, while the 12.0 inch wide members will be referred to as the 'wide' beams. The columns are indicated on the plan and are identified by numbers 1 to 16 inclusive. The structure is symmetrical about a diagonal joining column 4 to column 13. The modulus of elasticity of the floor was assumed to be 3670 ksi and a Poisson's ratio of 0.15 was used. The column stiffnesses were calculated from a column length of 42.375 inches and a 'fixed end' condition was assumed at the far ends of the columns. A single load case of 0.100 ksf was applied to the structure.

The finite element model for the floor system is shown in Figure 7.6. A total of 295 joints and 282 elements were used. The elements consist of 256 rectangles, 24 beams and 2 rectangular transition elements.

The edge stiffeners were modelled both as eccentric beam elements and as offset plate elements. The overall approach as described earlier was used to represent the cross section. The wide edge beams were modelled as line beams along the edge at X=0 and as offset plate elements along the edge at Y=45 feet. The narrow edge beams were modelled as line beams along the edge at Y=0 and as offset plate elements along the edge at X=45 feet. These two

different models were used in the same structure with the intent that the results from the two approaches could be compared and would serve as a cross-check on each other. The comparisons are possible because the structure is symmetrical about its diagonal. With the two different models, the values at points of symmetry will not remain identical, but it is expected that the differences will not be significant for design purposes. If this is true, then the designer is free to use the two models interchangeably.

The column cross sections were modelled by rectangular shaped elements with thicknesses equal to 100 times the slab thickness. This approach, which was discussed at the end of Chapter 5, is used to make a column head very stiff so that it undergoes a minimal amount of deformation and basically behaves as a rigid body.

In-plane displacements were permitted in the vicinity of the edge beams but were suppressed on the interior of the structure. The nodes at which the in-plane displacements were assumed to be zero are contained in the square block of nodes defined by joints 55, 65, 229, and 239.

The chosen gridwork resulted in a problem with 1195 unknowns and a semi-band of 97. The analysis required 35.3 seconds of execution time on the AMDAHL 470/V8 computing system. At current(1981) commerical computing rates this run would cost approximately $45.

To check the results from the program *HYBSLAB*, a number of statics checks were done on the structure. These checks

were done at midspan of each bay in both directions and confirmed that the conditions of statics were satisfied. Additional checks were done by calculating the axial load in each column based on an assumed tributary area. These results were found to be quite close to the values obtained from *HYBSLAB* and are not presented.

The effect of the two different beam models on the columns was studied by comparing the forces at the column centroids. The comparison of these values is indicated in Table 7.2. In this table, the bracketed number denotes the column which has symmetrical values. The percent difference for the axial loads is less than 3.5%, but the differences in the more significant column moments reach values as high as 18%. Some of the discrepancy in the column moments is expected to be due to the difference in elements used to model the column cross sections. Comparisons of transverse displacements were also done for each edge beam and the midspan values were found to be quite similar.

A study of the rotations of each column head indicated that all nodes on the perimeter had undergone the same amount of rotation to within 4 and 5 digits of accuracy. This indicates that the column heads are basically acting as rigid members.

To illustrate another plotting facility of the program, the isolines for the transverse displacement, *W*, were plotted as shown in Figure 7.7. Since the displacement profiles of this floor can be visualized rather easily, this

type of plot serves as a means of detecting gross errors in the analysis. As well, the plot can be folded about the diagonal of symmetry and deflections at points of symmetry can be compared.

The intent of running the program for this floor system was to indicate some additional capabilities of *HYBSLAB* and the versatility of the finite element method to handle such problems. The amount of checking done thus far has been aimed at verifying that the results from *HYBSLAB* satisfy the conditions of statics and that the output data looks reasonable. The checking is by no means complete and work is continuing on additional checking and comparing the finite element results to the experimental test data. The outcome of this correlation study will be made available under separate cover.

Typical Floor of High Rise Building:				
Nodes	Strip Width	Finite Element	Equivalent Frame	Ratio (Frame/FEM)
(Negative Moments)	(feet)	(ft.kips)	(ft.kips)	
24-->30	17.0	-162.1	-152.3	0.94
120-->125L	17.0	-101.9	-138.0	1.35
120-->125R	17.0	-62.5	-58.3	0.93
180-->186L	17.0	-39.4	-44.6	1.13
180-->186R	12.5	-47.5	-51.1	1.08
260-->264L	12.5	-56.2	-59.1	1.05
260-->264R	12.5	-53.9	-68.8	1.28
349-->353L	12.5	-60.5	-70.5	1.17
349-->353R	12.9	-64.9	-79.0	1.22
439-->444L	12.9	-41.5	-71.6	1.73
439-->444R	7.35	-28.3	-40.0	1.41
496-->498R	7.35	-13.1	-26.7	2.04
(Positive Moments)	(feet)	(ft.kips)	(ft.kips)	
82-->87	17.0	+67.9	+68.5	1.01
220-->224	12.5	+30.7	+28.5	0.93
302-->306	12.5	+29.2	+35.1	1.20
395-->399	12.9	+36.2	+39.7	1.10
476-->479	7.35	+14.6	+17.6	1.21
(Axial Load in Column)		(Kips)	(Kips)	
122	-	-66.6	-64.5	0.97
182	-	-41.2	-43.0	1.04
262	-	-55.0	-46.4	0.84
351	-	-45.9	-50.7	1.10
441	-	-37.9	-39.3	1.04
496	-	- 8.4	-12.1	1.44

Table 7.1 Comparison of Forces for the Finite Element Model and an Equivalent Frame Model.

Axial Loads and Moments in Columns:			
Column	Axial Load	X-axis Moment	Y-axis Moment
1 (16)	- 5.248	-10.488	- 8.144
2 (12)	-11.907	-20.746	+ 2.738
3 (8)	-11.857	-20.111	- 2.660
4	- 5.005	- 8.715	+ 9.626
5 (15)	-11.677	+ 1.861	-22.129
6 (11)	-24.118	+ 2.736	+ 2.713
7	-23.731	+ 2.612	- 1.499
8 (3)	-12.270	+ 2.911	+23.005
9 (14)	-11.602	- 1.684	-21.145
10	-23.968	- 2.405	+ 2.780
11 (6)	-23.595	- 2.314	- 1.596
12 (2)	-12.211	- 2.841	+23.334
13	- 5.567	+11.176	-10.898
14 (9)	-11.800	+22.621	+ 1.833
15 (5)	-11.676	+21.917	- 1.403
16 (1)	- 5.370	+ 9.234	+12.562

Table 7.2 Experimental Floor, Comparison of Column Forces.

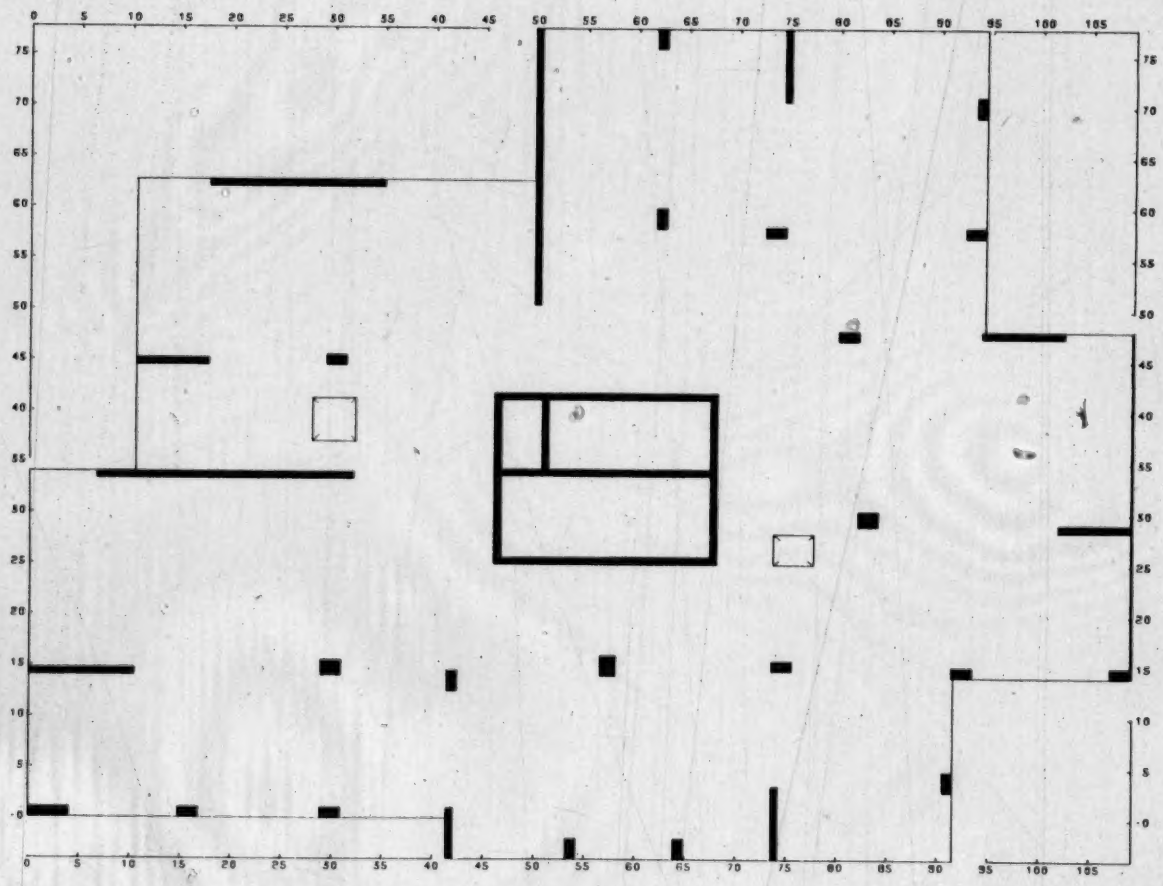

Figure 7.1 Typical Floor of a High-Rise Building.

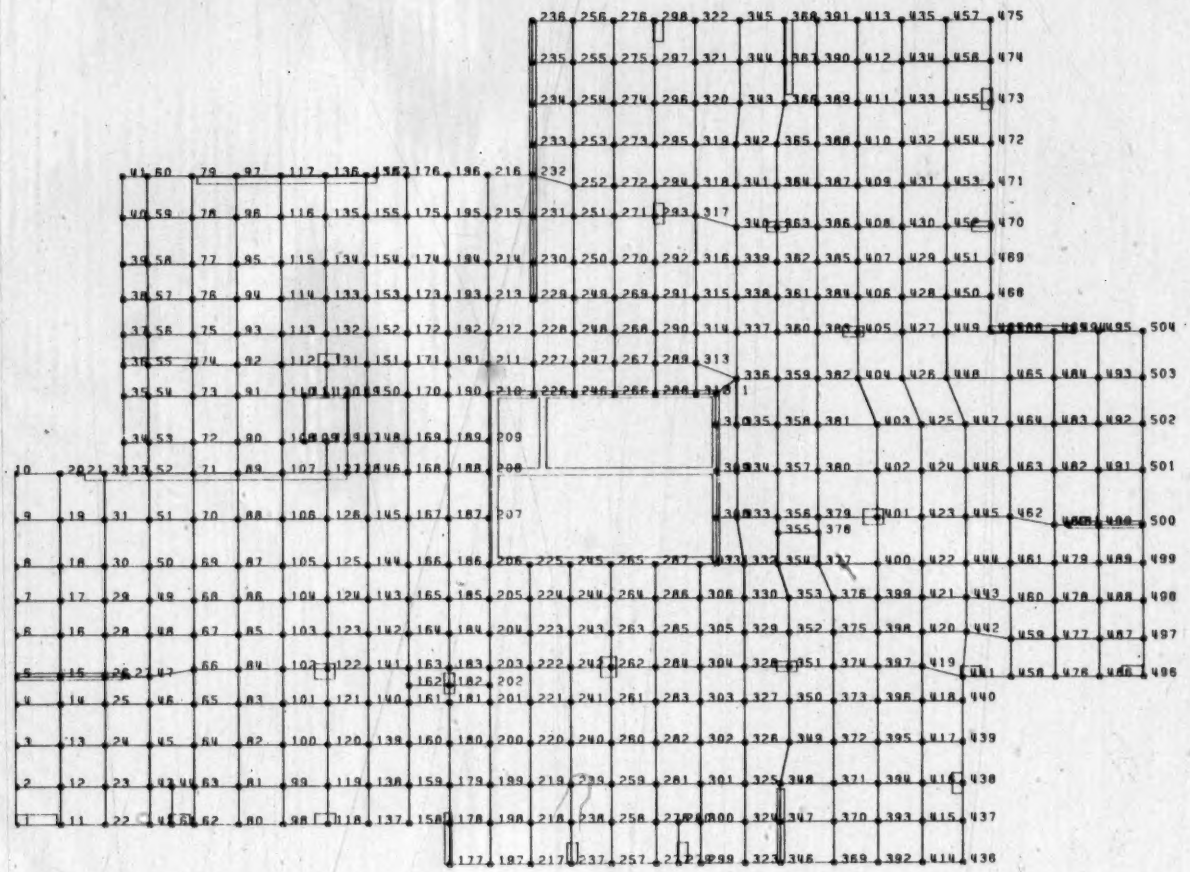

Figure 7.2 Finite Element Grid for Typical Floor.

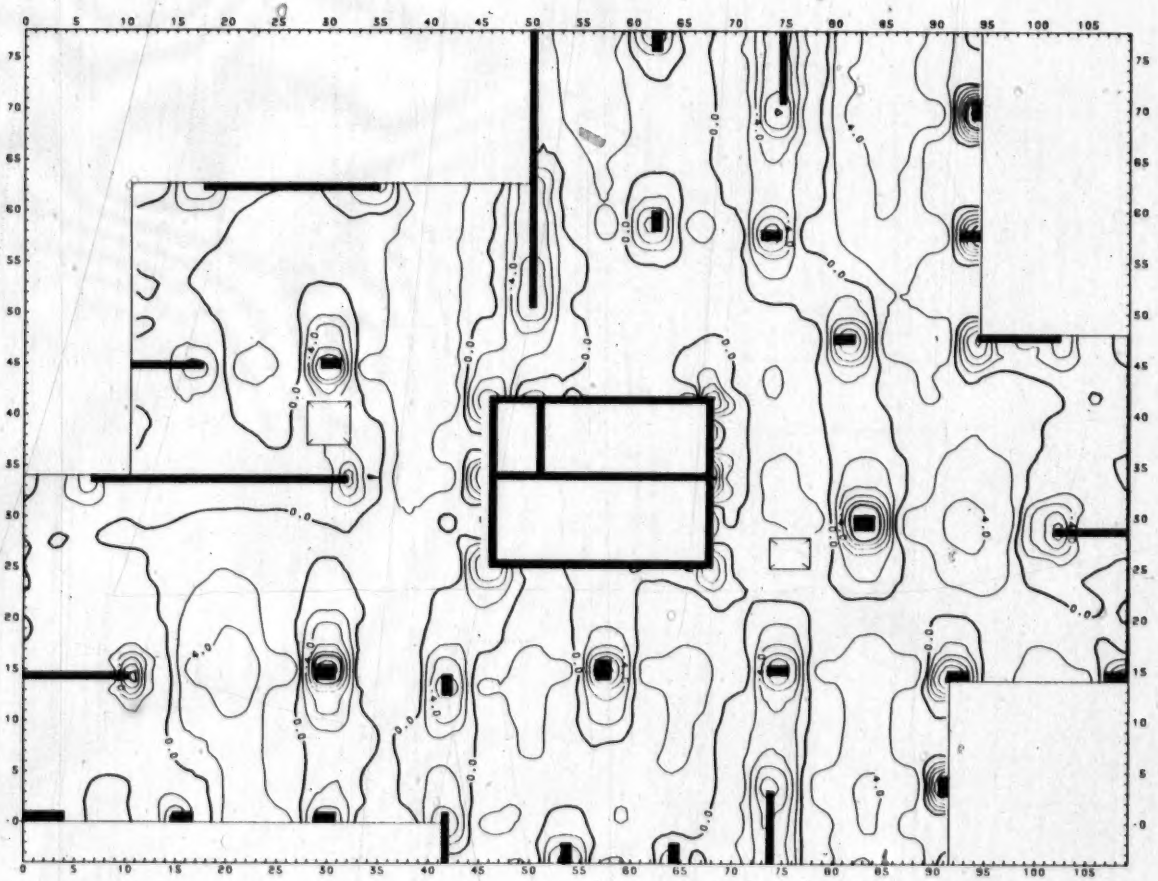

Figure 7.3 Contour Plots of Bending Moment *Mx*, (ft.kips/ft.).

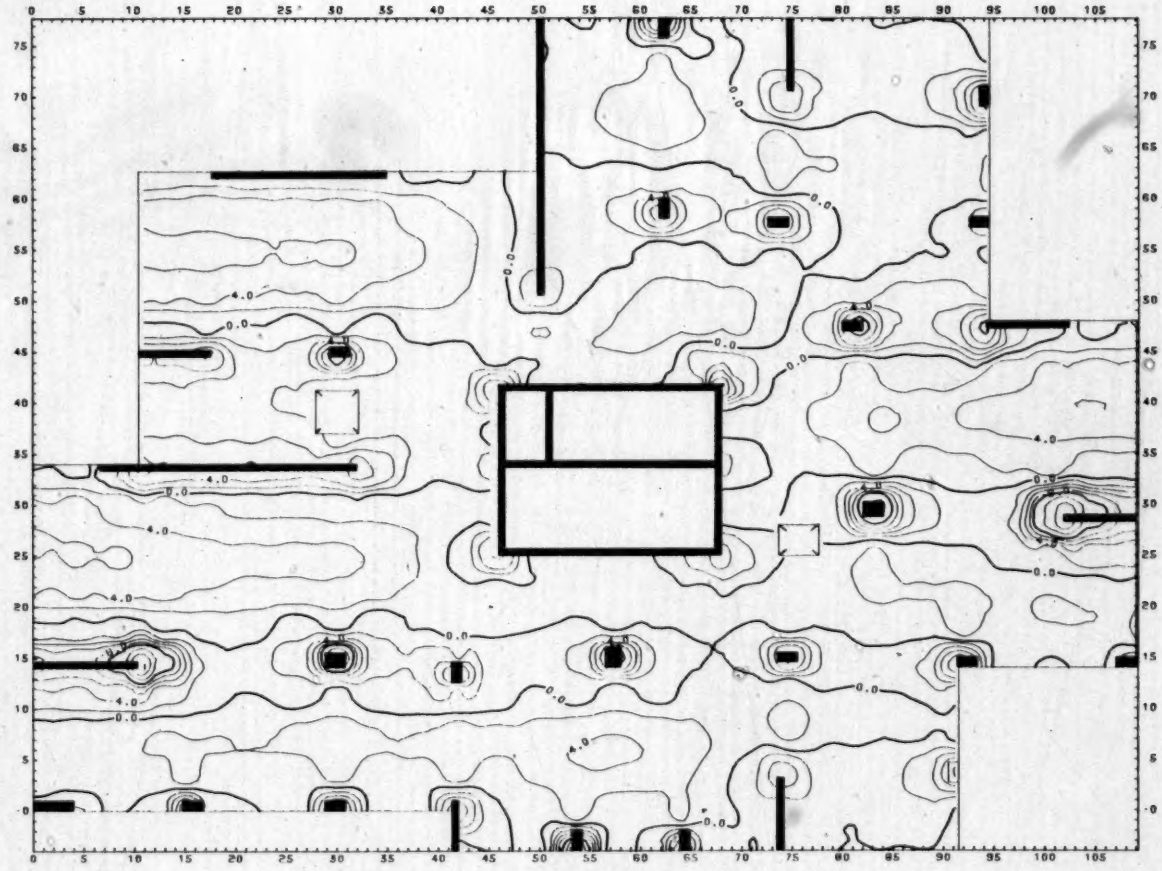

Figure 7.4 Contour Plots of Bending Moment My, (ft.kips/ft.).

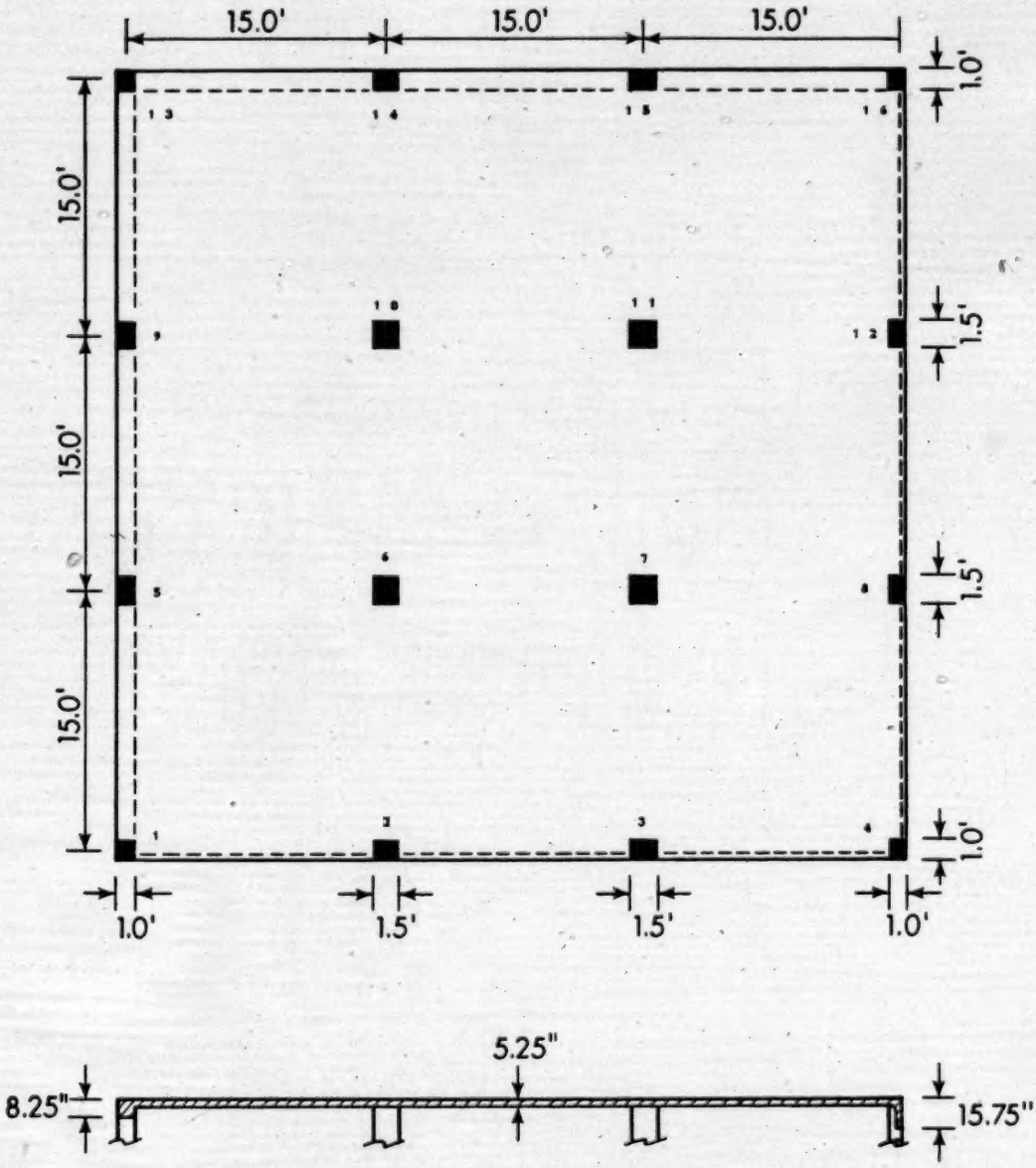

Figure 7.5 Experimental Test Slab.

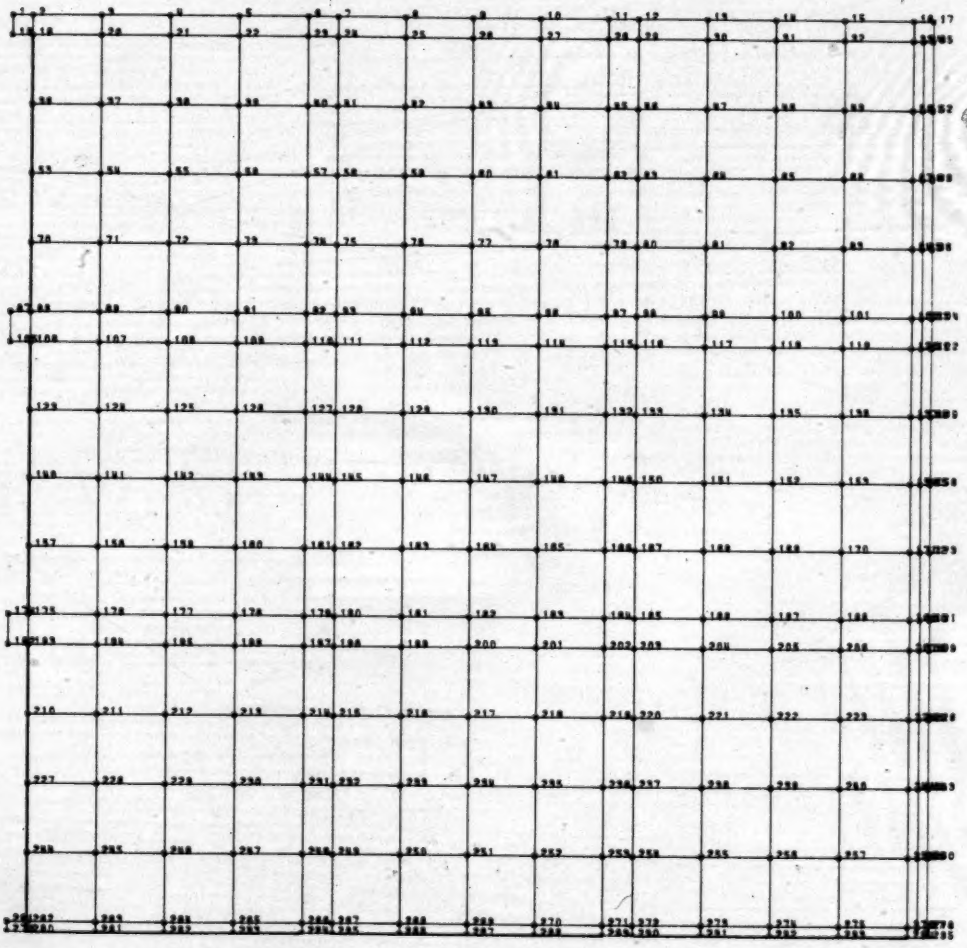

Figure 7.6 Finite Element Grid for Experimental Slab.

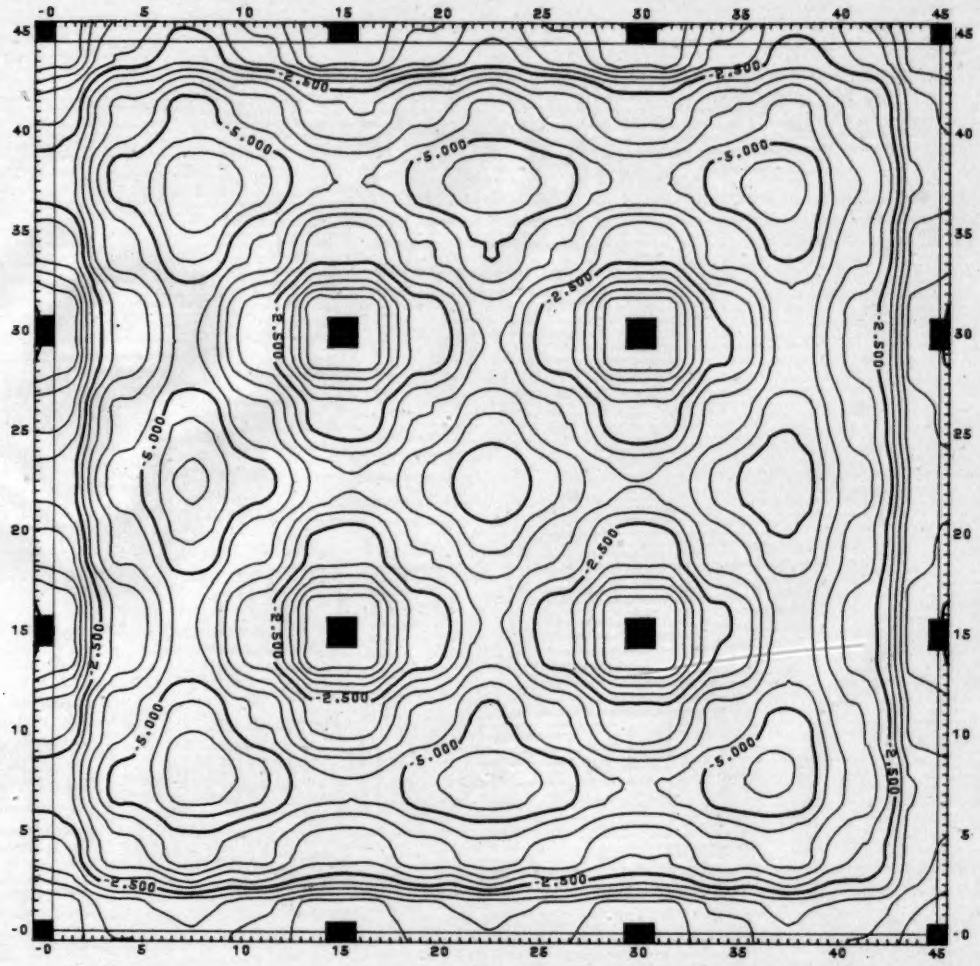

Figure 7.7 Contour Plots of Displacement *W*, (feet/1000).

Chapter 8

SUMMARY AND CONCLUSIONS

8.1 Summary

At the outset it was stated that this investigation was undertaken with two objectives in mind. The first of these was to develop a general purpose computer program for practical use. To this end the program *HYBSLAB* was written. The second objective was to present and use a formulation which could take into account the effects of stress singularities at reentrant corners of plates in flexure.

The program is based on the hybrid stress method and uses elements with only geometric degrees of freedom as nodal parameters. The choice to use the hybrid stress formulation was made after an extensive literature search and testing of a number of rectangular elements.

The theory of the hybrid stress method is reviewed and a formulation is proposed to include the effects of stress singularities at reentrant corners. This is followed by a presentation and discussion of the explicit forms of the various component matrices required to calculate stiffness matrices for multi-sided elements. With these matrices as a basis, the program *HYBSLAB* was developed. A general description of the program *HYBSLAB* is given and the methods used to model eccentric stiffeners and finite-sized columns are discussed.

To test the program and its variety of element shapes, a number of test cases are used. The patch test is used to verify that assemblages of elements with arbitrary configurations are capable of representing the constant strain states for plane stress and constant curvature states for flexure. Additional test cases with various grids are presented to demonstrate that the various element shapes do converge to the correct values. This is followed by the use of the singularity elements on plates with reentrant corners. In the vicinity of the reentrant corner, the singularity elements appear to be capable of providing significantly better results than analyses which do not consider the singularity.

The error caused by coupling eccentric stiffeners to a plate is considered. A T-beam is analysed and the cross section is represented by a 'layered' and an 'overall' model. As well, both line beams and offset plate elements are used to model the T-beam member. For all cases tested, the overall approach was found to be more accurate than the layered model.

In closing, it is demonstrated that the program *HYBSLAB* can be used for the analysis of actual floor systems. The first case considered is a typical floor of a high-rise building. This floor is modelled in a manner similar to that expected to be used by a design engineer. The structure is represented as a flat plate supported by point-sized columns and the effects of stress singularities

are not included. The second case is a slab which was tested by the Portland Cement Association in 1962. The finite element model for this floor takes into account the finite dimensions of the column cross section and the finite width of the beam stem. At present, another study is under way which is correlating the finite element values with the experimental results.

8.2 Conclusions

The work done in this investigation demonstrates that the finite element method is a viable alternative to some of the more approximate traditional methods presently being used by design engineers. From an economical point of view, it has been shown that the finite element method can be used competitively against equivalent frame methods to analyse floor systems. From an analytical point of view, there is no question as to which method is more appropriate for the analysis of plates.

The merits of using a finite element based program such as *HYBSLAB* are many. The most important is the nature of the solution. The analytical solution is for a structure which is represented by a series of finite-sized plate elements connected at the nodal points. First, the solution consists of nodal displacement values which are compatible. There are no discontinuities in the transverse displacement, the two nodal rotations and the two in-plane translations.

Second, the calculated nodal forces are such that each and every element is in equilibrium under the action of the applied loading. This is the type of solution that many designers intuitively feel is adequate for design purposes. Whether the numerical values come from a finite element solution or elsewhere is immaterial to most designers. No other method exists which is as simple to use as the finite element method and, at the same time, is as capable of providing the type of solution just discussed.

From a designer's point of view, another advantage of the finite element method is the consistency introduced into the design procedure. After the gridwork for the structure and the boundary conditions have been decided upon, the remaining procedure is straightforward. In contrast, non-standard floor systems designed by equivalent frame approaches leave much to the discretion of the engineer. This often leads to differences of opinions regarding matters such as the ziz-zagging of a frame to include nearby columns and the multiple branching or 'forking' of a frame to include columns on either side.

Other advantages of using the finite element method are the standardization which can be introduced into the design procedure. This has time-saving advantages in the sense that the checking of a design would simply consist of verifying that the input for the model is correct. This would be followed by spot checks on the output to determine if the results look reasonable. Additional time-saving

features which could be standardized are the graphical output of the connectivity data and the plotting of moment and displacement contours as illustrated in Chapter 7.

It is concluded that, although more traditional analysis techniques like the equivalent frame methods are quite satisfactory for many floor systems, there are situations where the finite element method offers a number of advantages while remaining competitive in terms of cost. Thus, while not proposing the abandonment of the frame methods, it is suggested that designers should give serious consideration to adopting the finite element method for problems to which it is particularly suited.

It is also felt that the automatic data generating capabilities of *HYBSLAB* make it competitive with the frame methods for floor systems with regular column layouts. Through repeated use of the program on simple structures the designer would become more efficient at this type of analysis and would be more qualified to model a complicated structure. The question of the importance of including the effects of stress singularities at reentrant corners is not addressed in any amount of detail in this study. A formulation to include the singularities has been proposed. This approach has been used to obtain stiffness matrices for L-shaped singularity elements, and plates with reentrant corners were analysed in Chapter 6. The results from the analysis appear to be reasonable and it is concluded that the formulation is valid.

8.3 Recommendations for Future Studies

Additional research is still required on a number of topics. Probably the most demanding of these is continuing the work on the singularity elements. As discussed in Chapter 4, only the real eigenvalue was considered for the L-shaped element with clamped reentrant edges. A considerable amount of work remains to be done in obtaining the matrices associated with the complex eigenvalue. For both the free edge and the fixed edge elements, a more indepth study is required to assess the importance of the singularities for a wide range of problems. The problems in Chapter 6 were done to demonstrate the use of the proposed formulation. The results look encouraging enough that further studies are warranted.

Regarding the program *HYBSLAB*, few technical revisions are envisioned. The program has been used for a wide range of problems and appears to be working satisfactorily. If the program continues to be used, errors will surface but these are not expected to cause major revisions to the program.

Additional testing is still required to assess more fully the behavior characteristics of a number of elements, such as the multi-sided elements and the offset elements used to model stiffeners. As well, the use of the five- and six-noded rectangular elements as transition elements for changing grid sizes has not been investigated.

A complete listing of the program *HYBSLAB* and a related user's manual[104] will be available from the University of Alberta where this research was done.

References

1. Abel, J.F., and Desai, C.S., "Comparison of Finite Elements for Plate Bending," *Journal of the Structural Division, ASCE*, Vol.98, No. ST9, Sept., 1972, pp. 2143-2148.

2. ACI Committee 318, "Building Code Requirements for Reinforced Concrete Structures (ACI 318-77)," *American Concrete Institute*, Detroit, Michigan, Aug., 1978.

3. Adini, A., and Clough, R.W., "Analysis of Plate Bending by the Finite Element Method," Report submitted to the National Science Foundation (Grant G7337), Washington, D.C., 1960.

4. Adini, A., "Analysis of Shell Structures by the Finite Element Method," thesis presented in partial fulfillment of the requirements for the degree of Doctor of Philosophy, Department of Civil Engineering, University of California, Berkeley, 1961.

5. Ahmad, S., Irons, B.M., and Zienkiewicz, O.C., "Curved Thick Shell and Membrane Elements with Particular Reference to Axisymmetric Problems," *Proceedings of the Second Conference on Matrix Methods in Structural Mechanics*, AFFDL-TR-68-150, Ohio, Oct. 15-17, 1968, pp. 539-572.

6. Ahmad, S., Irons, B.M., and Zienkiewicz, O.C., "Analysis of Thick and Thin Shell Structures," *International Journal for Numerical Methods in Engineering*, Vol.2, No.3, 1970, pp. 419-451.

7. Ali, R., Gopalacharyulu, S., and Sharman, P.W., "The Development of a Series of Hybrid-Stress Finite Elements," *Proceedings of the World Congress on Finite Element Methods in Structural Mechanics*, held at Bournemouth, Dorset, England, 1975, Vol.II, pp. 13.1-13.27.

8. Allman, D.J., "Triangular Finite Elements for Plate Bending with Constant and Linearly Varying Bending Moments," *The Proceedings of the IUTAM Symposium on High Speed Computing of Elastic Structures*, B. Fraeijs de Veubeke, ed., University of Liege, Belgium, Aug. 23-28, 1970, pp.105-136.

9. Allman, D.J., "A Simple Cubic Displacement Element for Plate Bending," *International Journal for Numerical Methods in Engineering*, Vol.10, No.2, 1976, pp. 263-281.

10. Allwood, R.J., and Cornes, G.M.M., "A Polygonal Finite Element for Plate Bending Problems Using the Assumed Stress Approach," *International Journal for Numerical Methods in Engineering*, Vol.1, No.2, 1969, pp. 135-150.

11. Anderheggen, E., "Finite Element Plate Bending Equilibrium Analysis," *Journal of the Engineering Mechanics Division, ASCE*, Vol.95, No. EM4, Aug., 1969, pp. 841-857.

12. Anderheggen, E., "A Conforming Triangular Finite Element Plate Bending Solution," *International Journal for Numerical Methods in Engineering*, Vol.2, No.2, 1970, pp. 259-264.

13. Argyris, J.H., "Continua and Discontinua," *Proceedings of the First Conference on Matrix Methods in Structural Mechanics*, AFFDL-TR-66-80, Ohio, Oct. 26-28, 1965, pp. 11-189.

14. Argyris, J.H., "Matrix Displacement Analysis of Anisotropic Shells by Triangular Elements," *The Aeronautical Journal of The Royal Aeronautical Society*, Vol.69, Nov., 1965, pp. 801-805.

15. Argyris, J.H., Buck, K.E., Scharpf, D.W., Hilber, H.M., and Mareczek, G., "Some New Elements for the Matrix Displacement Method," *Proceedings of the Second Conference on Matrix Methods in Structural Mechanics*, AFFDL-TR-68-150, Ohio, Oct. 15-17, 1968, pp. 333-397.

16. Argyris, J.H., Fried, I., and Scharpf, D.W., "The TUBA Family of Plate Elements for the Matrix Displacement Method," *The Aeronautical Journal of The Royal Aeronautical Society*, Vol.72, Aug., 1968, pp. 701-709.

17. Argyris, J.H., and Buck, K.E., "A Sequel to 'The TUBA Family of Plate Elements for the Matrix Displacement Method'," *The Aeronautical Journal of The Royal Aeronautical Society*, Vol.72, Aug., 1968, pp. 977-983.

18. Baldwin, J.T., Razzaque, A., and Irons, B.M., "Shape Function Subroutines for an Isoparametric Thin Plate Element," *International Journal for Numerical Methods in Engineering*, Vol.7, No.4, 1973, pp. 431-440.

19. Balmer, H.A., "Another Aspect of the Error in Eccentric Beam Formulation," *International Journal for Numerical Methods in Engineering*, Vol.11, No.11, 1978, pp. 1761-1771.

20. Ballesteros, P., and Lee, S.L., "Uniformly Loaded Rectangular Plate Supported at the Corners," *International Journal of Mechanical Science*, Vol.2, No.3, 1960, pp. 206-211.

21. Bares, R., *Tables for the Analysis of Plates, Slabs, and Diaphragms Based on Elastic Theory*, Bauverlag GmbH., Berlin, 1968.

22. Bartholomew, P., "Comment on Hybrid Finite Elements," *International Journal for Numerical Methods in Engineering*, Vol.10, No.4, 1976, pp. 968-973.

23. Batoz, J.L., Bathe, K.J., and Ho, L.W., "A Study of Three-Node Triangular Plate Bending Elements," *International Journal for Numerical Methods in Engineering*, Vol.15, No.12, 1980, pp. 1771-1812.

24. Bathe, K.J., Wilson, E.L., and Peterson, F.E., "SAP IV - A Structural Analysis Program for Static and Dynamic Response of Linear Systems," Report submitted to the National Science Foundation, Report No. EERC 73-11, College of Engineering, University of California, Berkeley, California, June, 1973.

25. Bazeley, G.P., Cheung, Y.K., Irons, B.M., and Zienkiewicz, O.C., "Triangular Elements in Plate Bending - Conforming and Non-Conforming Solutions," *Proceedings of the First Conference on Matrix Methods in Structural Mechanics*, AFFDL-TR-66-80, Ohio, Oct. 26-28, 1965, pp. 547-576.

26. Bell, K., "Analysis of Thin Plates in Bending Using Triangular Finite Elements," *Division of Structural Mechanics Engineering Report*, The Technical University of Norway, Trondheim, 1968.

27. Bell, K.,"Triangular Plate Bending Elements," Chapter 7 of *Finite Element Methods in Stress Analysis*, I. Holand and K. Bell, eds., TAPIR (Technical University of Norway Press), Trondheim, 1969.

28. Bell, K., "A Refined Triangular Plate Bending Finite Element," *International Journal for Numerical Methods in Engineering*, Vol.1, No.1, 1969, pp. 101-122.

29. Bergan, P.G., and Hanssen, L., "A New Approach for Deriving 'Good' Element Stiffness Matrices," *The Mathematics of Finite Elements and Applications*, J.R. Whiteman, ed., Academic Press, London, 1975, pp. 483-497.

30. Bicanic, N., and Hinton, E., "Spurious Modes in Two-Dimensional Isoparametric Elements," *International Journal for Numerical Methods in Engineering*, Vol.14, No.10, 1979, pp. 1545-1557.

31. Bogner, F.K., Fox, R.L., and Schmit, Jr., L.A., "The Generation of Inter-Element Compatible Stiffness and Mass Matrices by Use of Interpolation Formulas," *Proceedings of the First Conference on Matrix Methods in Structural Mechanics*, AFFDL-TR-66-80, Ohio, Oct. 26-28, 1965, pp. 397-443.

32. Boot, J.C., "On A Problem Arising from the Derivation of Finite Element Matrices Using Reissner's Principle," *International Journal for Numerical Methods in Engineering*, Vol.12, No.12, 1978, pp. 1879-1882.

33. Bosshard, W., "Ein Neues, Vollvertagliches Endliches Element fur Plattenbiegung," *International Association of Bridge and Structural Engineering Bulletin*, Zurich, Vol.28, 1968, pp. 27-40.

34. Bron, J.C., and Dhatt, G., "Mixed Quadrilateral Elements for Bending," *American Institute of Aeronautics and Astronautics Journal*, Vol.10, No.10, 1972, pp. 1359-1361.

35. Butlin, G.A., "A Refined Triangular Plate Bending Element," *International Journal for Numerical Methods in Engineering*, Vol.1, No.4, 1969, pp. 395.

36. Butlin, G.A., and Ford, R., "A Compatible Triangular Plate Bending Finite Element," *Engineering Department Report 68-15*, University of Leicester, Oct., 1968.

37. Butlin, G.A., and Ford, R., "A Compatible Triangular Plate Bending Finite Element," *International Journal of Solids and Structures*, Vol.6, No.3,1970, pp. 323-332.

38. Butlin, G.A., and Leckie, F.A., "A Study of Finite Elements Applied to Plate Flexure," presented at *The Symposium on Numerical Methods for Vibration Problems*, held at the University of Southampton, July, 1966.

39. Caramanlian, C., Selby, K.A., and Will, G.T., "A Quintic Conforming Plate Bending Triangle," *International Journal for Numerical Methods in Engineering*, Vol.12, No.7, 1978, pp. 1109-1130.

40. Chatterjee, A., and Setlur, A.V., "A Mixed Finite Element Formulation for Plate Problems," *International Journal for Numerical Methods in Engineering*, Vol.4, No.1, 1972, pp. 67-84.

41. Cheung, Y.K., and Chan, H.C., "A Family of Rectangular Bending Elements," *Computers and Structures*, Vol.10, 1979, pp. 613-619.

42. Cheung, Y.K., King, I.P, and Zienkiewicz, O.C., "Slab Bridges with Arbitrary Shape and Support Conditions: A General Method of Analysis Based on Finite Elements," *Proceedings of the Institution of Civil Engineers, London*, Vol.40, 1968, pp. 9-36.

43. Chu, T.C., and Schnobrich, W.C., "Finite Element Analysis of Translational Shells," *Computers and Structures*, Vol.2, 1972, pp. 197-222.

44. Clough, R.W., "The Finite Element Method in Structural Analysis," Chapter 7 of *Stress Analysis*, O.C. Zienkiewicz and G.S. Holister, eds., John Wiley and Sons, Inc., London, 1965.

45. Clough, R.W., "The Finite Element Method After Twenty-Five Years: A Personal View," *Computers and Structures*, Vol.12, pp. 361-370

46. Clough, R.W., and Felippa, C.A., "A Refined Quadrilateral Element for the Analysis of Plate Bending," *Proceedings of the Second Conference on Matrix Methods in Structural Mechanics*, AFFDL-TR-68-150, Ohio, Oct. 15-17, 1968, pp. 399-440.

47. Clough, R.W., and Tocher, J.L., "Finite Element Stiffness Matrices for the Analysis of Plate Bending," *Proceedings of the First Conference on Matrix Methods in Structural Mechanics*, AFFDL-TR-66-80, Ohio, Oct. 26-28, 1965, pp. 515-545.

48. Connor, J., and Will, G., "A Triangular Flat Plate Bending Element," Technical Report 68-3, Department of Civil Engineering, M.I.T., Cambridge, Mass., 1968.

49. Cook, R.D., "More on Reduced Integration and Isoparametric Elements," *International Journal for Numerical Methods in Engineering*, Vol.5, No.1, 1972, pp. 141-148.

50. Cook, R.D., "Two Hybrid Elements for Analysis of Thick, Thin and Sandwich Plates," *International Journal for Numerical Methods in Engineering*, Vol.5, No.2, 1972, pp. 277-288.

51. Cook, R.D., "Some Elements for Analysis of Plate Bending," *Journal of the Engineering Mechanics Division, ASCE*, Vol.98, No. EM6, Dec., 1972, pp. 1453-1470.

52. Cook, R.D., "A Note on Certain Incompatible Elements," *International Journal for Numerical Methods in Engineering*, Vol.6, No.1, 1973, pp. 146-147.

53. Cook, R.D., "Further Improvement of an Effective Plate Bending Element," *Computers and Structures*, Vol.6, 1976, pp. 93-97.

54. Cook, R.D., and Ladkany, S.G., "Observations Regarding Assumed-Stress Hybrid Plate Elements," *International Journal for Numerical Methods in Engineering*, Vol.8, No.3, 1974, pp. 513-520.

55. Courant, R., "Variational Methods for the Solution of Problems of Equilibrium and Vibrations," *Bulletin of the American Mathematical Society*, Vol.49, 1943, pp. 1-23.

56. Cowper, G.R., Kosko, E., Lindberg, G.M., and Olson, M.D., "Formulation of a New Triangular Plate Bending Element," *Transactions of the Canadian Aeronautics and Space Institute* , Vol.1, No.2, Sept., 1968, pp. 86-90.

57. Cowper, G.R., Kosko, E., Lindberg, G.M., and Olson, M.D., "Static and Dynamic Applications of a High-Precision Triangular Plate Bending Element," *American Institute of Aeronautics and Astronautics Journal*, Vol.7, No.10, Oct., 1969, pp. 1957-1965.

58. CSA/NBC Joint Committee, "Code for the Design of Concrete Structures for Buildings (CAN3-A23.3-M77)," Canadian Standards Association, Rexdale, Ontario, Dec., 1977.

59. Davies, J.D., Parekh, C.J., and Zienkiewicz, O.C., "Analysis of Slabs with Edge Beams," *International Symposium on Bridge Design*, Vol.1, 1969, pp. 142-163.

60. Dawe, D.J., "A Finite Element Approach to Plate Vibration Problems," *The Journal of Mechanical Engineering Sciences*, Vol.7, No.1, 1965, pp. 28-32.

61. Dawe, D.J., "Parallelogrammic Elements in the Solution of Rhombic Cantilever Plate Problems," *Journal of Strain Analysis*, Vol.1, No.3, 1966, pp. 223-230.

62. Dawe, D.J., "On Assumed Displacements for the Rectangular Plate Bending Element," *The Aeronautical Journal of The Royal Aeronautical Society*, Vol.71, Oct., 1967, pp. 722-724.

63. Deak, A.L., and Pian, T.H.H., "Application of Smooth-Surface Interpolation to the Finite-Element Analysis," *American Institute of Aeronautics and Astronautics Journal*, Vol.5, No.1, 1967, pp. 187-189.

64. Dhatt, G., "Numerical Analysis of Thin Shells by Curved Triangular Elements Based on Discrete Kirchhoff Hypothesis," *Proceedings of the Symposium on Application of Finite Element Methods in Civil Engineering*, held at the School of Engineering, Vanderbilt University, Nashville, Tennessee, Nov. 13-14, 1969, pp. 255-278.

65. Dhatt, G., "An Efficient Triangular Shell Element," *American Institute of Aeronautics and Astronautics Journal*, Vol.8, No.11, Sept., 1970, pp. 2100-2102.

66. Doherty, W.P., Wilson, E.L., and Taylor, R.L., "Stress Analysis of Axisymmetric Structures Using Higher Order Quadrilateral Elements," *Structural Engineering Lab. Report SESM 69-3*, University of California, Berkeley, 1969.

67. Dungar, R., Severn, R.T., and Taylor, P.R., "Vibration of Plate and Shell Structures Using Triangular Finite Elements," *Journal of Strain Analysis*, Vol.2, No.1, 1967, pp. 73-83.

68. Dungar, R., and Severn, R.T., "Triangular Finite Elements of Variable Thickness and Their Application to Plate and Shell Problems," *Journal of Strain Analysis*, Vol.4, No.1, 1969, pp. 10-21.

69. Dunne, P., "Complete Polynomial Displacement Fields for the Finite Element Method," *The Aeronautical Journal of The Royal Aeronautical Society*, Vol.72, March, 1968, pp. 246-247.

70. Elias, Z.M., "Duality in Finite Element Methods," *Journal of the Engineering Mechanics Division, ASCE*, Vol.94, No. EM4, Aug., 1968, pp. 931-946.

71. Ergatoudis, I., Irons, B.M., and Zienkiewicz, O.C., "Curved, Isoparametric, 'Quadrilateral' Elements for Finite Element Analysis," *International Journal of Solids and Structures*, Vol.4, No.1, 1968, pp. 31-42.

72. Ergatoudis, I., and Zienkiewicz, O.C., discussion of "Complete Ploynomial Displacement Fields for the Finite Element Method," by P. Dunne, Paper No.6726, *The Aeronautical Journal of The Royal Aeronautical Society*, Vol.72, Aug., 1968, pp. 710.

73. Felippa, C.A., "Refined Finite Element Analysis of Linear and Nonlinear Two-Dimensional Structures," thesis presented in partial fulfillment of the requirements for the degree of Doctor of Philosophy, Department of Civil Engineering, University of California, Berkeley, 1966.

74. Fraeijs de Veubeke, B., ed., "Upper and Lower Bounds in Matrix Structural Analysis," *Matrix Methods of Structural Analysis*, Pergamon Press, Oxford, 1964, pp. 165-201.

75. Fraeijs de Veubeke, B., "Displacement and Equilibrium Models in the Finite Element Method," Chapter 9 of *Stress Analysis*, O.C. Zienkiewicz and G.S. Holister, eds., John Wiley and Sons, Inc., London, 1965.

76. Fraeijs de Veubeke, B., "Bending and Stretching of Plates - Special Models for Upper and Lower Bounds," *Proceedings of the First Conference on Matrix Methods in Structural Mechanics*, AFFDL-TR-66-80, Ohio, Oct. 26-28, 1965, pp. 863-886.

77. Fraeijs de Veubeke, B. "A Conforming Finite Element for Plate Bending," *International Journal of Solids and Structures*, Vol.4, No.1, 1968, pp. 95-108.

78. Fraeijs de Veubeke, B. and Millard, A., "Discretization of Stress Fields in the Finite Element Method," *Journal of the Franklin Institute*, Vol.302, Nos.5 and 6, Dec., 1972, pp. 389-412.

79. Fraeijs de Veubeke, B. and Sander, G., "An Equilibrium Model for Plate Bending," *International Journal of Solids and Structures*, Vol.4, No.4, 1968, pp. 447-468.

80. Fraeijs de Veubeke, B. and Zienkiewicz, O.C., "Strain Energy Bounds in Finite Element Analysis by Slab Analogy," *Journal of Strain Analysis*, Vol.2, No.4, 1967, pp. 265-271.

81. Fried, I., "Shear in C^0 and C^1 Bending Finite Elements," *International Journal of Solids and Structures*, Vol.9, No.4, 1973, pp. 449-460.

82. Fried, I., and Yang, S.K., "Triangular 9 Degree of Freedom, C^0 Plate Bending Elements of Quadratic Accuracy," *Quarterly of Applied Mathematics*, Vol.31, No.3, Oct., 1973, pp. 303-312.

83. Gallagher, R.H., "Analysis of Plate and Shell Structures," *Proceedings of the Symposium on Application of Finite Element Methods in Civil Engineering*, held at the School of Engineering, Vanderbilt University, Nashville, Tennessee, Nov. 13-14, 1969, pp. 155-205.

84. Gallagher, O.C., *Finite Element Analysis: Fundamentals*, Prentice Hall, Inc., Englewood Cliffs, New Jersey, 1975.

85. Gallagher, R.H., and Dhalla, A.K., "Direct Flexibility Finite Element Elastoplastic Analysis," *International Conference on Structural Mechanics in Reactor Technology*, Paper M6/9, Berlin, 1971, pp. 443-462.

86. Gopalacharyulu, S., "A Higher Order Conforming, Rectangular Plate Bending Element," *International Journal for Numerical Methods in Engineering*, Vol.6, No.2, 1973, pp. 305-309.

87. Granheim, G.O., "Beregning av Skjeve Plater ved Elementmetode," *Division of Structural Mechanics Technical Report SKJPL-1002*, The Technical University of Norway, 1967.

88. Greene, B.E., Jones, R.E., McLay, R.W., and Strome, D.R., "Generalized Variational Principles in the Finite Element Method," *American Institute of Aeronautics and Astronautics Journal*, Vol.7, No.7, July, 1969, pp. 1254-1260.

89. Gupta, A.K., and Ma, P.S., "Error in Eccentric Beam Formulations," *International Journal for Numerical Methods in Engineering*, Vol.11, No.9, 1977, pp. 1473-1483.

90. Guralnick, S.A., and LaFraugh, R.W., "Laboratory Study of a 45-Foot Square Plate Structure," *Journal of the American Concrete Institute, Proceedings*, Vol. 60., Sept., 1963, pp. 1107-1185.

91. Hansteen, H., "Finite Element Displacement Analysis of Plate Bending Based on Rectangular Elements," presented at *The Symposium on the Use of Electronic Digital Computers in Structural Engineering*, held at the University of Newcastle, Tyne, 1966.

92. Hansteen, O.E.,"Finite Element Methods as Applications of Variational Principles," Chapter 15 of *Finite Element Methods in Stress Analysis*, I. Holand and K. Bell, eds., TAPIR (Technical University of Norway Press), Trondheim, 1969.

93. Harvey, J.W., and Kelsey, S., "Triangular Plate Bending Elements with Enforced Compatibility," *American Institute of Aeronautics and Astronautics Journal*, Vol.9, No.6, June, 1971, pp. 1023-1026.

94. Hellan, K., "Analysis of Elastic Plates in Flexure by A Simplified Finite Element Method," *Acta Polytechnica Scandinavia*, Ci. Ser. 46, 1967.

95. Hellan, K., "On the Unity of the Constant-Strain Constant-Moment Finite Elements," *International Journal for Numerical Methods in Engineering*, Vol.6, No.2, 1973, pp. 191-209.

96. Henshell, R.D., "On Hybrid Finite Elements," *The Mathematics of Finite Elements and Applications*, J.R. Whiteman, ed., Academic Press, London, 1973, pp. 299-311.

97. Henshell, R.D., Walters, D., and Warburton, G.B., "A New Family of Curvilinear Plate Bending Elements for Vibration and Stability," *Journal of Sound and Vibration*, Vol.20, No.3, 1972, pp. 381-397.

98. Herrmann, L.R., "A Bending Analysis for Plates," *Proceedings of the First Conference on Matrix Methods in Structural Mechanics*, AFFDL-TR-66-80, Ohio, Oct. 26-28, 1965, pp. 577-602.

99. Herrmann, L.R., "Finite Element Bending Analysis for Plates," *Journal of the Engineering Mechanics Division, ASCE*, Vol.93, No. EM5, Oct., 1967, pp. 13-26.

100. Hinton, E., and Bicanic, N., "A Comparison of Lagrangian and Serendipity Mindlin Plate Elements for Free Vibration Analysis," *Computers and Structures*, Vol.10, 1979, pp. 483-493.

101. Hinton, E., Razzaque, A., Zienkiewicz, O.C., and Davies, J.D., "A Simple Finite Element Solution for Plates of Homogeneous, Sandwich and Cellular Construction," *Proceedings of the Institution of Civil Engineers, London*, Vol.59, Part 2, March, 1975, pp. 43-46.

102. Holand, I.,"Stiffness Matrices for Plate Bending Elements," Chapter 5 of *Finite Element Methods in Stress Analysis*, I. Holand and K. Bell, eds., TAPIR (Technical University of Norway Press), Trondheim, 1969.

103. Holand, I., "Membrane and Flat Plate Elements," *Proceedings of the World Congress on Finite Element Methods in Structural Mechanics*, held at Bournemouth, Dorset, England, 1975, Vol. II, pp. 13.1-13.18.

104. Hrabok, M.M., and Hrudey, T.M., "HYBSLAB - A Finite Element Program for Stiffened Plate Analysis," *Structural Engineering Report No. 101*, Department of Civil Engineering, University of Alberta, Edmonton, Alberta, Nov., 1981.

105. Hughes, T.J.R., and Cohen, M., "The 'Heterosis' Finite Element for Plate Bending," *Computers and Structures*, Vol.9, 1978, pp. 445-450.

106. Hughes, T.J.R., and Cohen, M., "The 'Heterosis' Finite Element for Plate Bending," *Proceedings of the ASCE Conference on Electronic Computations*, Aug., 1979, pp. 1-10.

107. Hughes, T.J.R., Cohen, M., and Haroun, M., "Reduced and Selective Integration Techniques in the Finite Element Analysis of Plates," *Nuclear Engineering and Design*, Vol.46, 1978, pp. 203-222.

108. Hughes, T.J.R., and Taylor, R.L., "A New Finite Element for Plate Bending," *International Conference on Structural Mechanics in Reactor Technology*, Paper M2/1, San Franciso, Aug., 1977.

109. Hughes, T.J.R., Taylor, R.L., and Kanoknukulchai, W., "A Simple and Efficient Finite Element for Plate Bending," *International Journal for Numerical Methods in Engineering*, Vol.11, No.10, 1977, pp. 1529-1543.

110. Irons, B.M., "Numerical Integration Applied to Finite Element Methods," presented at *The Symposium on the Use of Electronic Digital Computers in Structural Engineering*, held at the University of Newcastle, Tyne, 1966.

111. Irons, B.M., discussion of "Complete Polynomial Displacement Fields for the Finite Element Method," by P. Dunne, Paper No.6726, *The Aeronautical Journal of The Royal Aeronautical Society*, Vol.72, Aug., 1968, pp. 709-710.

112. Irons, B.M., "A Conforming Quartic Triangular Element for Plate Bending," *International Journal for Numerical Methods in Engineering*, Vol.1, No.1, 1969, pp. 29-45.

113. Irons, B.M., "The Patch Test for Engineers," presented at the *Conference ot the Atlas Computing Center*, held at Harwell, United Kingdom, March, 1974.

114. Irons, B.M., "The Semi-Loof Element," Chapter 11 of *Finite Elements for Thin Shell and Curved Members*, G.H. Ashwell and G.H. Gallagher, eds., John Wiley and Sons, Inc., New York, 1976.

115. Irons, B.M., and Draper, K.J, "Inadequacy of Nodal Connections in a Stiffness Solution for Plate Bending", *American Institute of Aeronautics and Astronautics Journal*, Vol.3, No.5, 1965, pp. 961.

116. Irons, B.M., and Razzaque, A., "Experience with the Patch Test for Convergence of Finite Element Methods," *Conference on the Mathematical Foundations of the Finite Element Method with Applications to Partial Differential Equations*, A.R. Aziz, ed., Academic Press, London, 1972, pp. 557-587.

117. Irons, B.M., and Razzaque, A., "Shape Function formulations for Elements Other than Displacement Models," presented at the *Symposium on Variational Methods in Engineering*, held at the University of Southampton, 1972, pp. 4/59-71.

118. Jirousek, J., and Leon, N., "A Powerful Finite Element for Plate Bending," *Computer Methods in Applied Mechanics and Engineering*, Vol.12, 1977, pp. 77-96.

119. Jones, R.E., "A Generalization of the Direct-Stiffness Method of Structural Analysis," *American Institute of Aeronautics and Astronautics Journal*, Vol.2, No.5, 1964, pp. 821-862.

120. Kikuchi, F., and Ando, Y., "Some Finite Element Solutions for Plate Bending Problems by Simplified Hybrid Displacement Method," *Nuclear Engineering and Design*, Vol.23, 1972, pp. 155-178.

121. Loof, H.W., "The Economical Computation of Stiffness of Large Structural Elements," presented at *The Symposium on the Use of Electronic Digital Computers in Structural Engineering*, held at the University of Newcastle, Tyne, 1966.

122. Lyons, L.P.R., "A General Finite Element System with Special Reference to the Analysis of Cellular Structures," thesis presented in partial fulfillment of the requirements for the degree of Doctor of Philosophy, Department of Civil Engineering, Imperial College of Science Technology, London, 1977.

123. Malkus, D.S., and Hughes, T.J.R., "Mixed Finite Element Methods - Reduced and Selective Integration Techniques: A Unification of Concepts," *Computer Methods in Applied Mechanics and Engineering*, Vol.15, 1978, pp. 63-81.

124. Mang, H.A., and Gallagher, R.H., "A Critical Assessment of the Simplified Hybrid Displacement Method," *International Journal for Numerical Methods in Engineering*, Vol.11, No.1, 1977, pp. 145-168.

125. Martins, R.A.F., and Owen, D.R.J., "Thin Plate Semi-Loof Element for Structural Analysis Including Stability and Natural Vibrations," *International Journal for Numerical Methods in Engineering*, Vol.12, No.11, 1978, pp. 1667-1676.

126. Mason, V., "Rectangular Elements for Analysis of Plate Vibrations," *Journal of Sound and Vibration*, Vol.7, No.3, 1968, pp. 437-448.

127. Meek, J.L., "Redundant Structure Concepts in Finite Element Analysis," *International Journal for Numerical Methods in Engineering*, Vol.9, No.4, 1975, pp. 765-773.

128. Melosh, R.J., "A Stiffness Matrix for the Analysis of Thin Plates in Bending," *Journal of the Aeronautical Sciences*, Vol.28, No.1, 1961, pp. 34-42.

129. Melosh, R.J., "Basis for Derivation of Matrices for the Direct Stiffness Method," *American Institute of Aeronautics and Astronautics Journal*, Vol.1, No.7, July, 1963, pp. 1631-1637.

130. Miller, R.E., "Reduction of the Error in Eccentric Beam Modelling," *International Journal for Numerical Methods in Engineering*, Vol.15, No.4, 1980, pp. 575-582.

131. Mindlin, R.D., "Influence of Rotatory Inertia and Shear on Flexural Motions of Isotropic, Elastic Plates," *Journal of Applied Mechanics*, Vol.18, March, 1951, pp. 31-38.

132. Morley, L.S.D., *Skew Plates and Structures*, Pergamon Press, London, 1963.

133. Morley, L.S.D., "A Triangular Equilibrium Element with Linearly Varying Bending Moments for Plate Bending Problems," *The Aeronautical Journal of The Royal Aeronautical Society*, Vol.71, Oct., 1967, pp. 715-719.

134. Morley, L.S.D., "The Triangular Equilibrium Element in the Solution of Plate Bending Problems," *The Aeronautical Quarterly*, Vol.XIX, May, 1968, pp. 149-169.

135. Morley, L.S.D., "A Finite Element Application of the Modified Rayleigh-Ritz Method," *International Journal for Numerical Methods in Engineering*, Vol.2, No.1, 1970, pp. 85-98.

136. Morley, L.S.D., "The Constant Moment Plate Bending Element," *Journal of Strain Analysis*, Vol.6, No.1, 1971, pp. 20-24.

137. Morley, L.S.D., and Merrifield, B.C., "On the Conforming Cubic Triangular Element for Plate Bending," *Computers and Structures*, Vol.2, 1972, pp. 875-892.

138. Neale, B.K., Henshell, R.D., and Edwards, G. "Hybrid Plate Bending Elements," *Journal of Sound and Vibration*, Vol.22, 1972, pp. 101-112.

139. Olson, M.D., "Compatibility of Finite Elements in Structural Mechanics," *Proceedings of the World Congress on Finite Element Methods in Structural Mechanics*, held at Bournemouth, Dorset, England, 1975, Vol.I, pp. H.1-H.32.

140. Papenfuss, S.W., "Lateral Plate Deflection by Stiffness Matrix Methods with Application to a Marqee," thesis presented in partial fulfillment of the requirements for the degree of Master of Science, Department of Civil Engineering, University of Washington, Seattle, Washington, 1959.

141. Panc, V., *Theories of Elastic Plates*, Noordhoff International Publishing Company, Leyden, The Netherlands, 1975.

142. Pawsey, S.F., and Clough, R.W., "Improved Numerical Integration of Thick Shell Finite Elements," *International Journal for Numerical Methods in Engineering*, Vol.3, No.4, 1971, pp. 575-586.

143. Pawsey, S.F., "discussion of papers by O.C. Zienkiewicz, R.L. Taylor, and J.M. Too, and S.F. Pawsey and R.W. Clough," *International Journal for Numerical Methods in Engineering*, Vol.4, No.3, 1972, pp. 449-450.

144. Pian, T.H.H., "Derivation of Element Stiffness Matrices," *American Institute of Aeronautics and Astronautics Journal*, Vol.2, No.3, March, 1964, pp. 1332-1333.

145. Pian, T.H.H., "Derivation of Element Stiffness Matrices by Assumed Stress Distributions," *American Institute of Aeronautics and Astronautics Journal*, Vol.2, No.7, July, 1964, pp. 1333-1336.

146. Pian, T.H.H., "Element Stiffness Matrices for Boundary Compatibility and for Prescribed Boundary Stresses," *Proceedings of the First Conference on Matrix Methods in Structural Mechanics*, AFFDL-TR-66-80, Ohio, Oct. 26-28, 1965, pp. 457-477.

147. Pian, T.H.H., "Hybrid Models," *Numerical and Computer Methods in Structural Mechanics*," S.J. Fenves, et al., eds., Academic Press, New York, 1973, pp. 59-78.

148. Pian, T.H.H., "Variational Principles for Incremental Finite Element Methods," *Journal of the Franklin Institute*, Vol.302, Nos. 5 and 6, Dec., 1972, pp. 473-488.

149. Pian, T.H.H., "A Historical Note about 'Hybrid Elements'," *International Journal for Numerical Methods in Engineering*, Vol.12, No.5, 1978, pp. 891-892.

150. Pian, T.H.H., and Mau, S.T., "Some Recent Studies in Assumed Stress Hybrid Models," *Advances in Computational Methods in Structural Mechanics and Design*, J.T. Oden et al., eds., UAH Press, Alabama, 1972, pp. 87-106.

151. Pian, T.H.H., and Tong, P., "Rationalization in Deriving Element Stiffness Matrices by Assumed Stress Approach," *Proceedings of the Second Conference on Matrix Methods in Structural Mechanics*, AFFDL-TR-68-150, Ohio, Oct. 15-17, 1968, pp. 441-469.

152. Pian, T.H.H., and Tong, P., "Basis of Finite Element Methods for Solid Continua," *International Journal for Numerical Methods in Engineering*, Vol.1, No.1, 1969, pp. 3-28.

153. Pian, T.H.H., Tong, P., and Luk, C.H., "Elastic Crack Analysis by a Finite Element Hybrid Method," *Proceedings of the Third Conference on Matrix Methods in Structural Mechanics*, AFFDL-TR-71-160, Ohio, Oct. 19-21, 1971, pp. 661-682.

154. Poceski, A., "A Mixed Finite Element Method for Bending of Plates," *International Journal for Numerical Methods in Engineering*, Vol.9, No.1, 1975, pp. 3-15.

155. Popplewell, N., and McDonald, D., "Conforming Rectangular and Triangular Plate-Bending Elements," *Journal of Sound and Vibration*, Vol.19, 1971, pp. 333-347.

156. Prager, W., "Variational Principles for Elastic Plates with Relaxed Continuity Requirements," *International Journal of Solids and Structures*, Vol.4, No.9, 1968, pp. 837-844.

157. Pryor, C.W., Barker, R.M., and Frederick, D., "Finite Element Bending of Reissner Plates," *Journal of the Engineering Mechanics Division, ASCE*, Vol.96, No. EM6, Dec., 1970, pp. 967-983.

158. Przemieniecki, J.S., "*Theory of Matrix Structural Analysis*," McGraw Hill Book Company, New York, 1968.

159. Pugh, E.D.L., "The Static and Dynamic Analysis of Mindlin Plates by Isoparametric Elements," thesis presented in partial fulfillment of the requirements for the degree of Master of Science, Department of Civil Engineering, Department of Civil Engineering, University College, Swansea, Dec., 1976.

160. Pugh, E.D.L., Hinton, E., and Zienkiewicz, O.C., "A Study of Quadrilateral Plate Bending Elements with 'Reduced Integration'," *International Journal for Numerical Methods in Engineering*, Vol.12, No.7, 1978, pp. 1059-1079.

161. Ramstad, H., "Parallelogram Elements in Bending: Accuracy and Convergence of Results," Division of Structural Mechanics, The Technical University of Norway, 1967.

162. Ramstad, H., and Holand, I., "The Finite Element Method for Analysis of Skew Plates in Bending by Use of Parallelogram Elements," presented at *The Symposium on the Use of Electronic Digital Computers in Structural Engineering*, held at the University of Newcastle, Tyne, 1966.

163. Razzaque, A., "Finite Element Analysis of Plates and Shells," thesis presented in partial fulfillment of the requirements for the degree of Doctor of Philosophy, Department of Civil Engineering, University College, Swansea, 1972.

164. Razzaque, A., "Program for Triangular Bending Elements with Derivative Smoothing," *International Journal for Numerical Methods in Engineering*, Vol.6, No.3, 1973, pp. 333-343.

165. Reissner, E., "The Effect of Transverse Shear Deformation on the Bending of Elastic Plates," *Journal of Applied Mechanics*, ASME Transactions, Vol. 67, 1945, pp. A69-77.

166. Reissner, E., "On a Variational Theorem in Elasticity," *Journal of Mathematics and Physics*, Vol.29, 1950, pp. 90-95.

167. Rossow, M.P., and Ibrahimkhail, A.K., "Constraint Method Analysis of Stiffened Plates," *Computers and Structures*, Vol.8, 1978, pp. 51-60.

168. Rossow, M.P., "Observations on Numerical Modeling of an Obtuse Corner of a Simply Supported Plate," *Journal of Applied Mechanics*, Vol.45, Sept., 1978, pp. 689-690.

169. Sander, G., "Bornes Superieures et Inferieures dans L'Analyse Matricielle des Plaques en Flexion-Torsion," *Bulletin Societe Royale des Sciences de Liege*, 1964, pp. 167-207.

170. Sander, G., "Applications of the Dual Analysis Principle," *The Proceedings of the IUTAM Symposium on High Speed Computing of Elastic Structures*, B. Fraeijs de Veubeke, ed., University of Liege, Belgium, Aug. 23-28, 1970, pp. 167-207.

171. Severn, R.T., and Taylor, P.R., "The Finite Element Method for Flexure of Slabs when Stress Distributions are Assumed," *Proceedings of the Institution of Civil Engineers, London*, Vol.34, June, 1966, pp. 153-170.

172. Severn, R.T., and Taylor, P.R., closure to "The Finite Element Method for Flexure of Slabs when Stress Distributions are Assumed," *Proceedings of the Institution of Civil Engineers, London*, Vol.34, June, 1966, pp. 701-705.

173. Shieh, W., Lee, S.L., and Parmelee, R., "Analysis of Plate Bending by Triangular Elements," *Journal of the Engineering Mechanics Division, ASCE*, Vol.94, No. EM5, Oct., 1968, pp. 1089-1107.

174. Smith, I.M., "A Finite Element Method Analysis for 'Moderateley Thick' Rectangular Plates in Bending," *International Journal of Mechanical Science*, Vol.10, 1968, pp. 563-570.

175. Smith, I.M., and Duncan, W., "The Effectiveness of Excessive Nodal Continuities in the Finite Element Analysis of Thin Rectangular and Skew Plates in Bending," *International Journal for Numerical Methods in Engineering*, Vol.2, No.2, 1970, pp. 253-257.

176. Somervaille, I.J., "A Family of Equilibrium Plate Bending Elements," *Conference on Finite Element Methods in Engineering*, V. Pulmano and A. Kabaila, eds., University of New South Wales, Australia, 1974,, pp. 247-256.

177. Southwell, R.V., "On the Analogues Relating Flexure and Extension of Flat Plates," *Quarterly Journal of Mathematics and Applied Mechanics*, Vol. III, Part 3, 1950, pp. 257-270.

178. Speare, P.R.S., and Kemp, K.O., "A Simplified Reissner Theory for Plate Bending," *International Journal of Solids and Structures*, Vol.13, No.11, 1977, pp. 1073-1079.

179. Spilker, R.L., and Munir, N.I., "The Hybrid-Stress Model for Thin Plates," *International Journal for Numerical Methods in Engineering*, Vol.15, No.8, 1980, pp. 1239-1260.

180. Stricklin, J.A., Haisler, W.E., Tisdale, P.R., and Gunderson R., "A Rapidly Converging Triangular Plate Element," *American Institute of Aeronautics and Astronautics Journal*, Vol.7, No.1, 1969, pp. 180-181.

181. Svec, O.J., and Gladwell, G.M.L., "A Triangular Plate Bending Element for Contact Problems," *International Journal of Solids and Structures*, Vol.9, No.3, 1973, pp. 435-446.

182. Swedlow, J.L., "Singularity Computations," *International Journal for Numerical Methods in Engineering*, Vol.12, No.12, 1978, pp. 1779-1798.

183. Szabo, B., and Lee, G., "Stiffness Matrix for Plates by Galerkin's Method," *Journal of the Engineering Mechanics Division, ASCE*, Vol.95, No. EM3, June., 1969, pp. 571-585.

184. Timoshenko, S., and Woinowsky-Krieger, S., *Theory of Plates and Shells*, McGraw-Hill Book Company, Inc., New York, 1959.

185. Tocher, J.L., "Analysis of Plate Bending Using Triangular Elements," thesis presented in partial fulfillment of the requirements for the degree of Doctor of Philosophy, Department of Civil Engineering, University of California, Berkeley, 1962.

186. Tong, P., "New Displacement Hybrid Finite Element Models for Solid Continua," *International Journal for Numerical Methods in Engineering*, Vol.2, No.1, 1970, pp. 73-83.

187. Tong, P., Mau, S.T., and Pian, T.H.H., "Derivation of Geometric and Mass Matrices for Finite Element Hybrid Models," *International Journal of Solids and Structures*, Vol.10, No.8, 1974, pp. 919-932.

188. Tong, P., and Pian, T.H.H., "A Variational Principle and the Convergence of a Finite Element Model Based on Assumed Stress Distributions," *International Journal of Solids and Structures*, Vol.5, No.5, 1969, pp. 463-472.

189. Torbe, I., and Church, K., "A General Quadrilateral Plate Element," *International Journal for Numerical Methods in Engineering*, Vol.9, No.4, 1975, pp. 855-868.

190. Utku, S. "Stiffness Matrices for Thin Rectangular Elements of Non-Zero Gaussian Curvature," *American Institute of Aeronautics and Astronautics Journal*, Vol.5, No.9, Sept., 1967, pp. 1659-1667.

191. Utku, S., "On Derivation of Stiffness Matrices with C^0 Rotation Fields for Plates and Shells," *Proceedings of the Third Conference on Matrix Methods in Structural Mechanics*, AFFDL-TR-71-160, Ohio, Oct. 19-21, 1971, pp. 255-274.

192. Visser, W. "A Refined Mixed-Type Plate Bending Element," *American Institute of Aeronautics and Astronautics Journal*, Vol.7, No.9, Sept., 1969, pp. 1801-1803.

193. Watkins, D.S., "A Conforming Rectangular Plate Element," *The Mathematics of Finite Elements and Applications*, J.R. Whiteman, ed., Academic Press, London, 1975, pp. 77-83.

194. Watkins, D.S. "A Comment on Gopalacharyulu's 24 Node Element," *International Journal for Numerical Methods in Engineering*, Vol.10, No.2, 1976, pp. 471-474.

195. Wegmuller, A.W., "A Refined Plate Bending Finite Element," *International Journal of Solids and Structures*, Vol.10, No.11, 1974, pp. 1173-1178.

196. Wempner, G.A., Oden, J.T., and Kross, D.A., "Finite Element Analysis of Thin Shells," *Journal of the Engineering Mechanics Division, ASCE*, Vol.94, No. EM6, Dec., 1968, pp. 1273-1294.

197. Williams, M.L., "Surface Stress Singularities Resulting from Various Boundary Conditions in Angular Corners of Plates Under Bending," *Proceedings of the First U.S. National Congress of Applied Mechanics*, Illinois Institute of Technology, Chicago, June, 1951, pp. 325-329.

198. Williams, M.L., "Stress Singularities Resulting from Various Boundary Conditions in Angular Corners of Plates in Extension," *Journal of Applied Mechanics*, Vol.19, No.5, Dec., 1952, pp. 526-528.

199. Withum, D., "Berechnung von Platten nach dem Ritz'schen Verfahren mit Hilfe dreieckformiger Maschennetze," *Mitteilungen des Instituts fur Statik der Technischen Hochschule, Nr.9*, Hanover, June, 1966.

200. Wolf, J.P., "Generalized Hybrid Stress Finite Element Models," *American Institute of Aeronautics and Astronautics Journal*, Vol.11, No.3, March, 1973, pp. 386-388.

201. Wolf, J.P., "Alternate Hybrid Stress Finite Element Models," *International Journal for Numerical Methods in Engineering*, Vol.9, No.3, 1975, pp. 601-615.

202. Yamamoto, R., and Isshiki, H., "Variational Principles and Dualistic Scheme for Intersection Problems in Elasticity," *Journal of the Faculty of Engineering*, University of Tokyo, Vol. XXX, No.1, 1969.

203. Yoshida, Y., "Equivalent Finite Elements of Different Bases," *Advances in Computational Methods in Structural Mechanics and Design*, J.T. Oden et al., eds., UAH Press, Alabama, 1972, pp. 133-149.

204. Yoshida, Y., "A Hybrid Stress Element for Thin Shell Analysis," *Conference on Finite Element Methods in Engineering*, V. Pulmano and A. Kabaila, eds., University of New South Wales, Australia, 1974,, pp. 271-284.

205. Zenisek, A., "Interpolation Polynomials on the Triangle," *Numerische Mathematik*, Vol.15, 1970, pp. 283-296.

206. Zienkiewicz, O.C., "*The Finite Element Method in Engineering Science*," McGraw Hill Book Company, New York, 1977.

207. Zienkiewicz, O.C., and Cheung, Y.K., "The Finite Element Method for Analysis of Isotropic and Orthotropic Slabs," *Proceedings of the Institution of Civil Engineers, London*, Vol.28, 1964, pp. 471-488.

208. Zienkiewicz, O.C., and Hinton, E., "Reduced Integration, Function Smoothing and Non-Conformity in Finite Element Analysis," *Journal of the Franklin Institute*, Vol.302, Nos.5 and 6, Dec., 1976, pp. 443-461.

209. Zienkiewicz, O.C., Taylor, R.L., and Too, J.M., "Reduced Integration Technique in General Analysis of Plates and Shells," *International Journal for Numerical Methods in Engineering*, Vol.3, No.2, 1971, pp. 275-290.

210. Zienkiewicz, O.C., Taylor, R.L., and Too, J.M., discussion and closure on "Reduced Integration Technique in General Analysis of Plates and Shells," *International Journal for Numerical Methods in Engineering*, Vol.4, No.1, 1972, pp. 148-151.

APPENDIX A

THE LAGRANGE MULTIPLIER ELEMENT

In this section a formulation is presented for obtaining stiffness matrices from a method which combines Mindlin plate theory, the principle of minimum potential energy, and Lagrangian multipliers. A general form of the stiffness matrix is obtained first and then certain conditions are prescribed to obtain stiffness matrices for a number of different elements. Among these elements are the 'Lagrange' element and the selective reduced integration rectangles.

By using plate theories such as Mindlin's, the effects of transverse shear can be included in the formulation. As shown in Figure A.1, the total rotation of a plane section, initially normal to the midsurface, consists of a rotation due to flexure plus an additional rotation due to shear. The total rotations can be written as:

$$\theta x = W,y + \theta x$$
$$\theta y = W,x + \theta y \qquad (A.1)$$

where,

θx= total rotation of an equivalent plane section about the X axis,
θy= total rotation of an equivalent plane section about the Y axis,
W = transverse displacement of the plate's midsurface,
θx= rotation about the X axis of a normal with respect to a tangent at the midsurface,
θy= rotation about the Y axis of a normal with respect to a tangent at the midsurface,

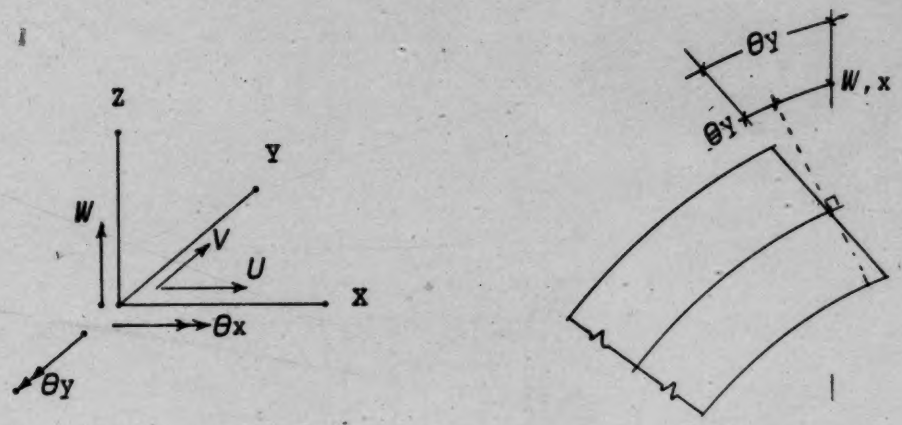

Figure A.1 Rotations at the Midsurface of the Plate.

The x and y displacements, U and V, respectively, of a point located at a distance 'z' above the neutral surface can be written as:

$$U = -z\,\theta y$$
$$V = -z\,\theta x \qquad \text{(A.2)}$$

From the above expressions for U and V, the following strains can be obtained:

$$\epsilon x = U,x \quad = -(z)(\theta y,x)$$
$$\epsilon y = V,y \quad = -(z)(\theta x,y)$$
$$\epsilon xy = \tfrac{1}{2}(V,x + U,y) = -\tfrac{1}{2}(z)(\theta x,x + \theta y,y)$$
$$\epsilon yz = \tfrac{1}{2}(W,y + V,z) = +\tfrac{1}{2}(W,y - \theta x) \qquad \text{(A.3)}$$
$$\epsilon xz = \tfrac{1}{2}(W,x + U,z) = +\tfrac{1}{2}(W,x - \theta y)$$

The finite element method has the unique feature that displacement functions can be specified independently for each element. The Mindlin plate theory is characterised by the assumption that midsurface rotations are not solely dependent on the transverse displacements. Therefore, the

element shape functions, $\langle N_i \rangle$, for plate flexure can be identical to those from plane elasticity. The importance of this aspect is that the elements can be distorted isoparametrically. In equation form, the field values of the independent variables can be related to their respective nodal values as:

$$\begin{aligned} W &= \langle N_1 \rangle \{\underline{W}\} \\ \theta x &= \langle N_2 \rangle \{\underline{\theta} x\} \\ \theta y &= \langle N_3 \rangle \{\underline{\theta} y\} \end{aligned} \tag{A.4}$$

Substituting the above expressions into the strain-displacement Equations A.3 results in Equations A.5 shown below. Partial differentiation is denoted by the comma notation.

$$\begin{aligned} \epsilon x &= -z \langle N_3,x \rangle \{\underline{\theta} y\} \\ \epsilon y &= -z \langle N_2,y \rangle \{\underline{\theta} x\} \\ \epsilon xy &= -\tfrac{1}{2}(z)(\langle N_2,x \rangle \{\underline{\theta} x\} + \langle N_3,y \rangle \{\underline{\theta} y\}) \\ \epsilon yz &= +\tfrac{1}{2}(\langle N_1,y \rangle \{\underline{W}\} - \langle N_2 \rangle \{\underline{\theta} x\}) \\ \epsilon xz &= +\tfrac{1}{2}(\langle N_1,x \rangle \{\underline{W}\} - \langle N_3 \rangle \{\underline{\theta} y\}) \end{aligned} \tag{A.5}$$

The constitutive matrix is assumed to relate stresses to strains according to the following equations:

$$\{\sigma\} = [E]\{\epsilon\} \tag{A.6}$$

where,

$$[E] = \begin{bmatrix} Ex & E_1 & . & . & . \\ E_1 & Ey & . & . & . \\ . & . & Exy & . & . \\ . & . & . & Eyz & . \\ . & . & . & . & Exz \end{bmatrix}$$

The potential energy of the structure, $\prod$, consists of the strain energy, ξ, and the potential of external or applied loads, Ve. The expression for the strain energy can be written as:

$$\xi = 1/2 \int \sigma ij \, \epsilon ij \, dV \qquad (A.7)$$

$$= \tfrac{1}{2} <\underline{\theta}y>[K^{(1)}]\{\underline{\theta}y\} + <\underline{\theta}x>[K^{(2)}]\{\underline{\theta}y\} + \tfrac{1}{2} <\underline{\theta}x>[K^{(3)}]\{\underline{\theta}x\}$$
$$+\tfrac{1}{2} <\underline{\theta}x>[K^{(4)}]\{\underline{\theta}x\} + <\underline{\theta}x>[K^{(5)}]\{\underline{\theta}y\} + \tfrac{1}{2} <\underline{\theta}y>[K^{(6)}]\{\underline{\theta}y\}$$
$$+\tfrac{1}{2} <\underline{W}>[K^{(7)}]\{\underline{W}\} - <\underline{W}>[K^{(8)}]\{\underline{\theta}x\} + \tfrac{1}{2} <\underline{\theta}x>[K^{(9)}]\{\underline{\theta}x\}$$
$$+\tfrac{1}{2} <\underline{W}>[K^{(10)}]\{\underline{W}\} - <\underline{W}>[K^{(11)}]\{\underline{\theta}y\} + \tfrac{1}{2} <\underline{\theta}y>[K^{(12)}]\{\underline{\theta}y\}$$

where,

$$[K^{(1)}] = (t^3/12) \int \{N_3,x\} \, Ex \, <N_3,x> \, dA$$

$$[K^{(2)}] = (t^3/12) \int \{N_3,y\} \, E_1 \, <N_3,x> \, dA$$

$$[K^{(3)}] = (t^3/12) \int \{N_3,y\} \, Ey \, <N_3,y> \, dA$$

$$[K^{(4)}] = (t^3/24) \int \{N_3,x\} \, Exy \, <N_3,x> \, dA$$

$$[K^{(5)}] = (t^3/24) \int \{N_3,x\} \, Exy \, <N_3,y> \, dA$$

$$[K^{(6)}] = (t^3/24) \int \{N_3,y\} \, Exy \, <N_3,y> \, dA$$

$$[K^{(7)}] = (\gamma t/2) \int \{N_1,y\} \, Eyz \, <N_1,y> \, dA$$

$$[K^{(8)}] = (\gamma t/2) \int \{N_1,y\} \, Eyz \, <N_2> \, dA$$

$$[K^{(9)}] = (\gamma t/2) \int \{N_2\}\ Eyz\ \langle N_3 \rangle\ dA$$

$$[K^{(10)}] = (\gamma t/2) \int \{N_1,x\}\ Exz\ \langle N_1,x \rangle\ dA$$

$$[K^{(11)}] = (\gamma t/2) \int \{N_1,x\}\ Exz\ \langle N_3 \rangle\ dA$$

$$[K^{(12)}] = (\gamma t/2) \int \{N_3\}\ Exz\ \langle N_3 \rangle\ dA$$

In the above equations, 'γ' is the shear factor which accounts for the nonuniform distribution of the shear stresses in the Z direction.

The potential of the external loads can be written as:

$$Ve = \int q\ W\ dA + \int My\ \theta x\ dA + \int Mx\ \theta y\ dA \qquad (A.8)$$

$$= \langle \underline{W} \rangle \{F_1\} + \langle \underline{\theta}x \rangle \{F_2\} + \langle \underline{\theta}y \rangle \{F_3\}$$

where,

$$\{F_1\} = \int \{N_1\}\ (q)\ dA$$

$$\{F_2\} = \int \{N_2\}\ (My)\ dA$$

$$\{F_3\} = \int \{N_3\}\ (Mx)\ dA$$

For thick plates, the functional $\prod$ could now be minimized with respect to the displacement vectors $\{\underline{W}\}$, $\{\underline{\theta}x\}$, and $\{\underline{\theta}y\}$ to obtain a reasonable stiffness matrix. However, for thin plates the shear rigidity is so large that it causes the element to 'lock' or become so stiff that when loaded it virtually undergoes no displacement. To rectify the situation, researchers such as Clough, Zienkiewicz,

Hughes, and Hinton have developed the technique of using selective reduced integration. A second method is to impose the Kirchhoff conditions of normality as constraints at discrete locations; this was done by Lyons in 1977. The third method, the one being presented here, is to impose the Kirchhoff constraints in an integral sense through the use of Lagrangian multipliers. The Kirchhoff conditions of normality for thin plates are:

$$W,y - \theta x = 0$$
$$W,x - \theta y = 0 \qquad (A.9)$$

A convenient approach for minimizing the functional Π subject to these constraints is to use Lagrangian multipliers and work with the augmented functional Πg.

The field values of the Lagrangian multipliers are assumed to be related to their respective nodal values by shape functions similar to those used for displacements. In matrix equation form this can be written as:

$$\lambda x = \langle N_4 \rangle \{\underline{\lambda} x\}$$
$$\lambda y = \langle N_5 \rangle \{\underline{\lambda} y\} \qquad (A.10)$$

The modified functional, Πg, can be written as:

$$\Pi g = \Pi + \mp \qquad (A.11)$$

where,

$$\mp = \int (\lambda x)(W,y - \theta x)\, dA + \int (\lambda y)\,(W,x - \theta y)\, dA$$

$$= \langle \underline{\lambda} x \rangle [L^{(1)}]\{\underline{W}\} - \langle \underline{\lambda} x \rangle [L^{(3)}]\{\underline{\theta} x\}$$
$$+ \langle \underline{\lambda} y \rangle [L^{(3)}]\{\underline{W}\} - \langle \underline{\lambda} y \rangle [L^{(4)}]\{\underline{\theta} y\}$$

where,

$$[L^{(1)}] = \int \{N_4\} \langle N_1, y \rangle \, dA$$

$$[L^{(2)}] = \int \{N_4\} \langle N_2 \rangle \, dA$$

$$[L^{(3)}] = \int \{N_5\} \langle N_1, x \rangle \, dA$$

$$[L^{(4)}] = \int \{N_5\} \langle N_3 \rangle \, dA$$

To obtain a stationary value, the functional $\prod g$ is minimized with respect to $\{\underline{W}\}$, $\{\underline{\theta}x\}$, $\{\underline{\theta}y\}$, $\{\underline{\lambda}x\}$, and $\{\underline{\lambda}y\}$. The results of this operation are shown in the set of equations below.

$$\begin{bmatrix} [K^{(7)}]+[K^{(10)}] & -[K^{(8)}] & -[K^{(11)}] & +[L^{(1)}]^T & +[L^{(3)}]^T \\ -[K^{(8)}]^T & [K^{(3)}]+[K^{(4)}]+[K^{(9)}] & [K^{(2)}]+[K^{(5)}] & -[L^{(2)}]^T & . \\ -[K^{(11)}]^T & [K^{(2)}]^T+[K^{(5)}]^T & [K^{(1)}]+[K^{(6)}]+[K^{(12)}] & . & -[L^{(4)}]^T \\ +[L^{(1)}] & -[L^{(2)}] & . & . & . \\ +[L^{(3)}] & . & -[L^{(4)}] & . & . \end{bmatrix} \begin{bmatrix} \{\underline{W}\} \\ \{\underline{\theta}x\} \\ \{\underline{\theta}y\} \\ \{\underline{\lambda}x\} \\ \{\underline{\lambda}y\} \end{bmatrix} = \begin{bmatrix} \{F_1\} \\ \{F_2\} \\ \{F_3\} \\ \{o\} \\ \{o\} \end{bmatrix} \tag{A.12}$$

In the above equations, the Lagrangian multipliers can be set equal to zero and stiffness matrices obtained for the Bi.MPT element, the higher order Lagrangian and Serendipity rectangles, and the heterosis elements. Setting $\{\underline{\lambda}x\}$ and

{λ_y} to zero eliminates the last two rows and columns of submatrices, and Equations A.12 become identical to those typically associated with a Mindlin type of formulation. For thick plate elements these equations are usually evaluated exactly, while for thin plates selective reduced integration is used.

To obtain the stiffness matrix for the Lagrange element of Chapter 3, the following procedure was used. The element was initially assumed to have 4 corner nodes and 4 midside nodes. The A C M element shape functions were used to represent W and its first derivatives at the corner nodes. Complete quadratic Serendipity shape functions were used for θ_x, θ_y, λ_x, and λ_y. The resulting element has 44 degrees of freedom; the parameters at the corner nodes are $< W\ W,_x\ W,_y\ \theta_x\ \theta_y\ \lambda_x\ \lambda_y >$, and $< \theta_x\ \theta_y\ \lambda_x\ \lambda_y >$ at the midside nodes. The resulting matrix from Equation A.12 is 44×44 and can be reduced to 12×12 by using static condensation. The condensed element has corner nodes only with $< W\ \theta_x\ \theta_y >$ as nodal degrees of freedom.

In using the above element two separate cases were considered. For the first case, Eyz and Exz were assigned equal to Exy. For the second case, Eyz and Exz were assigned zero values relative to Exy. For the 4x4 and finer grids of Chapter 3, the results from the two cases were very similar and only the results from the second case were reported.

The element from the first case is a Mindlin element and the Lagrange multipliers prevent the 'locking' normally experienced by these elements when analysing thin plates. The element derived from the second case is, in essence, a Kirchhoff element because the strain energy from transverse shear deformations is not included.

The stiffness matrix for either case can be evaluated by numerically evaluating the coefficients of Equation A.12 and then eliminating the Lagragian multipliers by static condensation. The remaining stiffness matrix contains only the geometric degrees of freedom. This is the approach which was used to obtain the 12×12 stiffness matrix for the Lagrange element of Chapter 3. The results of this operation were checked by using a separate approach where transverse shear strains were neglected from the beginning and the Lagrange multipliers were eliminated from the explicit form of the stiffness matrix.